

**The biorefinery of the heterotrophic marine microalga
Cryptocodinium cohnii grown on low-cost substrates:
Production of DHA and biodiesel**

Daniela Fonseca Martins

Dissertation to obtain the Master's Degree in
Food Science and Engineering

Supervisors: Dr. Patrícia Maria Azevedo Moniz

Prof. Dr. Maria Suzana Leitão Ferreira Dias Vicente

Jury:

Presidente: Doutor Vítor Manuel Delgado Alves, Professor auxiliar do(a) Instituto Superior de Agronomia da Universidade de Lisboa

Vogais: Doutora Carla Sofia Ramos Tecelão, Professora adjunta do(a) Escola Superior de Turismo e Tecnologia do Mar do Instituto Politécnico de Leiria

Doutora Patrícia Maria Azevedo Moniz, Investigadora do(a) Laboratório Nacional de Energia e Geologia, orientadora

Preface

The work presented in this dissertation was performed at the National Laboratory of Energy and Geology - LNEG (Lisbon, Portugal), at the Bioenergy and Biorefineries Unit, within the project "OMEGAFUEL - New platform for the production of biofuels and compounds ω -3, from the sustainable biorefinery of the marine microalgae *Cryptocodinium cohnii*", with the reference PTDC 2017 - PTDC/EAM-AMB/30169/2017, funded by FCT (Fundação para a Ciência e Tecnologia). This study was accomplished during the period of February to July of 2022, under the supervision of Dr. Patrícia Maria Azevedo Moniz and Dr. Maria Teresa Lopes da Silva. The thesis was co-supervised at Instituto Superior de Agronomia, Universidade de Lisboa, by Prof. Suzana Ferreira Dias.

The results reported in this study were published in the scientific article "The Biorefinery of the Marine Microalga *Cryptocodinium Cohnii* as a Strategy to Valorise Microalgal Oil Fractions", in *Fermentation* journal, authored by Patrícia Moniz, Daniela Martins, Ana Cristina Oliveira, Alberto Reis and Teresa Lopes da Silva (<https://doi.org/10.3390/fermentation8100502>).

Acknowledgments

This thesis would never be completed if I did not thank all those who, in their own way, contributed to its elaboration and to my growth. Therefore, I would like to start to thank my supervisors Dr. Patrícia Moniz and Dr. Teresa Lopes da Silva for all the support provided, for all the knowledge transmitted, for all the experiences shared in laboratory over the last months of work and for the infinite patience over my mistakes. Your passion and dedication to the work you do has always motivated me a lot and this last months in LNEG really made me grow at professional, academical and personal level.

To everyone else I met on LNEG, for their patience, sympathy, and constant assistance in the laboratory. I would like to thank to Inês, Francisca, Ângela and Filipe, for the time we shared and for the constant good company for lunch.

To Professor Suzana Ferreira Dias, for first giving me the contact that led to my participation in this project, for always speaking to me with the greatest sympathy and for being available to help me whenever I needed.

On a personal note, I would like to give thanks to all my family and friends, for their love, friendship and unconditional support during my entire academic career and, specially, during this challenge that was my master's thesis. I would like to give a very special thanks to my mother Cristina, my father Américo and my sister Beatriz, that always gave me motivation, supported my choices, helped me following my dreams and ambitions and helped me grow and succeed in the challenges I faced during my life. I'm eternally grateful for all your support.

To António, my boyfriend and my best friend, thank you for always cheering me up, for believing in me and for your endless support and patience with me. You make all my days better. There are not enough words for you.

Finally, I would also like to thank FCT (Fundação para a Ciência e Tecnologia) for funding the project "OMEGAFUEL - New platform for the production of biofuels and compounds ω -3, from the sustainable biorefinery of the marine microalgae *Cryptothecodinium cohnii*" (PTDC 2017 - PTDC/EAM-AMB/30169/2017) and providing the resources for conducting this work.

Abstract

The present work explored the use of low-cost substrates for the cultivation of the marine heterotrophic microalga *Cryptocodinium cohnii*, to produce high concentrations of docosahexaenoic acid (DHA) and fatty acids for biodiesel production.

Three cultivations were conducted, in a benchtop bioreactor operated under fed-batch regime, using different nutrient sources: crude glycerol, sugarcane molasses and corn steep liquor (CSL), all industrial by-products. The use of crude glycerol and CSL as carbon and nitrogen sources (Assay I), presented the best results, with a biomass concentration of 10.69 g L⁻¹, total fatty acids (TFA) content of 28.29% (w/w), TFA productivity of 19.31 mg L⁻¹ h⁻¹ and DHA productivity of 6.64 mg L⁻¹ h⁻¹.

After the cultivation, the lyophilized biomass obtained underwent a saponification reaction, to produce fatty acid soaps, which were further converted into fatty acid ethyl esters (FAEE). These compounds were fractionated, using the urea complexation method at different temperatures, to obtain a polyunsaturated FAEE rich fraction (with potential for food, pharmaceutical and cosmetic purposes) and a saturated and monounsaturated FAEE rich fraction (potentially for biodiesel purposes). At the crystallization temperature of -18°C, in Assay I fractions with 91.6% purity of DHA ethyl ester and 88.0% purity of saturated and monounsaturated FAEE were obtained. In Assay III, fractions with 69.91% purity of DHA ethyl ester and 97.4% purity of saturated and monounsaturated FAEE were attained. Finally, physical parameters of the fractions rich in saturated and monounsaturated FAEE were estimated and confirmed to be appropriate for biodiesel production, after a hydrogenation step, according to limits defined by the European Standard EN 14214.

The attained results represent an innovative and sustainable method for producing DHA and biodiesel from *C. cohnii*, increasing the potential revenue generated by the entire process, since all compounds produced are valorised and no waste is generated, respecting the circular economy.

Keywords: *Cryptocodinium cohnii*, Docosahexaenoic acid, Biodiesel, Low-cost Substrates, Circular Bioeconomy

Resumo

O presente estudo permitiu explorar a utilização de substratos de baixo custo no cultivo da microalga heterotrófica marinha *Cryptocodinium cohnii*, para produzir elevadas concentrações de ácido docosahexaenóico (DHA) e ácidos gordos para produção de biodiesel.

Foram realizados três ensaios em biorreator de bancada, em regime *fed-batch*, utilizando subprodutos industriais como substrato: glicerol bruto, melação de cana-de-açúcar e *corn steep liquor* (CSL). Foi possível concluir que a utilização de glicerol bruto e CSL (Ensaio I), conduziu a melhores resultados, atingindo-se uma concentração em biomassa de 10.69 g de L⁻¹, um teor em ácidos gordos totais (TFA) de 28.29% (m/m), produtividade em TFA de 19.31 mg L⁻¹ h⁻¹ e produtividade em DHA de 6.64 mg L⁻¹ h⁻¹.

Após cultivo, a biomassa liofilizada produzida foi saponificada, permitindo formação de sabões de ácidos gordos, que foram convertidos em ésteres etílicos e, seguidamente, fracionados, através do método de complexação com ureia a diferentes temperaturas. Este método permitiu a obtenção de uma fração rica em ésteres etílicos polinsaturados (com potencial utilização nas indústrias alimentar, farmacêutica e cosmética) e uma fração rica em ésteres etílicos saturados e monoinsaturados (potencialmente para produção de biodiesel). À temperatura de cristalização de -18°C foram obtidas frações com 91.6% e 69.91% de pureza em ésteres etílicos de DHA e frações com 88.0% e 97.4% de pureza de esteres etílicos saturados e monoinsaturados nos Ensaios I e III, respetivamente. Por último, foram estimados os parâmetros físicos das frações para biodiesel, verificando-se que, após uma etapa de hidrogenação, são adequadas para produção deste biocombustível, de acordo com os limites definidos pela Norma Europeia EN 14214.

Os resultados obtidos permitiram concluir que este se trata de um método inovador e sustentável para produção de DHA e biodiesel, uma vez que todos os compostos produzidos são valorizados e não são gerados resíduos, respeitando a economia circular.

Palavras-chave: *Cryptocodinium cohnii*, Ácido Docosahexaenóico, Biodiesel, Substratos de Baixo Custo, Bioeconomia Circular

Resumo Alargado

O presente estudo permitiu explorar a utilização de substratos de baixo custo no cultivo da microalga heterotrófica marinha *Cryptocodinium cohnii*, para produzir elevadas concentrações de ácido docosahexaenóico (DHA) e ácidos gordos para produção de biodiesel.

Foram realizados três ensaios em biorreator de bancada, em regime *fed-batch*, sendo utilizados subprodutos industriais como substrato: glicerol bruto (subproduto da indústria de produção de biodiesel), melão de cana-de-açúcar (subproduto industrial resultante do refinamento de açúcar a partir de cana-de-açúcar) e *corn steep liquor* (CSL) (subproduto resultante da maceração do milho). As fermentações realizadas foram monitorizadas em tempo real através de observação microscópica, densidade ótica e citometria de fluxo. Para além disso, procedeu-se à quantificação do carbono consumido ao longo do tempo de fermentação, bem como do conteúdo em azoto total presente no meio de cultura, e foi avaliado o perfil de ácidos gordos produzidos ao longo do cultivo.

Foi possível concluir que a utilização de glicerol bruto e CSL no Ensaio I, deu origem a melhores resultados, atingindo-se uma concentração em biomassa de 10.69 g L⁻¹, um teor de ácidos gordos totais (TFA) de 28.29% (m/m), produtividade em TFA de 19.31 mg L⁻¹ h⁻¹ e produtividade em DHA de 6.64 mg L⁻¹ h⁻¹. De facto, operar em regime *fed-batch*, adicionando pulsos nutritivos de glicerol bruto, extrato de levedura e CSL (subproduto industrial resultante do processamento de amido de milho), permitiu, efetivamente, um prolongamento da fase estacionária do crescimento celular, o que resultou num aumento da produção de lípidos.

Por outro lado, no Ensaio II, ao utilizar o melão de cana-de-açúcar como fonte de carbono, os resultados não foram tão satisfatórios, uma vez que apenas foi possível a produção de 7.84 g L⁻¹ de biomassa e obtenção de um teor de TFA de 7.92% (m/m), constituindo resultados pouco satisfatórios quando comparando com os restantes ensaios realizados neste estudo ou com outros estudos reportados na literatura. Este resultado verificou-se devido à falta de carbono no meio de cultura, que induziu uma situação de stress celular, levando ao consumo dos lípidos de reserva já acumulados, reduzindo assim a quantidade de lípidos de reserva nas células no final da fermentação. No entanto, elevadas produtividades em TFA (31.82 mg L⁻¹ h⁻¹) e em DHA (10.94 mg L⁻¹ h⁻¹) foram atingidas, o que evidencia que a extensão desta fermentação, através de adição de mais pulsos de nutrientes (hidrolisado de melão de cana-de-açúcar, extrato de levedura e CSL), permitiria um aumento na produção de biomassa e, conseqüentemente, na acumulação de lípidos. Deste modo, futuramente deverão ser realizadas novas fermentações em biorreator, permitindo avaliar se, de facto, o melão de cana-de-açúcar constitui uma fonte de baixo custo promissora como substrato para crescimento da microalga *C. cohnii*.

No Ensaio III foram novamente utilizados glicerol bruto e CSL como substratos, sendo atingida uma concentração em biomassa de 9.19 g L⁻¹, um teor de TFA de 24.07% (m/m), produtividade em TFA de 10.52 mg L⁻¹ h⁻¹ e produtividade em DHA de 5.57 mg L⁻¹ h⁻¹. Os resultados obtidos neste ensaio apresentaram-se como semelhantes aos obtidos no Ensaio I.

A utilização de substratos de baixo custo neste estudo, como glicerol bruto e CSL, para a produção de lípidos *C. cohnii* e DHA, pode representar até 84% na poupança de custos, relativamente ao uso de fontes convencionais como glucose e extrato de levedura. De facto, o custo médio da cultura pode

representar até 30% dos custos totais de produção das fermentações comerciais, o que significa que é importante encontrar medidas alternativas para reduzir este custo médio, sendo uma delas a utilização de substratos de baixo custo, tais como subprodutos industriais. Esta abordagem contribui não só para a redução dos custos globais deste bioprocessos, como também respeita a economia circular, baseada em três princípios: eliminar o desperdício e a poluição, reciclar produtos e materiais e regenerar a natureza.

A monitorização da fermentação de *C. cohnii* através de citometria do fluxo permitiu ainda concluir que o cultivo industrial desta microalga, utilizando fontes de carbono de baixo custo, não só é possível como tem pouco ou nenhum impacto negativo no crescimento das células, uma vez que foi possível verificar que as células permaneceram saudáveis, apresentando atividade enzimática e membrana celular intacta, ao longo dos ensaios realizados.

A extração de lípidos a partir da biomassa produzida em cada ensaio foi realizada através do método de extração acelerada com solvente (ASE) e do método convencional de extração por Soxhlet, sendo este último considerado no presente estudo como o processo de referência para a quantificação de lípidos. De modo geral, o rendimento em lípidos totais obtido através de extração por Soxhlet e ASE apresentou valores semelhantes para cada ensaio, o que é bastante vantajoso, uma vez que foi assim possível obter um mesmo rendimento em lípidos utilizando uma menor quantidade de biomassa e sendo consumido menos solvente, durante um reduzido tempo de extração.

A biomassa produzida nos Ensaios I e III foi submetida a uma reação de saponificação, permitindo formação de sabões de ácidos gordos, que foram convertidos em ésteres etílicos e, seguidamente, fracionados, através do método de complexação com ureia a diferentes temperaturas. A utilização de produtos químicos não tóxicos e sustentáveis do ponto de vista ambiental foi uma das principais preocupações desta investigação, uma vez que o principal objetivo da obtenção de uma fração lipídica rica em ácidos gordos polinsaturados (PUFA) se prende com o seu uso para consumo humano, através da sua aplicação nas indústrias alimentar, farmacêutica e cosmética. Deste modo, sendo o etanol um reagente menos tóxico do que o metanol, os ácidos gordos livres obtidos após a saponificação foram convertidos em ésteres etílicos de ácidos gordos (FAEE), antes de realizar o procedimento de cristalização com complexos de ureia.

Este método permitiu então a obtenção de uma fração rica em ésteres etílicos polinsaturados (potencialmente apropriada para utilização nas indústrias mencionadas) e uma fração rica em ésteres etílicos saturados e monoinsaturados (com potencial para produção de biodiesel). À temperatura de cristalização de -18°C, que permitiu obtenção de melhores resultados de entre as diferentes temperaturas de cristalização testadas, foi obtida uma fração lipídica com 91,6% de pureza em ésteres etílicos de DHA e uma outra fração com 88,0% de pureza de esterios etílicos saturados e monoinsaturados, no Ensaio I. No Ensaio III foi obtida uma fração com 69,91% de pureza em ésteres etílicos de DHA e uma fração com 97,4% de pureza de esterios etílicos saturados e monoinsaturados. No entanto, foi possível concluir que a taxa de recuperação de lípidos, para a soma de ambas as frações obtidas, atingiu um valor de cerca de 70%, o que indica que ocorreu perda de 30% de ésteres etílicos de ácidos gordos durante o processo. No futuro, para a obtenção de frações mais concentradas e para uma recuperação mais eficiente de todos os ésteres etílicos de ácidos gordos, deverá ser

estudado um passo alternativo para a separação das duas frações (em substituição da filtração) ou, por exemplo, o procedimento deverá ser modificado de modo a que seja realizado um maior número de lavagens utilizando n-hexano.

Por último, foram estimados os parâmetros físicos das frações para biodiesel, de um ponto de vista teórico, de modo a assegurar a sua viabilidade e verificar se as frações obtidas são adequadas e cumprem os requisitos definidos pela Norma Europeia EN 14214. Para tal, foram estimados valores teóricos para parâmetros como viscosidade, número de cetano, valor de iodeto e teor de ésteres de etílicos polinsaturados, através da utilização de correlações previamente estabelecidas e descritas na literatura. Deste modo, foi possível concluir que os parâmetros calculados se encontram em conformidade com as normas da União Europeia, com exceção do teor de ésteres etílicos polinsaturados, cuja percentagem se apresentou como superior ao limite estabelecido pela EN 14214. Consequentemente, de modo a permitir a utilização das frações lipídicas obtidas para a produção de biodiesel (ricas em ésteres etílicos saturados e monoinsaturados), deverá ser efetuado, por exemplo, um passo adicional de hidrogenação, a fim de reduzir a presença de ésteres etílicos polinsaturados para um nível inferior a 1% (m/m).

Os resultados obtidos permitiram concluir que o presente estudo aborda um método inovador e sustentável, a nível económico e ambiental, através da utilização de subprodutos industriais (substratos de baixo custo) para produção de DHA e biodiesel, num processo que permite a valorização de todos os compostos gerados no cultivo da microalga *C. cohnii*, não sendo gerados resíduos e respeitando a economia circular. Assim sendo, para avaliar a viabilidade prática e económica deste processo de biorrefinaria a nível industrial, o próximo passo será a realização futura de fermentações de *C. cohnii* em larga escala.

Table of Contents

Preface	ii
Abstract.....	iv
Resumo Alargado.....	vi
Table of Contents	ix
Index of Figures.....	xii
Index of Tables	xiv
Index of Symbols and Abbreviations	xv
1. Introduction.....	1
1.1. Lipid production by Oilseed Microalgae	1
1.2. Microalgal biomass biorefinery	2
1.2.1. Docosahexaenoic acid production.....	4
1.2.2. Biodiesel production	5
1.3. <i>Cryptocodinium cohnii</i>	7
1.3.1. <i>C. cohnii</i> growth conditions.....	8
1.4. Low-cost carbon sources	9
1.4.1. Sugarcane molasses	9
1.4.2. Crude glycerol.....	10
1.5. Flow Cytometry.....	11
1.6. Lipid extraction and fractionation.....	13
1.7. Applications of oil free microalgae biomass	14
1.8. Aims of the study	15
2. Methodology	16
2.1. Material and Equipment.....	16
2.2. Microorganism and Culture Maintenance.....	16
2.3. <i>C. cohnii</i> bioreactor fermentation conditions	16
2.4. Analysis and processing of complex substrates	18
2.4.1. Crude glycerol.....	18
2.4.2. Sugarcane Molasses	18
2.4.3. Corn Steep Liquor (CSL)	19
2.5. <i>C. cohnii</i> bioreactor culture monitoring.....	19

2.5.1. Microscopical observations.....	19
2.5.2. Dry cell weight measurements.....	19
2.5.3. Flow Cytometry	20
2.5.4. Carbon source quantification and consumption	20
2.5.5. Total nitrogen content determination	21
2.5.6. Moisture and ash contents.....	21
2.5.7. Fatty acid profile analysis	22
2.5.8. Calculation of kinetic parameters	23
2.6. <i>C. cohnii</i> biomass processing.....	23
2.7. Lipid extraction methods.....	24
2.7.1. Soxhlet extraction	24
2.7.2. Accelerated solvent extraction.....	25
2.8. Lipid fractionation with urea complexes	26
2.8.1. Saponification and ethylation.....	26
2.8.2. Urea complexation.....	26
2.9. Characterization of monounsaturated and saturated fractions	27
3. Results and Discussion	28
3.1. Assay I.....	28
3.1.1. <i>C. cohnii</i> bioreactor fermentation.....	28
3.1.2. <i>C. cohnii</i> biomass yield.....	36
3.1.3. Lipid extraction.....	37
3.1.4. Lipid fractionation with urea complexes.....	38
3.1.5. Evaluation of the fraction for biodiesel production.....	40
3.2. Assay II.....	42
3.2.1. <i>C. cohnii</i> bioreactor fermentation.....	42
3.2.2. <i>C. cohnii</i> biomass yield.....	50
3.2.3. Lipid extraction.....	51
3.3. Assay III.....	54
3.3.1. <i>C. cohnii</i> bioreactor fermentation.....	54
3.3.2. Lipid extraction.....	62
3.3.3. Lipid fractionation with urea complexes.....	63

3.3.4. Evaluation of the fraction for biodiesel production.....	66
3.4. Discussion of results obtained in this study	68
4. Conclusions and future prospects	72
References	75
Annex I – Materials and Reagents	79
Annex II – EU Standard for Biodiesel.....	80
Annex III – Calculation of the Specific Growth Rate	81
Annex IV – Calibration curves to determine carbon content in the culture medium by HPLC	82

Index of Figures

Figure 1 - Flow diagram of an heterotrophic biorefinery process.	3
Figure 2 - Chemical structure and ball-and-stick model of docosahexaenoic acid (DHA).	4
Figure 3 - Biodiesel production: transesterification reaction.	5
Figure 4 - Microscopical photographs of <i>C. Cohnii</i> : (a) 400x magnification; (b) 1000x magnification. The larger and immobile cysts can be observed near the centre with the smaller, motile cells surrounding it.	7
Figure 5 - Schematic diagram of flow cytometer.	11
Figure 6 – Flow cytometry: (a) Measurement of forward and side scatter; (b) Graphic representation of cells according to its size and complexity. Source: (CD Creative Diagnostics, 2022)	12
Figure 7 - Heterotrophic metabolism and applications of microalgae biomass.	14
Figure 8 - Bioreactor used in <i>C. cohnii</i> fermentations.	17
Figure 9 - Conventional Soxhlet extractor.	24
Figure 10 - Schematic view of accelerated solvent extraction system.	25
Figure 11 – <i>C. cohnii</i> cell count performed by flow cytometry and optical density (corrected) obtained in Assay I.	28
Figure 12 - Evolution of <i>C. cohnii</i> biomass concentration over time in Assay I.	29
Figure 13 - Natural logarithm profile of the biomass over time in Assay I.	29
Figure 14 - Glycerol concentration in the culture medium over time in Assay I.	30
Figure 15 - Speed rate and dissolved oxygen over time in Assay I.	31
Figure 16 - Total nitrogen concentration in the culture medium over time in Assay I.	32
Figure 17 - Total fatty acid content and productivity in Assay I.	33
Figure 18 - DHA content and productivity and other fatty acid content in Assay I.	34
Figure 19 - Controls used for the CFDA (FITC-A) and PI (PC5.5-A) staining: (a) Unstained healthy culture (autofluorescence); (b) Healthy culture stained with both CFDA and PI; (c) Culture stained with CFDA and PI after boiling water bath.	35
Figure 20 - <i>C. cohnii</i> cell subpopulations profiles for Assay I, after staining with CFDA and PI: subpopulation CFDA-/PI- includes cells with intact membrane and no enzymatic activity; subpopulation CFDA+/PI- includes cells with intact membrane and enzymatic activity; subpopulation CFDA+/PI+ includes cells with permeabilised membrane and enzymatic activity; subpopulation CFDA-/PI+ comprises cells with damaged membrane and no enzymatic activity.	36
Figure 21 - Fatty acids profile of total lipids extracted by ASE from biomass obtained in Assay I. The obtained values resulted from an average of 2 duplicates.	38
Figure 22 - Saturated, Monounsaturated and Polyunsaturated FAEE before and after urea crystallization of biomass obtained in Assay I, expressed in %(w/w) of total fatty acids ethyl esters. ...	39
Figure 23 - <i>C. cohnii</i> cell count performed by flow cytometry and optical density (corrected) obtained in Assay II.	42
Figure 24 - Evolution of <i>C. cohnii</i> biomass concentration over fermentation time in Assay II.	42
Figure 25 - Natural logarithm profile the biomass over time in Assay II.	43

Figure 26 - Glucose and fructose concentrations in the culture medium over time in Assay II.	44
Figure 27 - Speed rate and dissolved oxygen over time in Assay II.	45
Figure 28 - Total nitrogen concentration in the culture medium over time in Assay II.	46
Figure 29 - Total fatty acid content and productivity in Assay II.	48
Figure 30 - DHA content and productivity and other fatty acid content in Assay II.	49
Figure 31 – <i>C. cohnii</i> cell subpopulations profiles for Assay II, after staining with CFDA and PI: subpopulation CFDA-/PI includes cells with intact membrane and no enzymatic activity; subpopulation CFDA+/PI- includes cells with intact membrane and enzymatic activity; subpopulation CFDA+/PI+ includes cells with permeabilised membrane and enzymatic activity; subpopulation CFDA-/PI+ comprises cells with damaged membrane and no enzymatic activity.	50
Figure 32 - Fatty acids profile of total lipids extracted in Assay II: (a) Soxhlet Extraction; (b) ASE. The obtained values resulted from an average of 2 duplicates.	52
Figure 33 - <i>C. cohnii</i> cell count performed by flow cytometry and optical density (corrected) obtained in Assay III.	54
Figure 34 - Evolution of <i>C. cohnii</i> biomass concentration over fermentation time in Assay III.	55
Figure 35 - Natural logarithm profile of the biomass over time in Assay III.	55
Figure 36 - Glycerol concentration in the culture medium over time in Assay III.	56
Figure 37 - Speed rate and dissolved oxygen over time in Assay III.	56
Figure 38 - Total nitrogen concentration in the culture medium over time in Assay III.	58
Figure 39 - Total fatty acid content and productivity in Assay III.	59
Figure 40 - DHA content and productivity and other fatty acid content in Assay II.	60
Figure 41 - <i>C. cohnii</i> cell subpopulations profiles for Assay III, after staining with CFDA and PI: subpopulation CFDA-/PI includes cells with intact membrane and no enzymatic activity; subpopulation CFDA+/PI- includes cells with intact membrane and enzymatic activity; subpopulation CFDA+/PI+ includes cells with permeabilised membrane and enzymatic activity; subpopulation CFDA-/PI+ comprises cells with damaged membrane and no enzymatic activity.	61
Figure 42 - Fatty acids profile of total lipids extracted in Assay III: (a) Soxhlet Extraction; (b) ASE. The obtained values resulted from an average of 2 duplicates.	63
Figure 43 - Saturated, Monounsaturated and Polyunsaturated FAEE before and after urea crystallization of biomass obtained in Assay III, expressed in %(w/w) of total fatty acids ethyl esters.	64
Figure 44 - Recovery yields for the final FAEE fractions, obtained after urea crystallization at -18°C in Assay III, relatively to the initial ethyl esters mixture before urea addition.	65
Figure 45 - Natural logarithm of dry cell weight (DCW) of the assays over fermentation time for the points used to calculate specific growth rate, along with the trendlines used.	81
Figure 46 - Calibration curve for glycerol.	82
Figure 47 - Calibration curves for glucose and fructose.	82

Index of Tables

Table 1 - Main ω -3 polyunsaturated fatty acids.	2
Table 2 - Crude glycerol composition in percentage (w/w).	18
Table 3 - Distribution of the most important fatty acids detected over fermentation time in Assay I, as percentage of total fatty acids (%(w/w) TFA). The obtained values resulted from an average of 2 duplicates.	32
Table 4 - Results obtained by ASE and Soxhlet extraction method, using hexane as solvent. The yields in total lipids, TFA, DHA and fatty acids for biodiesel production are presented in g/100g of dry biomass and without ash. The obtained values resulted from an average of 2 duplicates.	37
Table 5 – <i>C. cohnii</i> FAEE % (w/w) in total fatty acid ethyl esters before and after crystallization with urea complexes of biomass obtained in Assay I. The obtained values resulted from an average of 2 duplicates.	39
Table 6 - Theoretical estimate of FAEE quality for biodiesel production, according to EN 14214. The obtained values were determined through the Average Unsaturation (AU) calculation.	41
Table 7 - Distribution of the most important fatty acids detected over fermentation time in Assay II, as percentage of total fatty acids (%(w/w) TFA). The obtained values resulted from an average of 2 duplicates.	47
Table 8 - Results obtained by ASE and Soxhlet extraction method, using hexane as solvent. The yields in total lipids, TFA, DHA and fatty acids for biodiesel production are presented in g/100g of dry biomass and without ash. The obtained values resulted from an average of 2 duplicates.	51
Table 9 - Distribution of the most important fatty acids detected over fermentation time in Assay III, as percentage of total fatty acids (%(w/w) TFA). The obtained values resulted from an average of 2 duplicates.	58
Table 10 - Results obtained by ASE and Soxhlet extraction method, using hexane as solvent. The yields in total lipids, TFA, DHA and fatty acids for biodiesel production are presented in g/100g of dry biomass and without ash. The obtained values resulted from an average of 2 duplicates.	62
Table 11 - <i>C. cohnii</i> FAEE % (w/w) in total fatty acid ethyl esters before and after crystallization with urea complexes of biomass obtained in Assay III. The obtained values resulted from an average of 3 triplicates.	64
Table 12 - Theoretical estimate of FAEE quality for biodiesel production, according to EN 14214. The obtained values were determined through the Average Unsaturation (AU) calculation.	66
Table 13 - Summary table of the conditions and results obtained in previous studies, reported in the literature, in which <i>C. cohnii</i> cultivations were conducted with a view to DHA production and the results attained in the present study (Assays I, II and III).	69
Table 14 - Materials and reagents used in this work.	79
Table 15 - Requirements of biodiesel properties according to the European standard EN 14214.	80
Table 16 - Specific growth rate, calculated standard deviation and coefficient of determination (R^2) for each assay.	81
Table 17 - Glycerol, glucose and fructose correlations.	83

Index of Symbols and Abbreviations

μ	Specific growth rate
ALA	α -linolenic acid (Lipid number 18:3 ω 3)
ASE	Accelerated Solvent Extraction
ATCC	American Type Culture Collection
AU	Average Unsaturation
CFDA	Carbofluorescein diacetate (Dye used in flow cytometer)
CSL	Corn Steep Liquor (Low-cost nitrogen source)
DAD	Diod Array Detector (HPLC detector)
DCW	Dry Cell Weight (Volumetric concentration of biomass)
DHA	Docosahexaenoic acid (Lipid number 22:6 ω 3)
DMSO	Dimethyl sulfoxide
DO	Dissolved Oxygen
DPA	Docosapentaenoic (Lipid number 22:5 ω 3)
EPA	Eicosapentaenoic (Lipid number 20:5 ω 3)
FAEE	Fatty Acid Ethyl Ester (Class of molecules similar to fatty acids that have the carboxylic acid (-OOH) group replaced with a -OOC ₂ H ₅ radical and that are the result of the ethylation reaction of triglycerides using ethanol)
FA _{<i>i</i>}	Fatty acid <i>i</i>
FAME	Fatty Acid Methyl Ester (Class of molecules similar to fatty acids that have the carboxylic acid (-OOH) group replaced with a -OOCH ₃ radical and that are the result of the transmethylation reaction of triglycerides using methanol)
FITC-A	Flow cytometry fluorescence detector
FSC	Forward Scatter (Flow cytometry dispersion detector)
GLY	Crude Glycerol (Low-cost carbon source)
HPLC	High Performance Liquid Chromatography
PBS	Phosphate buffered saline
PC5.5-A	Flow cytometry fluorescence detector
PI	Propidium iodide (Dye used in flow cytometer)
PUFA	Polyunsaturated Fatty Acid (Fatty acids with more than one double bond in their carbon chain)
RI	Refractive Index Detector (HPLC detector)
SDA	Stearidonic (Lipid number 18:4 ω 3)
SM	Sugarcane Molasses (Low-cost carbon source)
SSC	Side Scatter (Flow cytometry dispersion detector)
TFA	Total fatty acids
X:Y ω Z	Lipid number used as nomenclature for fatty acids. X is the length of carbon chain atoms; Y is the number of double bonds in the carbon chain; Z is the position of the first unsaturated carbon from the methyl (CH ₃) end of the fatty acid chain.
YE	Yeast Extract

1. Introduction

1.1. Lipid production by Oilseed Microalgae

Microalgae are microorganisms that have complex metabolic capacity and great strength and versatility, presenting high potential for the food and pharmaceutical industries, reasons why they are currently widely studied. The fact that they have a fast growth rate, high productivity in biomass and the ability to synthesize complex metabolites with minimal resources are some of their main advantages. The wide biochemical diversity among the various species of microalgae makes them a resource of biomolecules with high industrial and biomedical importance. Thus, microalgae have been continuously exploited to the production of a wide range of molecular compounds, which have industrial interest, such as carbohydrates, proteins, pigments and lipids (Kumar, et al., 2020).

Microalgae may have autotrophic, heterotrophic or mixotrophic metabolisms. Autotrophic microalgae use carbon dioxide as carbon source and require light to grow, while heterotrophic microalgae do not require light and use organic carbon for their development (Lopes da Silva, et al., 2021). In most research about the production of biofuels and value-added products, there are used autotrophic microalgae, however, heterotrophic microalgae can have particular interest in countries located at higher latitudes, such as European countries, since their cultivation does not imply light supply and does not depend on weather factors. In addition, heterotrophic microalgae crops are carried out in conventional fermenters, under sterility conditions, being less prone to microbial contamination than autotrophic crops, which are conducted outdoors. The development of heterotrophic microalgae also leads to higher productivity in biomass and lipids, when compared to the production of autotrophic microalgae. It is also important to note that in most cases the maintenance of heterotrophic cultivation systems is cheaper, easier to conduct on a large scale and the facilities are simpler to construct (Lopes da Silva, Moniz, & Reis, 2020). Some of the heterotrophic microalgae produce high lipid contents that can be extracted and fractionated into ω -3 compounds, with interest in several industries, and biodiesel, in an approach based on the concept of algal biomass biorefinery, which is in line with the objective of this work.

The lipid content produced by oilseed microalgae include polyunsaturated fatty acids (PUFA), that constitute a large group of unsaturated fatty acids containing long-chain carbonic molecules, including ω -3 polyunsaturated fatty acids. This family is based on the position of the first double bond from the methyl end group in the fatty acid chain (Remize, et al., 2021).

PUFA, particularly ω -3 polyunsaturated fatty acids, are essential to human organism and they are obtained exclusively from the food ingested in the diet, since the organism cannot synthesize *de novo* ω -3 PUFA or produce them from their precursors in enough quantities. The essential role played by ω -3 PUFA in the organism is recognized for the beneficial effects related to the maintenance of normal blood pressure and triglyceride levels, prevention of cardiovascular diseases and for the development of infant brain and visual systems (Castejón, Luna, & Senorans, 2021). Table 1 shows the main ω -3 polyunsaturated fatty acids. These are considered essential fatty acids, since they cannot be synthesized by all organisms (Remize, et al., 2021).

Table 1 - Main ω -3 polyunsaturated fatty acids.

Type	Common name	Carbon number	Double bonds C-C	Formula
ω-3 polyunsaturated fatty acids	α -Linoleic	18	3	C18:3 ω 3
	Stearidonic	18	4	C18:4 ω 3
	EPA	20	5	C20:5 ω 3
	DPA	22	5	C22:5 ω 3
	DHA	22	6	C22:6 ω 3

The ω -3 linolenic acid (ALA, 18:2 ω 6) is considered an essential fatty acid from which all other ω -3 polyunsaturated fatty acids result metabolically. This fatty acid can be converted by elongation and desaturation pathways, in the human body, into bioactive acids such as stearidonic (SDA, 18:4 ω 3), eicosapentaenoic (EPA, 20:5 ω 3), docosapentaenoic (DPA, 22:5 ω 3) and docosahexaenoic (DHA, 22:6 ω 3). Due to their role in human nutrition and disease prevention, DHA and EPA are considered the most important polyunsaturated fatty acids (Mendes, Lopes da Silva, & Reis, 2007). DHA, in particular, has several applications in pharmaceutical, nutraceutical, biomedicine and food industries, as it has several benefits in human health.

The percentage of DHA produced by microalgae depends on the species and on the productivity rate and the growth conditions of the microorganism. Microalgae richer in DHA consequently present a higher nutritional value for consumers than microalgae with lower ω -3 PUFA levels (Remize, et al., 2021). The large-scale production of these ω -3 PUFA from microalgae is possible using heterotrophic microalgae, in conventional fermentation systems, that allow the production of biomass under highly controlled and monitored conditions, resulting in a high-quality product (Sharma, Sarmah, & Bishnoi, 2020). Therefore, the demand for heterotrophic microalgae is of potential importance, in order to achieve high biomass concentrations and higher productivity in polyunsaturated fatty acids such as DHA.

1.2. Microalgal biomass biorefinery

Oilseed microalgae produce intracellular oils above 20% of their dry weight, enriched in PUFA, such as DHA, for animal supplementation and human diet, and rich in saturated and monounsaturated fatty acids, that can be extracted and converted into biofuels, such as biodiesel. Besides, these microalgae can be used to produce a variety of valuable products such as pigments, proteins, carbohydrates, biofuels and biofertilizers that are object of interest in diverse industries such as food, pharmaceutical, nutraceutical, cosmetic and chemical, as real biorefinery alternatives (Lopes da Silva, et al., 2021).

However, the cost of the DHA products derived from microorganisms is still high, limiting their wide applications (Horrocks & Yeo, 1999). Also, it is important to consider that biodiesel obtained by microbial route is not yet economically sustainable, also presenting high production costs, which are not competitive with current fossil fuel prices. Therefore, it is essential to consider new approaches to circumvent the high costs associated with the process of production and extraction of lipids from microalgae (Lopes da Silva, et al., 2019).

Currently, microalgae have become increasingly important due to their ability to produce value-added compounds from low-cost resources such as by-products or industrial effluents. Thus, a way to reduce the costs of this process consists in the use of low-cost substrates in the culture medium, for the development of microalgae, such as industrial or domestic effluents and industrial wastes or by-products. The development of microalgae for production of compounds with commercial interest from these wastes and effluents also aims at the removal of pollutants, contributing to the sustainability and development of the world bioeconomy (Lopes da Silva, et al., 2021).

Another approach to reduce the costs of DHA and biodiesel production of microbial origin is by using all the several products synthesized by microalgae, maximizing the value of the entire process, allowing waste reduction, in a biorefinery concept applied to the biomass of microalgae. Therefore, the economic value of the whole process is increased, and several value-added products are obtained from the same raw material – not only DHA and biodiesel, but also pigments, carotenoids, proteins and carbohydrates. This approach makes it possible to take advantage of the total microalgal biomass and the various products synthesized by its cells, maximizing the value derived from the whole process, considering concepts of circular economy (Kumar, et al., 2020). Figure 1 shows the biorefinery process flow diagram of an oilseed microalga, with heterotrophic metabolism, to the production of ω -3 compounds of added value and biodiesel.

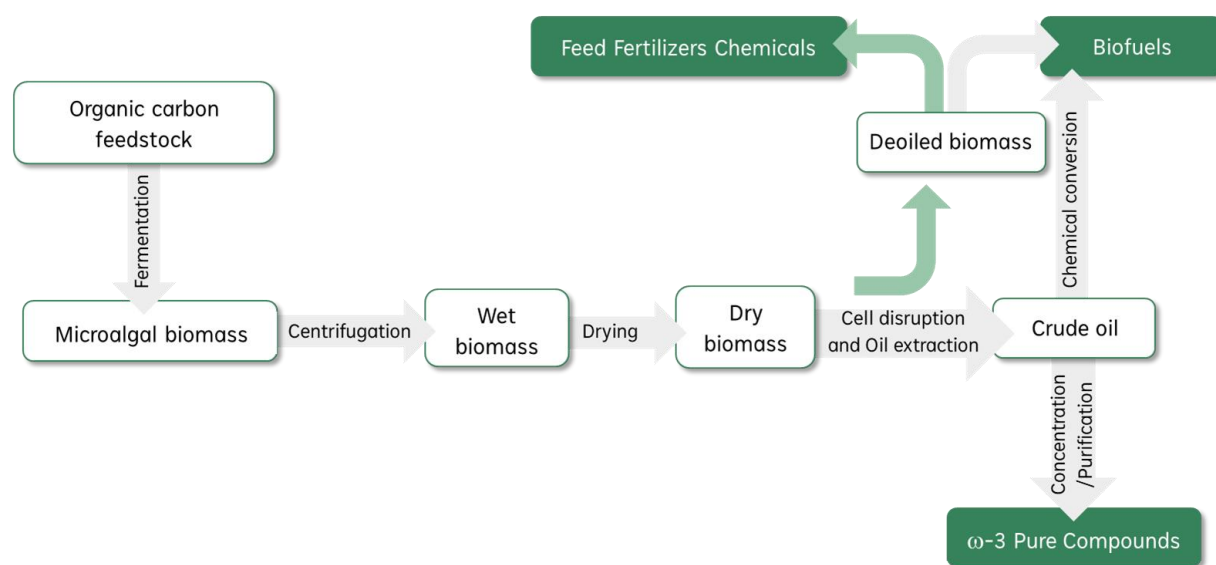


Figure 1 - Flow diagram of an heterotrophic biorefinery process.

Source: (Lopes da Silva, et al., 2019) - Adapted

1.2.1. Docosahexaenoic acid production

Docosahexaenoic acid (DHA), lipid number 22:6 ω 3, is a long chain ω -3 PUFA with 22 carbon atoms and 6 double bonds in its fatty acid chain. Figure 2 shows the representation of the docosahexaenoic acid molecule.

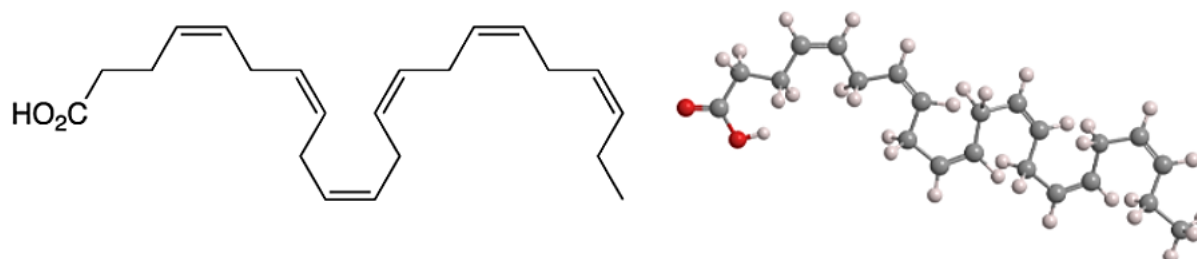


Figure 2 - Chemical structure and ball-and-stick model of docosahexaenoic acid (DHA).

Source: (American Chemistry for Life, 2020)

DHA resulting from microalgae metabolism is of high interest to the pharmaceutical, food and biomedicine industries, as it has benefits in human health, playing an important role in membrane fluidity and cell metabolism and transport mechanisms (Swanson, Block, & Mousa, 2012). It is a particularly important ω -3 fatty acid, that is a major component of brain phospholipids and the retina, being essential for the growth and functional development of the brain in infants. Besides, this molecule is also required for preservation of normal brain cells function in adults (Horrocks & Yeo, 1999). This PUFA is an important component of the brain and nervous system, performing various neurological functions such as neurogenesis, neurotransmission and protection against oxidative stress-induced brain damage (Taborda, et al., 2021). Also, DHA is highly used in the treatment of cardiovascular diseases, such as atherosclerosis, diabetes, cancer, rheumatoid arthritis, Alzheimer's or psoriasis (Lopes da Silva, et al., 2019).

DHA is a ω -3 PUFA that acts on the cell membranes of nervous, visual and reproductive tissues, being considered essential for the visual and neurological development of children and it is present, for example, in breast milk. Consequently, one of the main uses of this PUFA is its incorporation into infant formulations (Mendes, et al., 2007). The use of DHA has increased following several research reports, claiming that many babies fed with formulated milks have lower levels of docosahexaenoic acid and arachidonic acid compared to babies who are breastfed, so these compounds have been introduced into these types of food formulations. Thus, there was an overall increase in the market for the production of DHA by microalgae, associated with the growing public awareness of health care and chronic diseases, which led to the expansion of DHA applications and the emergence of greater regulation on this compound uses, supporting its use in infant formulations (Lopes da Silva, et al., 2019).

Traditionally, the main sources of ω -3 PUFA, such as DHA, are oils extracted from fish species such as herring, mackerel, sardines or salmon (Lopes da Silva, Moniz, & Reis, 2020). However, the extraction of these fatty acids from fish oil presents some disadvantages, such as the fact that the world's fish stocks are in decline and cannot guarantee, in a sustainable and long-term way, the production of these compounds. Another problem is the quality of the extracted oil, which can be variable according to fish species, the season and the place where the fish is caught. It should also be noted that fish oil usually has an unpleasant odor and may be contaminated with polychlorinated biphenyls or heavy metals,

whose presence prohibits its incorporation into pharmaceutical and food formulations (Lopes da Silva, et al., 2019). In addition, fish oil consists of a complex mixture of fatty acids with different saturation degrees and chain lengths, so it is necessary to proceed to a purification method to obtain DHA, which makes the process more expensive (Lopes da Silva, et al., 2019). It is considered that the use of microalgal biomass for lipid production has several advantages over the traditional methods, being more suitable for the extraction and purification of DHA, since the extracted oil is free of cholesterol and contaminants and has a taste that is highly appreciated and less intense (Mendes, Lopes da Silva, & Reis, 2007).

Given that the most prevalent sources of DHA are from animal origin, people following a vegetarian or vegan diet often consume little to no DHA. Although the health impact of the absence of DHA in adults is not yet established, it should be noted that it is very likely to impact fetal and pos-natal development in children of vegan mothers (Sanders, 2009). Therefore, it is fundamental that DHA from vegetarian and vegan-compatible sources, namely microalgae oil, becomes widespread in infant formula and in supplements for adults.

1.2.2. Biodiesel production

Considering the existing paradigm of increasing concerns towards our petrol-based economy and its impact on the global climate, biodiesel is a resource with great interest and it can be a solution to reduce the amount of carbon dioxide discharged into the atmosphere, contributing to reduce the greenhouse gas emissions (Ma & Hanna, 1999).

Biodiesel it's the name given to long-chain alkyl esters, usually methyl esters, produced from renewable lipid sources such as vegetable oils, animal fats or lipids from microorganisms, for use as a more environmentally friendly substitute for conventional petrol-based diesel fuel (petrodiesel). It is biodegradable and nontoxic, has low emission profiles and so is environmentally beneficial. It is produced by chemical reaction (transesterification or esterification) between lipids and an alcohol, usually methanol but ethanol can also be used, to produce lipid esters of that alcohol, as shown in Figure 3. When using methanol, these are called fatty acid methyl esters (FAME) and when using ethanol these are called fatty acid ethyl esters (FAEE).

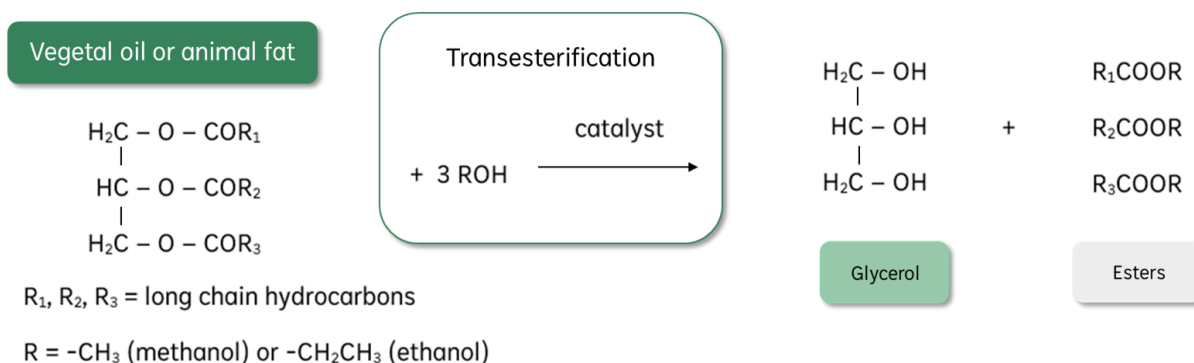


Figure 3 - Biodiesel production: transesterification reaction.
Source: (Leoneti, Araújo-Leoneti, & Oliveira, 2012) - Adapted

The use of non-toxic and environmentally friendly chemicals was a major concern in this research, given that the main aim of the present study was to produce PUFA for human consumption. Thus, given that ethanol is less toxic than methanol, lipids produced for biodiesel purposes may undergo an ethylation process, resulting in FAEE (Cardoso, et al., 2019) (Brunschwig, Mossavou, & Blin, 2012).

Since the chemical properties of biodiesel are very similar to those of petrodiesel, it can be used in conventional diesel engines, pure or in any ratio with the latter, with little or no prior modification of the engine (Ma & Hanna, 1999). However, the carbon footprint of biodiesel is contested and highly variable depending on its source. Biodiesel produced from vegetable oils should be near carbon neutral, as the source of the carbon in the biodiesel molecules is the carbon dioxide removed directly from the atmosphere by the photosynthetic organisms producing the lipids. Even so, the manufacturing process, transportation of the product, plant materials not converted to oil, raw materials like methanol (most of which comes from petrol) and side-products from the lipid-to-oil conversion (glycerol) should be considered when determining the overall eco-friendliness of this biofuel, since these production steps have negative impact on the environment. Additionally, the waste produced during oils production would also have to be accounted for (Fargione, et al., 2008).

Several social impacts are associated with biodiesel production from vegetable oils, namely in food supply and in food prices, and also environmental concerns with water consumption and soil quality (Ho, Ngo, & Guo, 2014). In response to these concerns, alternative biodiesel sources have been studied, including microalgae oil. When comparing to other plant oils, microbial oils have many advantages, such as short life cycle, less labor required, present more resistance to climate changes and easier to scale up. Besides, the effluents generated by microalgae production are less aggressive when compared to fossil fuels. This rapid expansion of biodiesel over the years, enabled microbial oils to become one of potential oil feedstocks for biodiesel production in the future (Li, Du, & Liu, 2008). Microalgae are very versatile microorganisms that can provide several different types of renewable biofuels, that include not only biodiesel derived from microalgal oil, but also methane produced by anaerobic digestion of the algal biomass and photobiologically produced biohydrogen (Chisti, 2007). Nevertheless, as already mentioned, biodiesel obtained by microbial route is not yet economically sustainable, presenting high production costs, which are not competitive with current fossil fuel prices. The only way for this process to be sustainable and achievable is by using the various products synthesized by microalgae, maximizing the value of the entire process, allowing waste reduction, in a biorefinery concept applied to the biomass of microalgae.

Biodiesel standards

The European Union specifies in its standard EN 14214 the requirements and test methods for FAME to be used as biodiesel. In order to biodiesel produced be used as a substitute for a fuel derived from petroleum, it is important that the final product does not contain any chemical residue (such as a secondary product or a catalyst). Properties such as viscosity, cetane number, density, iodine value and specific gravity, must be within the parameters presented in the standard EN 14214.

Viscosity is the resistance of a fluid to deformation at a given rate, having influence in the operation of injecting fuel into the equipment and dispersing it. This property is related to the fatty acids unsaturation, since higher unsaturation corresponds to lower viscosity. A given diesel's viscosity is a

fundamental parameter to determine its quality, considering that it affects the injector lubrication and the atomization of the fuel. A fuel with low viscosity may not provide sufficient lubrication of the fuel injection pumps, resulting in leakage and potential power loss. On the other hand, a fuel with a high viscosity may stop the pump from providing enough fuel to fill the pumping chamber, also resulting in power loss (Pratas, et al., 2011).

The cetane number is a measure of diesel's ignition capability and one of the most important factors for determining the quality of the fuel. Cetane is a hydrocarbon which easily ignites under pressure and is thus given a cetane number of 100, serving as the baseline against which all diesel is compared to. A high cetane number translates into smoother running and better performing engine.

Density is an important diesel property, since injection systems, pumps and injectors must deliver a precise amount of fuel to provide proper combustion. The specific gravity is related to density and corresponds to the weight of a substance when comparing to water, at a specified constant temperature (4°C), being related to the ease of outflow of a fluid.

The iodine value verifies the unsaturation of the oil, allowing the evaluation of the tendency for oxidation of the fuel. The higher the unsaturation, the higher the iodine content. The existence of double bonds in the chemical structure of FAME has a negative impact on the oxidative stability of biodiesel, so the standard EN 14213 defined a maximum limit of 12% of linolenic acid (C18:3) (Islam, Heimann, & Brown, 2017).

Table 15 in Annex II contains the requirements of several biodiesel properties according to the standard EN 14214.

1.3. *Cryptocodinium cohnii*

Currently the most used microalgae for ω -3 lipid production belong to *Thraustochytriaceae* and *Cryptocodiniaceae*, which are found in the oceans. Among the various dinoflagellate marine microalgae, *Cryptocodinium cohnii* has been identified as an interesting source for DHA production, being *Cryptocodinium* a genus of the *Cryptocodiniaceae* family. This marine microalga is represented in Figure 4.

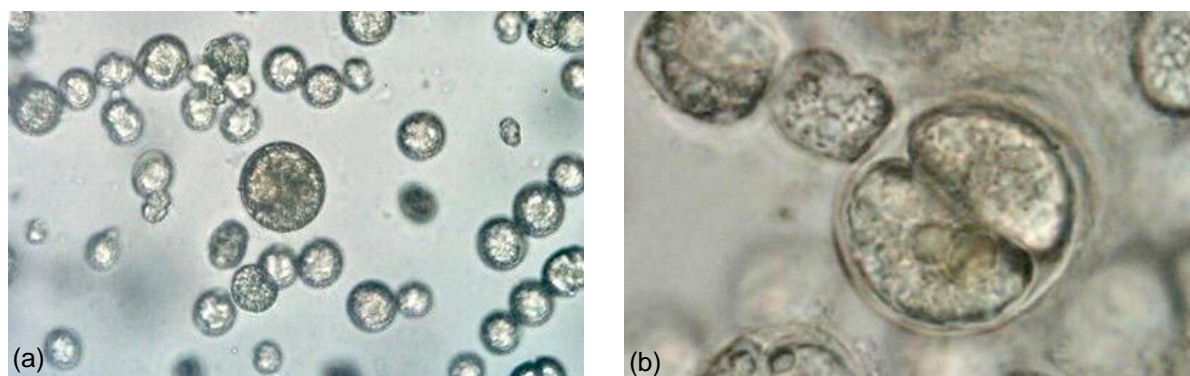


Figure 4 - Microscopical photographs of *C. Cohnii*: (a) 400x magnification; (b) 1000x magnification. The larger and immobile cysts can be observed near the centre with the smaller, motile cells surrounding it.

Cryptocodinium cohnii is a marine heterotrophic dinoflagellate that is widespread in tropical and temperate waters worldwide, having the ability to grow in environments with no light, using only a substrate rich in organic carbon as carbon source. It is a complex species with multiple isolated sibling

species that are otherwise indistinguishable by their morphology. In Nature, they appear to feed on decomposing macrophytes (marine macroalgae), especially the *Fucus spp* (Beam & Himes, 1982).

C. cohnii cells can be found in different forms: motile, swimming cells and cysts, with different dimensions. Cysts can either stand dormant or divide into 2 to 8 daughter cells. The motile cells have two unequal flagella, one is flat and encircles the cell in a transverse groove and provides propulsion and spinning force and the other is longitudinal and presumably works as a rudder for steering (Mendes, et al., 2008).

This oilseed microalga is capable of producing significant amounts of lipids (20 to 50% of their cell weight), namely DHA, which constitutes about 30 to 50% of the total fatty acid content and no other polyunsaturated fatty acid above 1% is present. Therefore, the extraction and purification of DHA is simpler and involves less costs (Mendes, Lopes da Silva, & Reis, 2007). The lipid fraction remaining from production and extraction of DHA is frequently neglected, however, this fraction, obtained after DHA removal, is mainly composed of saturated and monounsaturated fatty acids that can be used for biodiesel production: capric acid (10:0), lauric acid (12:0), myristic acid (14:0), palmitic acid (16:0), stearic acid (18:0), linoleic acid (18:2 ω 6) and oleic acid (18:1 ω 9). This way, all microalgal lipidic fractions can be valorized and used.

1.3.1. *C. cohnii* growth conditions

The fermentation of *C. cohnii* crops has been studied in laboratory since the beginning of the 20th century and several variables have been studied for the optimal growth of this microorganism. Its growth can be carried out in both liquid and solid culture medium, by adding a carbon source and a source of nitrogen and other nutrients. In addition, the development of a high cell density culture of *C. cohnii* depends on conditions such as the substrate used and its concentration, incubation temperature, oxygen supply, pH, salinity and luminosity (Mendes, et al., 2007). At an experimental level, several studies have been conducted that test various conditions of cultivation of this microalga, in order to optimize its growth and consequent production and accumulation of DHA (Mendes, et al., 2008).

C. cohnii grows in several different carbon sources, including glucose, acetic acid or acetate, ethanol, glycerol, sucrose, galactose and complex sources such as crude glycerol, rapeseed meal hydrolysate supplemented with waste molasses, cheese whey and carob pulp (Taborda, et al., 2021) (Gong, et al., 2015) (Isleten-Hosoglu & Elibol, 2017) (Asimakopoulou, et al., 2021). Growth of this microalga was not observed when using carbon sources such as fructose, maltose, rhamnose, arabinose, lactose, galacturonic acid and aldose (Mendes, et al., 2008).

To encourage high productivity in DHA, fermentation medium also includes a complex organic nitrogen source, such as yeast extract and inorganic salts, like ammonium sulfate ((NH₄)₂SO₄), glutamic acid (NH₄HCO₃), urea ((NH₂)₂CO) and sodium nitrate (NaNO₃) (Safdar, et al., 2017). Corn steep liquor (CSL) has also been identified as a potential nitrogen source in biochemical industries and a good substitute for other expensive complex medium. It is a major by-product found during corn starch processing (Zhou, et al., 2022).

As a marine species, this microalga also needs sodium chloride and other inorganic salts for its optimal growth, that must be added to the growth medium when performing a fermentation. Although

there is no exact optimal salt concentration, concentrations between 16 and 29 g L⁻¹ of salt have no relevant impact on cell growth (Isleten-Hosoglu & Elibol, 2017).

The ideal pH for *C. cohnii* is in the range of 6 to 7, with the maximum growth rate obtained at pH 6.5 (Safdar, et al., 2017). The range of optimal temperature is between 25 and 30°C (Safdar, et al., 2017). Also, for efficient oxygen supply, moderate agitation is needed (from 100 to 200 rpm), since *C. cohnii* is an obligate aerobic organism (Mendes, et al., 2008). All these parameters can be variable depending on the *C. cohnii* strain used.

The *C. cohnii* fermentation process can be performed in batch, however, in the present study, it was processed in fed-batch, a semi-continuous process, that is carried out in two phases, in order to enhance cell and lipid production. The first phase consists of the active growth of the microalgae in conditions of excess nutrients, allowing cell proliferation, and during this phase the lipid content is only about 20% of the dry weight and the carbon supplied is directed to cell division. Once the nitrogen source is exhausted, carbon is continuously supplied to the fermenter. The lack of nitrogen for the production of *de novo* proteins and nucleotides will disrupt cell growth and division and the carbon that is supplied is converted into storage lipids, DHA-rich triglycerides. Then, a second phase is followed, consisting of the accumulation of lipids produced by *C. cohnii* cells. The maintenance of carbon concentration is an important factor in optimizing lipid accumulation, not only to promote its synthesis, but also to avoid the use of these reserve lipids by cells (Lopes da Silva, et al., 2019).

Several authors reported different results, when performing *C. cohnii* fermentations, using different carbon sources. In each of them, different biomass concentrations and variable growth rates were obtained. Safdar, et al. (2017) have grown *C. cohnii* in 1L and 5L fermenters using glucose as carbon source, obtaining biomass concentrations up to 15.82 g L⁻¹ DCW and growth rates of 212 mg L⁻¹ h⁻¹). Ratledge, et al. (2001) obtained biomass concentrations of 30 g L⁻¹, in a bioreactor of 3.5L, by performing fed-batch cultivations with acetic acid as carbon source. De Swaaf, Sijtsma, & Pronk (2003) fermented with glucose, ethanol and yeast extract, in 2L fed-batch cultivation, attaining 83 g L⁻¹ DCW when using ethanol, the highest biomass concentration biomass reported at time.

1.4. Low-cost carbon sources

To reduce the costs of the microalgae biomass production process and, consequently, turning this process into a competitive alternative, low-cost carbon sources have been studied. Low-cost carbon sources resulting from industrial waste are of particular interest, such as sugarcane molasses, a by-product of sugarcane sugar industry, or crude glycerol, a by-product of biodiesel production industry, which were both used in this study for *C. cohnii* growth (Lopes da Silva, et al., 2021).

1.4.1. Sugarcane molasses

Sugarcane molasses is a thick, dark, sweet syrup, that is a valuable agro-industrial by-product of the refinement of sugar obtained from sugar beet or sugar cane. It is an inevitable side product of the crystallization process used to obtain the sucrose crystals that make table sugar. Molasses contains unextractable sugar, vitamins and minerals, such as calcium, sodium, potassium and magnesium (Nikodinovic-Runic, et al., 2013). Molasses is used as a soil fertilizer, a cattle feed supplement, in

specialized yeast fermentations, as a flavoring agent in some foods or as a feedstock for bioethanol production in specialized distilleries. As a result of price fluctuations and the difficulty of storing molasses, international trade of this product is rather limited (Nikodinovic-Runic, et al., 2013). Despite this, the production of excess molasses as a residue from sugar processing is still occurring resulting in waste management costs. Thus, the use of molasses as a carbon feedstock for the propagation of various microorganisms, such as *C. cohnii*, is a good alternative to the disposal of molasses. Since sugarcane molasses contain mostly sucrose in its composition, a previous hydrolysis of this carbon source into fructose and glucose is necessary, given that the latter is the preferred substrate for growth of this microalga. Fructose is not consumed at all by this microorganism.

The first study using molasses as the only carbon source for *C. cohnii* fermentation was recently conducted, by Taborda, et al. (2021), where its use was compared to glucose, acetate, pure glycerol and crude glycerol. In this study, the maximum biomass concentration achieved when using sugarcane molasses was 3.91 g L⁻¹ and the lipid and DHA content obtained were 11.12% (w/w DCW) and 5.51% (w/w DCW), respectively.

1.4.2. Crude glycerol

Crude glycerol is a by-product of biodiesel industry, as observed previously in Figure 3, independently of the used source of lipids. Cells store lipids as triglycerides, which are three fatty acids attached to a glycerol backbone by ester bonds. Biodiesel is produced through transesterification and in this chemical reaction the bonds between fatty acids and glycerol are destroyed. During this process, the fatty acids are transformed into methyl esters (FAME) or ethyl esters (FAEE), while the now free glycerol is separated from the biodiesel (Li, Du, & Liu, 2008).

Crude glycerol's chemical composition is primarily determined by the type of catalyst used to produce biodiesel, the transesterification efficiency, the biodiesel recovery efficiency and other impurities in the feedstock (Yang, Hanna, & Sun, 2012). Its major components are glycerol (25-95% w/w), water (up to 15%), salts (up to 5%) and methanol/ethanol (up to 10%). At present, crude glycerol is of little economic value due to the presence of various impurities such soaps, FAME or FAEE and alkaline catalyst residues and its purification is a complex process (Hu, et al., 2012).

Therefore, crude glycerol can be used for animal feedstuff, as feedstock for various chemicals and for the propagation of various microorganisms to produce various high-value products. Thus, the use of crude glycerol as a carbon feedstock for the propagation of various microorganisms, such as *C. cohnii*, for DHA and biodiesel production, is a good alternative to the disposal of glycerol, thus reducing waste and promoting circular economy.

In the same study mentioned previously by Taborda, et al. (2021), the maximum biomass concentration achieved when using crude glycerol was 5.05 g L⁻¹ and the lipid and DHA content obtained were 14.7% (w/w DCW) and 7.15% (w/w DCW), respectively.

1.5. Flow Cytometry

In most works reporting microalgae lipid production from heterotrophic microalgae, culture development is usually monitored using traditional methods such as optical density, dry cell weight and cell counting. Nevertheless, these techniques provide no information about the physiological state of the microorganism cells (Lopes da Silva, et al., 2019).

Flow cytometry is an advanced technique for bioprocess monitoring that gives near real-time information on several cell functions and compartments at the individual cell level. This is an efficient method that allows not only the evaluation of culture cellular growth, but also other physiological characteristics such as enzymatic and respiratory activities, intracellular pH or cellular membrane integrity. This technique allows the development of more efficient bioprocess control strategies and, consequently, the achievement of highest product yields and optimal process performance (Lopes da Silva, et al., 2021). Besides, microalgae cells are ideal for flow cytometric analysis since they are unicellular and larger than most microorganisms, being easily differentiated from the background and noise.

The flow cytometer is a system constituted by a light source (laser), a flow chamber, an optical filter unit, signal detectors (dispersion and fluorescence detectors) and an electronic processing unit for the collected data. Figure 5 shows a diagram of the equipment.

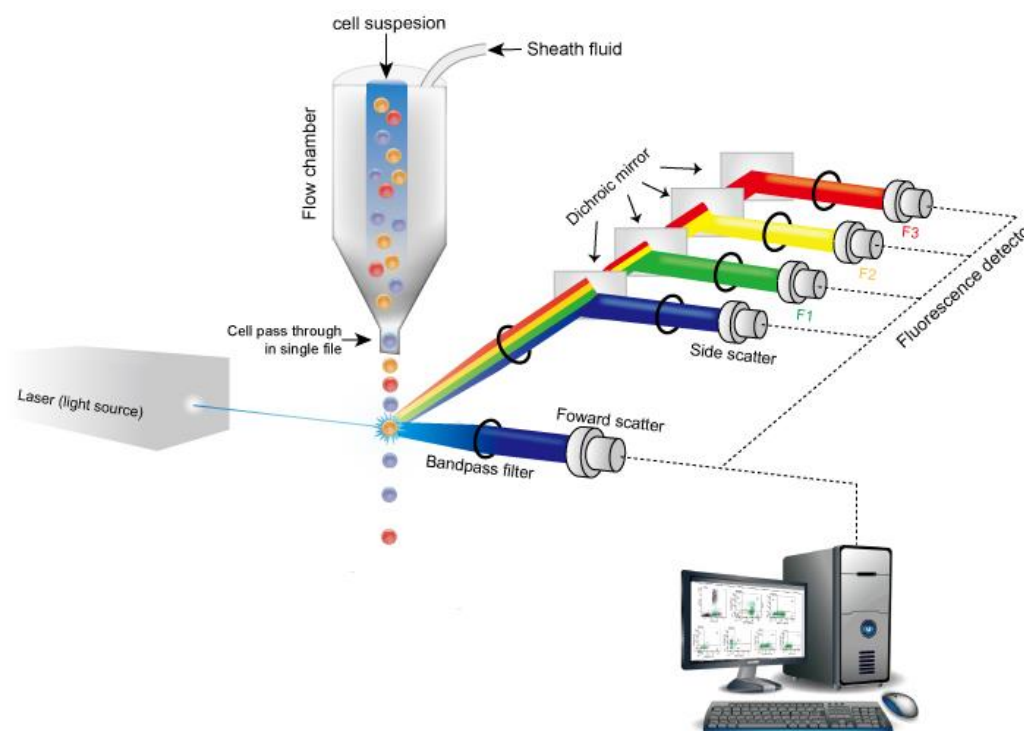


Figure 5 - Schematic diagram of flow cytometer.

Source: (CD Creative Diagnostics, 2022)

The cells to be analysed are suspended in a fluid and injected into the instrument. The passage of cells, one by one, is obtained through the hydrodynamic focus of the sample flow, since the cell suspension is injected into a saline solution (sheath fluid) that crosses the chamber at a higher speed. This difference of speed between the sheath fluid and the cell suspension injected allows a laminar flow

of the cells. The laser light then intercepts perpendicularly the cell flow, allowing light scattering forward and sideways. Scattered radiation is then channelled through a series of mirrors and lens, finally being detected on several different detectors (each detecting a specific wavelength) after going through one final filter specific for that detector (Lopes da Silva, et al., 2004).

The optical filters for different wavelength are FSC (Forward Scatter) and SSC (Side Scatter), both dispersion detectors, and 13 different fluorescence detectors (ex.: FITC-A, PC5.5-A).

FSC detector obtains information about the size of the cell and SSC detector evaluates cell complexity (Lopes da Silva, et al., 2004). By analysing the data of forward and side scatter together, cell populations can often be distinguished based on differences in their size, shape and internal complexity, as shown in Figure 6.

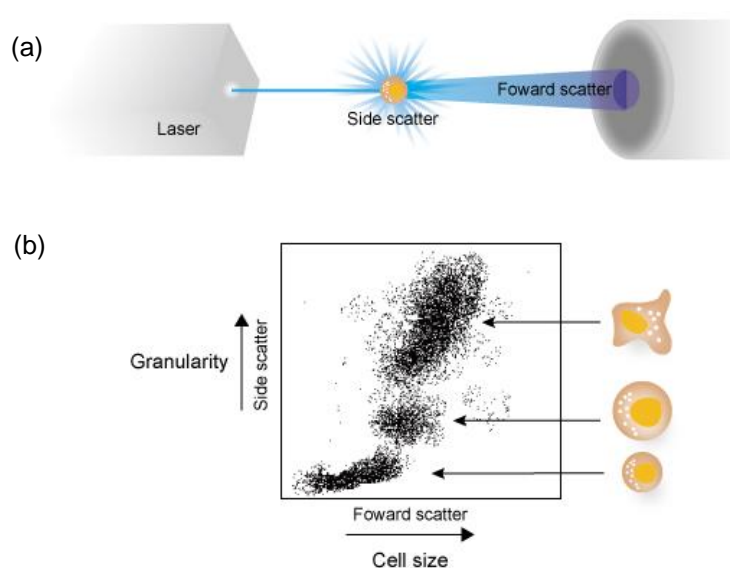


Figure 6 – Flow cytometry: (a) Measurement of forward and side scatter; (b) Graphic representation of cells according to its size and complexity. Source: (CD Creative Diagnostics, 2022)

To study other cellular characteristics, that are not possible to evaluate using simple scattering and autofluorescence of cells, fluorescent dyes can be used to label cells. These can be detected by fluorescent detectors, according to the emission wavelength. Signals collected from the several detectors are then processed and sent to a computer, that organizes information in dot plots, density plots and histograms.

In this study, *C. cohnii* physiological state was monitored by double staining procedure with fluorescent dyes coupled with flow cytometry analysis of the stained samples. This method allowed analysis of membrane integrity and enzymatic activity of cells, both indicative of cell's stress response. Membrane permeability is a good indicator of cell viability, as a damaged cell membrane exposes the intracellular medium to the outside, hindering cellular processes. Enzymatic activity is a good measure of cellular activity, as it indicates normal cell metabolism.

Therefore, the fluorescent dyes used were carboxyfluorescein diacetate (CFDA) and propidium iodide (PI). CFDA is a non-fluorescent dye that enters the cell by diffusion to evaluate its physiological state. When inside the cell, CFDA is hydrolyzed by esterases, producing a fluorescent compound, that binds to amine residues in the cell. The activity of esterases is a measure of normal cell function. Therefore,

when a cell is dyed with CFDA it means that it has enzymatic activity. PI is used to evaluate membrane integrity, since it bonds to cell DNA, but can't cross healthy cytoplasmic membrane. Thus, when a cell is dyed with PI it means the cell membrane is damaged. CFDA was detected in the FITC-A detector and PI was detected in the PC5.5-A detector.

1.6. Lipid extraction and fractionation

At the end of microalgae cultivation, the biomass is separated from the culture medium and is usually dried, in order to produce stable biomass, free of water, that can be stored for long periods of time without deterioration. Special attention should be paid to intracellular triglycerides, due to the fact that these compounds are very sensitive to heat, avoiding exposure of biomass to high temperatures, as these compounds can oxidate and degrade at temperatures above 50°C.

Before lipid extraction, a rupture cell method must follow, to facilitate the oil extraction from cells, such as high-pressure homogenization, hydrodynamic cavitation, treatment with pulsed electric field, microwave or ultrasound, solvent extraction, ball milling, ionic liquids, surfactants, direct saponification, hydrolytic enzymes or algicide treatments (Lopes da Silva, Moniz, & Reis, 2020).

The microalgal oil is usually extracted using several processes, such as mechanical pressing, homogenization, milling, solvent extraction, supercritical fluid extraction, enzymatic extractions, ultrasonic-assisted extraction, and osmotic shock (Mercer & Armenta, 2011). Organic solvents have shown to be effective when used on microalgae biomass since they degrade microalgal cell walls and extract the oil. Thus, it should be noted that microbial lipids intended for the pharmaceutical and food industries cannot be extracted with toxic solvents in order to avoid solvent residues in medicinal products or food. The most economical procedure is still hexane extraction, especially when extracted lipids are intended for food, pharmaceutical and nutraceutical applications, but it is necessary to ensure that no residual solvent remains in the oil (Lopes da Silva, Moniz, & Reis, 2020). In this study, conventional Soxhlet extraction and accelerated solvent extraction (ASE) were used, both using n-hexane as solvent (Luque de Castro & Priego-Capote, 2010). ASE is a fully automated rapid extraction technique for organic compounds that utilizes common solvents at elevated temperatures and pressures to increase extraction efficiency. When comparing to conventional Soxhlet extraction, this method requires less extraction time (15 to 25 min), consumes only 15-45 mL of solvent (n-hexane), which remains in liquid state during the entire process, and allows high lipid extraction yield using small amounts of biomass (Mottaleb & Sarker, 2012).

After lipid extraction from biomass, it can be further fractionated and several lipid fractions with different degrees of saturation are obtained: an unsaturated fraction, rich in ω -3 PUFA, such as DHA, and a saturated fraction, with potential use as biodiesel (Lopes da Silva, Moniz, & Reis, 2020).

There are several methods for PUFA concentration/purification, but most of them are expensive and not suitable for large-scale production. These methods include molecular distillation, low-temperature crystallization, simulated moving bed chromatography, supercritical fluid chromatography and preparative HPLC (Oh, et al., 2020). However, the urea complexation seems to be one of the most appropriate methods for PUFA enrichment. This method allows the formation of solid-phase complexes between urea molecules and saturated and monounsaturated fatty acids, but not with polyunsaturated

faty acids, what allows separation of these compounds. Compared to other processes, this method allows handling larger quantities of material, using simple equipment, requires inexpensive solvents (ethanol or hexane) and is more cost-effective. Furthermore, urea complexation protects the ω -3 PUFA from autoxidation (Moniz, et al., 2022).

1.7. Applications of oil free microalgae biomass

The biomass obtained, after oil extraction, is a by-product resulting from the process that can also be used as fertilizer, for biogas or biofuel production with drop-in properties, capable of being used as a fuel for terrestrial transport (Lopes da Silva, Moniz, & Reis, 2020). This way, the value of the entire process is maximized, through the use of low-cost substrates and the use of the several products resulting from the metabolism of *C. cohnii*, which contributes to the sustainability and profitability of the entire production process. Figure 7 shows a synthesis scheme of the heterotrophic metabolism of *C. cohnii* and the microalgal biomass applications, considering an integrated approach based on the use of a microalgal biorefinery with multiple applications, which efficiently uses all lipid fractions of microalgae biomass, for various purposes, through a sustainable process based on the concept of circular bioeconomy.

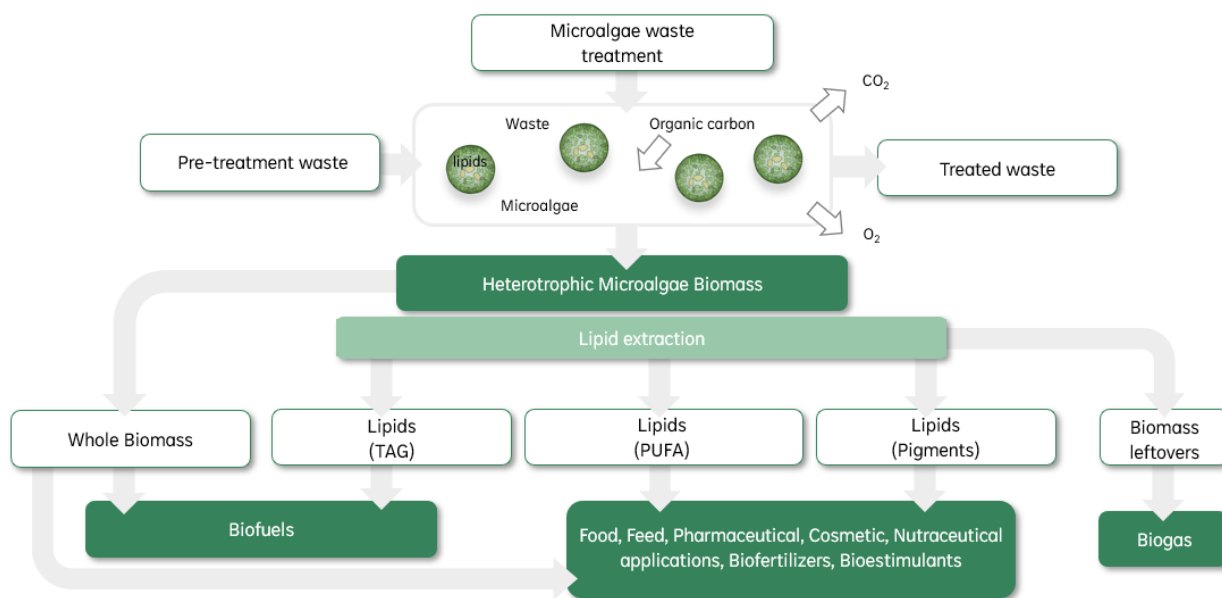


Figure 7 - Heterotrophic metabolism and applications of microalgae biomass.

Source: (Lopes da Silva, et al., 2021) - Adapted

1.8. Aims of the study

The present study aims to implement a simple and sustainable process, which supports the circular economy, for the production of docosahexaenoic acid (DHA) and biodiesel, from the biomass biorefinery of the microalga *Cryptocodinium cohnii*.

In the first part of the study, *C. cohnii* fermentations were conducted, under previous optimized conditions, using crude glycerol and sugarcane molasses as sustainable carbon sources, to obtain high density cell cultures with high content in intracellular lipids. The produced cultures were monitored in real time by microscopical observation, optical density and flow cytometry. Also, carbon consumption was quantified over time, as well as total nitrogen content, and the profile of fatty acids produced during cultivation was evaluated.

After microalgae cultivation, lipid extraction from microalgal biomass produced was carried out through accelerated solvent extraction (ASE) and conventional Soxhlet extraction, that, in this study, was considered the reference process for lipid quantification. Profile evaluation of the obtained fatty acids was performed by gas-liquid chromatography.

Lastly, the fatty acids present in the microalgal biomass produced were subjected to ethylation, in order to obtain the correspondent FAEE, which were then fractionated at different crystallization temperatures (-18°C, 4°C and 25°C), using urea complexes. After crystallization with urea, the FAEE were separated in non-urea complexing and urea complexing fractions, according to the structure of these molecules. Therefore, it was possible to separate lipidic fractions with different degrees of saturation: a polyunsaturated fatty acid fraction, rich in DHA, that can be used for pharmaceutical, nutraceutical and food purposes, and a lipid fraction rich in saturated and monounsaturated fatty acids, for biodiesel purposes.

From a theoretical approach, biodiesel fraction's characteristics were assessed, following the European standard for this product (EN 14214).

2. Methodology

2.1. Material and Equipment

The materials and reagents used in this work are described in Table 14 in Annex I. The equipment used in this work will be referred in the text as necessary.

2.2. Microorganism and Culture Maintenance

The *Cryptocodinium cohnii* strain (ATCC 30772) used in the present study was obtained from the American Type Culture Collection (ATCC). The initial cells were propagated and subsequently maintained in 250 mL flasks, using 150 mL of starter medium composed of yeast extract (1.8 g L⁻¹), sea salt (23 g L⁻¹) and a carbon source (9 g L⁻¹). Glucose and pure glycerol were the carbon sources used for maintenance of the cultures. This medium was sterilized using an autoclave (Uniclave 88, A. J. Costa LDA, Portugal), at 121°C for 20 min, and then inoculated using a *C. cohnii* cell suspension (10% v/v). The starter cultures were kept in a static incubator at 25°C in the dark, being subsequently re-inoculated in the same medium every month. The starters were then used to inoculate the inoculum cultures.

Inoculum cultures were used to produce enough biomass to inoculate the bioreactor at the start of each assay. These cultures were prepared in shake-flask cultures of 500 mL, containing 150 mL of medium composed of yeast extract (2 g L⁻¹), sea salt (25 g L⁻¹) and a carbon source (20 g L⁻¹), that was sterilized using an autoclave (Uniclave 88, A. J. Costa LDA, Portugal), at 121°C for 20 min, and then inoculated with 10% v/v of starter culture. Once again, glucose and pure glycerol were the carbon sources used for maintenance of these cultures. The inoculum cultures were incubated in the darkness at 27°C and 150 rpm for 6-8 days. After the incubation period, these culture cells in exponential growth phase were used to inoculate the bioreactors with 10% v/v inoculum.

For these culture mediums, the initial pH was adjusted to 6.5 using NaOH and HCl solutions before sterilization. The pH was determined using a Consort C3021 potentiometer (Consort, Belgium), calibrated regularly.

2.3. *C. cohnii* bioreactor fermentation conditions

Each fermentation of *C. cohnii* was carried out in a 7L benchtop bioreactor (Fermac 360, Electrolab Biotech, Tewkesbury, UK), equipped with two Rushton disk turbines and coupled to a module that controls agitation, temperature, pH and dissolved oxygen. Figure 8 illustrates the bioreactor used in this study.

The tests were performed under fed-batch regime, being the most used in the industry, since it has the advantage of allowing the prolongation of the exponential phase of microalgae growth, reaching a higher cell density. Thus, whenever cell growth slowed down, nutrient pulses (300 mL solutions of 10 times concentrated culture medium) were added, previously centrifuged and sterilized in the autoclave.



Figure 8 - Bioreactor used in *C. cohnii* fermentations.

The growth medium contained 0.5 g L^{-1} yeast extract, 5.5 g L^{-1} corn steep liquor, 27 g L^{-1} sea salt and a complex carbon source 20 g L^{-1} , being centrifuged (for residues removal) and then sterilized inside the bioreactor at 120°C for 30 min (Uniclave 88, A. J. Costa LDA, Portugal). The carbon sources used in the assays were crude glycerol or sugarcane molasses, present in the growth medium in concentrations of 23.4 g L^{-1} (in order to assure a 20 g L^{-1} of pure glycerol) or 20 g L^{-1} , respectively. When using sugarcane molasses in the medium, this carbon source was previously hydrolyzed (separated to the rest of the medium and later added to the bioreactor, in sterile conditions) to break down sucrose into glucose and fructose. Both complex carbon sources characterization is described below in section 2.4. The initial culture volume in the bioreactor was 2.7 L, to which it was added 300 mL of inoculum culture (10% v/v). Thus, the useful volume of the bioreactor was 3L.

Temperature was kept constant at the optimal temperature of 27°C . The pH of the fermentation medium was measured using a Mettler Toledo steam-sterilizable pH electrode (Columbus, USA) being controlled automatically through the addition of 2.5 M NaOH and 2.5 M HCl, on demand, to 6.5 ± 0.1 . Sterile air was added at the aeration rate of 1 v/v/m, being used a sterile in-line Millex® filter unit (Merck, Germany) to keep the asepsis conditions. The dissolved oxygen (DO) in the medium was measured using a Mettler Toledo oxygen electrode (Columbus, USA) and kept above 40%, by control of the stirring rate and airflow control, to avoid limiting the microorganism growth due to the oxygen deficiency. Thus, the stirring rate (100-300 rpm) was manually increased whenever the DO was below 40%.

To prevent from the appearance of contaminations, antibiotic and antifungal were added to the bioreactor, each one in the concentration of 0.1% (v/v). The added antibiotic mixture is a combination of Chloramphenicol (5 g L^{-1}), Penicillin G potassium salt (62 g L^{-1}) and Streptomycin Sulfate (100 g L^{-1}). The antifungal used was Amphotericin B (2 g L^{-1}), diluted in DMSO.

Since *C. cohnii* is a heterotrophic microalga, this species grows in environments without light, thus the bioreactor was protected using common aluminium foil.

Nutrient pulses (carbon source, yeast extract and CSL) were added whenever the residual carbon concentration in the broth decreased below 10 g L^{-1} and the dissolved oxygen increased above 80%,

except at the end of the fermentation. This approach allows the exponential phase to be followed by a nutritional limitation, other than the carbon source used, in order to enhance the production of lipids (Tuttle & Loeblich, 1975).

C. cohnii sampling was carried out at least two times per day, in sterile conditions, and the culture samples were observed microscopically and analyzed by optical density and flow cytometry, to check the culture growth and the viability of the cells. The culture samples were centrifuged (Sigma 2-16KL benchtop centrifuge, Sartorius, Germany) at 6000 rpm for 10 min, at RT. The resultant pellet (microalgal biomass) and supernatant were both freeze-dried and stored under nitrogen atmosphere at -18°C for further fatty acids analysis (section 2.5.7.) and carbon source consumption (section 2.5.4.) and total nitrogen determinations (section 2.5.5.), respectively.

2.4. Analysis and processing of complex substrates

The complex carbon sources used in *C. cohnii* fermentations were crude glycerol and sugarcane molasses, both low-cost industrial by-products. Also, as nitrogen source, it was used corn steep liquor (CSL) in *C. cohnii* cultivations, a major by-product found during corn starch processing.

2.4.1. Crude glycerol

The crude glycerol used in the assays was provided by Iberol (Sociedade ibérica de biocombustíveis e oleaginosas, S.A., Alhandra, Portugal) as a by-product of biodiesel production industry. The composition of the crude glycerol was previously analyzed in-lab by Taborda, et al. (2021) and it is described in Table 2.

Table 2 - Crude glycerol composition in percentage (w/w).

Source: (Taborda, et al., 2021)

Crude Glycerol (distilled)						
Glycerol	Water	Methanol	Non-glycerol organic matter	Ashes	Sodium	Potassium
85.5%	11.2%	0.013%	0.89%	4.74%	1.04%	<0.0005%

2.4.2. Sugarcane Molasses

The sugarcane molasses was supplied by Sidul Açúcares (Santa Iria de Azóia, Portugal), a by-product of sugarcane sugar industry, and its composition was previously determined by HPLC. A total sugar (sucrose, fructose and glucose) concentration of 459.3 g L⁻¹ was determined, of which 61% was sucrose, 22.3% was glucose and 16.7% was fructose (w/w).

The sugarcane molasses was hydrolyzed prior to use, to break the sucrose into glucose and fructose, by decreasing its pH to 3 with HCl 50% (w/w) and autoclaving at 120°C for 20 min. The pH was subsequently raised to 6.5 using NaOH 50% (w/w). The hydrolyzed molasses was then analyzed using HPLC and no traces of sucrose were found, the hydrolysis was determined to have been complete. The glucose and fructose concentrations after hydrolysis are 249,89 g L⁻¹ and 224,16 g L⁻¹, respectively (Taborda, et al., 2021).

2.4.3. Corn Steep Liquor (CSL)

Corn steep liquor (CSL) is a major by-product that results from corn starch processing and has been identified as a potential nitrogen source in biochemical industries and a good substitute for expensive complex medium. It is a viscous concentrate of corn solubles which contains amino acids, vitamins and minerals, so it can be used as a constituent of some growth media. The CSL used in the assays contains 0.035g of nitrogen/g and some residual sugars in its composition. These sugars are not accounted as carbon source in media formulation due to the small amounts used.

2.5. *C. cohnii* bioreactor culture monitoring

When performing each assay for the *C. cohnii* fermentation, all the cultures were monitored and analyzed in real time to ensure healthy cell growth and high lipid production.

2.5.1. Microscopical observations

All cultures were monitored through microscopic observation using the Olympus BX60 microscope (Olympus Corporation, Japan) under visible for contaminations screening, using a microscope equipped with a digital camera, which was used to take the photographs presented in this study.

For each microscopic observation using visible light, a small portion of the broth was removed from the bioreactor (culture sample), under sterile conditions, and observed under 100x, 400x and 1000x magnification.

2.5.2. Dry cell weight measurements

Cell biomass concentration over fermentation time was determined by optical density at 470 nm, using an UV-Vis spectrophotometer (Genesys 20 Visible Spectrophotometer, Thermo Scientific, USA). All samples collected were analyzed by optical density, as well as the culture medium before inoculation, to correct the optical density values of all samples (blank). The optical density of the added nutrient pulses was also analyzed. All measurements were performed in triplicate. Dry cell weight (g L^{-1}) was then estimated through the correlation between the values of optical density (OD), properly corrected (correction for dilution and subtraction of the blank value or pulse), and the dry weight, previously established and shown in Equation 1.

$$\text{Dry Cell Weight (g L}^{-1}\text{)} = (1.0889 \times \text{OD}) - 0.2497 \quad (1)$$

When performing assays using sugarcane molasses, the cell concentration was also quantified gravimetrically, by dry cell weight, on 1 mL per culture sample (in duplicate), from which cells were centrifugated and dried for 24 h at 100°C.

The use of wastes and effluents as substrates for culture medium formulations can interfere with the estimation of cell concentrations, when using quantification methods such as optical density and dry cell weight. For example, corn steep liquor, crude glycerol and sugarcane molasses contain high concentration of particles. Consequently, to minimize the particles interference in the biomass quantification, the number of *C. cohnii* cells per mL was also evaluated by flow cytometry, as described in the following section.

2.5.3. Flow Cytometry

Flow Cytometry analysis was used to monitor cell viability of the microalgal cultivations. Flow cytometry analysis was performed in a Cytoflex Beckman-Coulter (Beckman Coulter, USA) flow cytometer, equipped with a blue laser, FSC/SSC light scattering detectors and fluorescence detectors.

For flow cytometry analysis, the collected samples were previously subjected to ultrasound treatment for 15 seconds to disintegrate cellular aggregates and ensure the analysis of individual cells.

For *C. cohnii* biomass quantification, the autofluorescence of the cells was detected. The microalgal cell suspension was diluted in PBS buffer, in a total sample volume of 500 mL, to keep the event count constant between different analysis (~300 events/s). *C. cohnii* cells population was gated in the FSC/SSC dot-plot and the number of events for that gate was recorded for each sample. The medium culture without cells was previously analyzed by flow cytometry, in order to target dust and particles in the FSC/SSC dot-plot.

Dry cell weight (g L^{-1}) was determined through the correlation between the autofluorescence, given by the number of cells (per unit of volume), and the dry weight, previously established and shown in Equation 2.

$$\text{Dry Cell Weight (g L}^{-1}\text{)} = (0.0000009 \times \text{Cells/mL}) - 0.4133 \quad (2)$$

For the detection of *C. cohnii* cell enzymatic activity and membrane integrity, samples were also diluted in PBS buffer, using the double staining procedure. The dyes used were carbofluorescein diacetate (CFDA) and propidium iodide (PI), that were simultaneously added to the samples. A total of 3 μL of CFDA stock solution (10 mg mL^{-1}) and 2 μL PI stock solution (1 mg mL^{-1}) was added to the cell suspension, in a total sample volume of 500 mL, and incubated for 15 min in the darkness, before flow cytometry analysis.

All analysis were carried out in triplicate and each analysis was stopped after more than 5000 events were detected. The data was analyzed using CytExpert 2.5 software.

2.5.4. Carbon source quantification and consumption

To determine the carbon concentration throughout fermentation (glycerol or glucose, depending on the carbon source used in each assay), the samples were centrifuged and the supernatant collected was filtrated and analyzed by high performance liquid chromatography (HPLC), equipped with the injector Agilent 1260 Infinity II LC System (Agilent Technologies, USA). Two different chromatographic columns were used: Aminex™ HPX-87P (Bio-Rad, California, USA) and SugarPack™ (Waters, USA), the last one being used for assays containing sucrose (sugarcane molasses) and the former being used for assays containing glycerol. The columns were combined with a cation H^+ - guard column (Bio-Rad), equipped with a diode array detector (DAD) and a refractive index detector (RI). Elution took place at 50°C with $5 \text{ mmol L}^{-1} \text{ H}_2\text{SO}_4$ at a flow rate of 0.6 mL min^{-1} .

Before injecting the samples, correlations were established to relate the peak areas with the carbon concentration in each sample, through HPLC analysis of glycerol, glucose, fructose and sucrose standard solutions of known concentration. The correlations calculated are shown in Annex IV.

The chromatograms were analyzed using the Agilent OpenLab CDS 2.6 software.

2.5.5. Total nitrogen content determination

From each sample collected during fermentation process, a volume of supernatant was freeze-dried and reserved for the determination of total nitrogen content in the bioreactor over time. This content was estimated by the Kjeldahl method (Lim, 1992).

This method is based on three steps: a wet acidic digestion (mineralization), neutralization with alkali and distillation of the ammonia and titration of the solution from the distillation apparatus (Sáez-Plaza, et al., 2013).

The digestion step consists in the reaction between the sample (about 5 mL of supernatant) with 20 mL of sulfuric acid 96%, in the presence of 1 g of a catalyst mixture (9 parts of potassium sulphate and 1 part of copper sulphate, both anhydrous and nitrogen free). The mixture is placed and heated in the heating unit of the digestion appliance (Kjeldahl digestion unit B-435, Büchi Laboratoriums-Technik AG, Switzerland) for 2 hours.

The distillation of the sample was carried out by steam drag with 60 mL of NaOH 40% (w/v) and the ammonia was released to an Erlenmeyer containing 50 mL of boric acid 4% (w/v) and 1 drop of bromothymol blue pH indicator. The apparatus used for the distillation step was a Kjeldahl distillation unit K-350 (Büchi Laboratoriums-Technik AG, Switzerland).

The titration of the resultant solution from the distillation apparatus was performed with HCL 0.1 M, being the turning point of the indicator at a pH of 5.4. All samples were analyzed in duplicate.

The total nitrogen content in each sample, expressed as a percentage (nitrogen mass in g mL⁻¹ of sample), was calculated using Equation 3, where V is the volume of HCL 0.1 M spent on titration, expressed in mL, and m is the mass of the initial sample, expressed in g.

$$\% (w/v) \text{ Total Nitrogen Content} = \frac{0.14 \times V}{m} \quad (3)$$

2.5.6. Moisture and ash contents

To correct the weight of the biomass used for lipid quantification, moisture and ash percentages were determined for each sample. The moisture content was determined by weighing 0.5 g of dry biomass in pre-weighed crucibles and dried at 100°C for 24 h. The crucibles were then placed in a desiccator to cool down to room temperature and then weighed. The moisture content was calculated from the weight difference of the samples before and after drying, as shown in Equation 4.

$$\text{Moisture (\% w/w)} = \frac{W_{\text{crucible + biomass}} - W_{\text{crucible}}}{W_{\text{initial biomass}}} \quad (4)$$

The ash content was obtained in follow-up of the moisture determination, by placing the crucibles with dried samples in a muffle furnace at 550°C for 2 h. The crucibles were then removed from the furnace, placed in a desiccator to cool down to room temperature and then weighed. The ash content was calculated as shown in Equation 5.

$$\text{Ash (\% w/w)} = \frac{W_{\text{crucible + ash}} - W_{\text{crucible}}}{W_{\text{initial biomass}}} \quad (5)$$

The moisture and ash data resulted from the average of a minimum of two representative samples.

2.5.7. Fatty acid profile analysis

Gas-liquid chromatography was used to determine the fatty acids profile of the samples collected during fermentation, including the final biomass obtained. Lipids produced by *C. cohnii* were extracted, for analysis of the fatty acids profile, according to the following protocol described by Lepage & Roy (1986), with modifications.

The microalgal biomass collected over fermentation time, through sampling, was freeze-dried (Heto PowerDry LL3000 Freeze Dryer, Thermo Scientific, USA, coupled with a vacuum pump from Vacuubrand, Germany) after centrifugation of the broth. The freeze-dried samples of *C. cohnii* (100 mg) were transferred to vials under nitrogen atmosphere and transmethylated at 80°C for 1 h, with 2 mL of methanol/acetyl chloride (19:1 v/v) and 0.2 mL heptadecanoic acid (C:17) (5 mg mL⁻¹ petroleum ether) as internal standard. After cooling, each vial was diluted with 1 mL of water and the lipids were extracted using 2 mL of n-heptane. The organic phase was then separated from the aqueous phase, dried using anhydrous sodium sulphate (Na₂SO₄) and placed in a vial adequate for gas chromatography analysis.

The methyl esters were then analyzed by gas-liquid chromatography (Brucker Scion 436-GC, Germany) equipped with a flame ionization detector. Separation was carried out on a 0.32 mm × 30 m fused silica capillary column (film 0.32 mm) Supelcowax 10 (Supelco, USA) with helium as a carrier gas, at a flow rate of 3.5 mL min⁻¹. The column temperature was programmed at an initial temperature of 200°C for 8 min, then increased at 4°C per min to 240°C and held there for 16 min. Injector and detector temperatures were 250°C and 280°C, respectively, and split ratio was 1:50 for 5 min and then 1:10 for the remaining time. The column pressure was 13.5 psi. Peak identification and response factor calculation were carried out using known standards (GLC 459, GLC 85, GLC 75, Nu-check-Prep).

The fatty acids quantification was determined by comparing the peak area of each fatty acid with the peak area of the heptadecanoic acid (17:0), used as the internal standard, as shown in Equation 6. In this equation w_{FA_i} is the weight of the fatty acid i , A_{FA_i} is the peak area of this fatty acid, $A_{(17:0)}$ is the peak area of the internal standard and RF_{FA_i} is the response factor of the fatty acid. Each sample was analyzed in duplicate.

$$w_{FA_i} = \frac{A_{FA_i}}{A_{(17:0)}} \times RF_{FA_i} \quad (6)$$

Fatty Acids Composition

The percentage of each fatty acid in the total mass of fatty acids (% FA_i (w_{FA_i}/w_{TFA})) can be calculated using Equation 7, where w_{FA_i} is the weight of the fatty acid i and w_{TFA} is the weight of the total fatty acids.

$$\% FA_i (w_{FA_i}/w_{TFA}) = \frac{w_{FA_i}}{w_{TFA}} \times 100 \quad (7)$$

The percentage of total fatty acids in the biomass is calculated through Equation 8, where w_{TFA} is the weight of total fatty acids and $w_{biomass}$ is the weight of dry and without ashes biomass.

$$\% TFA_{(w_{TFA}/w_{biomass})} = \frac{w_{TFA}}{w_{biomass}} \quad (8)$$

2.5.8. Calculation of kinetic parameters

Specific Growth Rate

The specific growth rate (μ) is defined as the rate of increase of biomass of a cell population per unit of biomass concentration. It can be calculated by Equation 9, in the period between the lag and stationary phases (exponential phase), in which the logarithm of the dry weight over time fits a straight line. In this equation, DCW is the dry cell weight, DCW_0 is the dry cell weight in the beginning of the fermentation and t is the time.

$$\ln(DCW) = \mu t + \ln(DCW_0) \quad (9)$$

Volumetric Average Productivity

The average productivity in biomass of the fermentation process (P_A) is given by Equation 10, where C_{final} is the concentration of biomass in the final instant, $C_{initial}$ is the concentration of biomass in the initial instant and t is the total fermentation time. Equation 11 gives the instant productivity.

$$P_A(t) = \frac{C_{final} - C_{initial}}{t} \quad (10)$$

$$P_A(t_2) = \frac{C_2 - C_1}{t_2 - t_1} \quad (11)$$

The volumetric average productivity in total fatty acids (P_{TFA}) is determined through Equation 12, where P_A is the average productivity in biomass and $\% TFA_{(w_{TFA}/w_{biomass})}$ is the percentage of total fatty acids in biomass (dry and without ashes). Equation 12 is also used to calculate the DHA productivity.

$$P_{TFA} = P_A \times \frac{\% TFA_{(w_{TFA}/w_{biomass})}}{100} \quad (12)$$

2.6. *C. cohnii* biomass processing

After finishing the *C. cohnii* fermentation, the broth obtained was centrifugated (Sigma 6-16KS centrifuge, Germany) at 7000 rpm for 10 min, in room temperature. This step allowed the separation of the biomass produced from the remaining culture medium, for subsequent extraction of lipids from the microalgal biomass. The supernatant was stored, for example, for posterior biogas production, and the cell pellets were washed with deionized water. The cells were then centrifuged to discard the washing solution. The microalgal cells collected from this process were then freeze-dried (Heto PowerDry LL3000 Freeze Dryer, Thermo Scientific, USA, coupled with a vacuum pump from Vacuubrand, Germany), allowing to stability of biomass, free of water, which can be stored for long periods of time

without suffering deterioration. After freeze-drying, the dry biomass was stored at 4°C, being ready for the lipid extraction and analysis.

The final biomass dry cell weight (DCW) obtained in each assay was measured gravimetrically.

2.7. Lipid extraction methods

For lipid extraction the methods used were the traditional Soxhlet extraction and the accelerated solvent extraction (ASE), both using n-hexane as solvent. After extraction, lipids were gravimetrically measured and the fatty acids of the extracted oils were analyzed by gas-liquid chromatography, to evaluate their profile.

2.7.1. Soxhlet extraction

The extraction of total lipids presents in the final biomass obtained in each fermentation was performed using the conventional method by Soxhlet extraction, using n-hexane as solvent.

For each assay, 0.5 g of freeze-dried biomass was weighed (in duplicate) and subject to grinding using a ball mill (Retsch, model MM400, Germany). The grinding was performed at 25 Hz, for 3 min and 30 seconds, using 4 metal spheres (AISI 316) of 1 cm diameter. Then, the grinded biomass was transferred to a cellulose extraction thimble that was covered with cotton in order to prevent biomass to escape. The cellulose extraction thimble with the biomass was placed in a Soxhlet extracting tube and 160 mL of n-hexane were used in the distillation flask. The extraction was performed for 6 hours. Figure 9 shows a diagram of the Soxhlet extraction method.

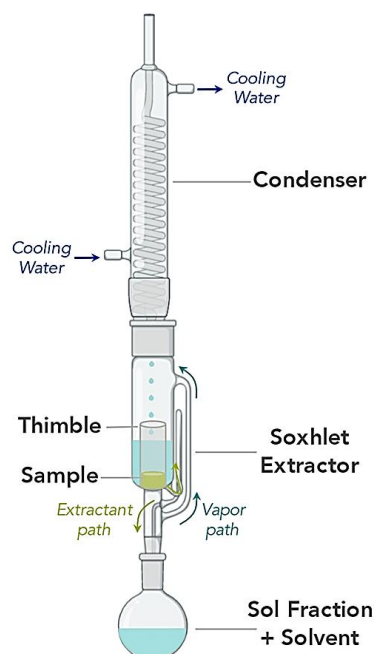


Figure 9 - Conventional Soxhlet extractor.

Source: (Danielsen, et al., 2021)

After extraction, the solution containing the lipidic extract obtained in the distillation flask was concentrated using a rotary vacuum evaporator (Büchi Rotavapor R-110, Switzerland) in order to

evaporate completely the solvent used. The concentrated extracted lipids obtained were then quantified gravimetrically. The lipidic extract was dried at 30°C for 1 hour, in the dark and under nitrogen atmosphere (to prevent from lipid degradation), for complete evaporation of the n-hexane. The extract was then placed in a desiccator to cool down to room temperature and weighed.

The calculation of the lipid percentage obtained in each Soxhlet extraction was calculated using Equation 13, where $w_{biomass}$ is the biomass weighed (dry and without ashes, previously determined).

$$\text{Lipids (\%)} = \frac{W_{flask+lipidic\ extract} - W_{flask}}{W_{biomass}} \times 100 \quad (13)$$

The fatty acids profile was analyzed by gas-liquid chromatography, as described in section 2.5.7.

2.7.2. Accelerated solvent extraction

The accelerated solvent extraction method (ASE) was another extraction method used for the obtainment of the lipidic extract present in the final biomass of each fermentation. The yield in lipids obtained when using this process is similar to the one obtained when using Soxhlet extraction method. However, the accelerated solvent extraction method is more advantageous and eco-friendlier than the Soxhlet extraction method since it requires a small amount of biomass to carry out the extraction, the extraction time is reduced and the solvent consumption is relatively low. Figure 10 shows a schematic representation of the ASE method.

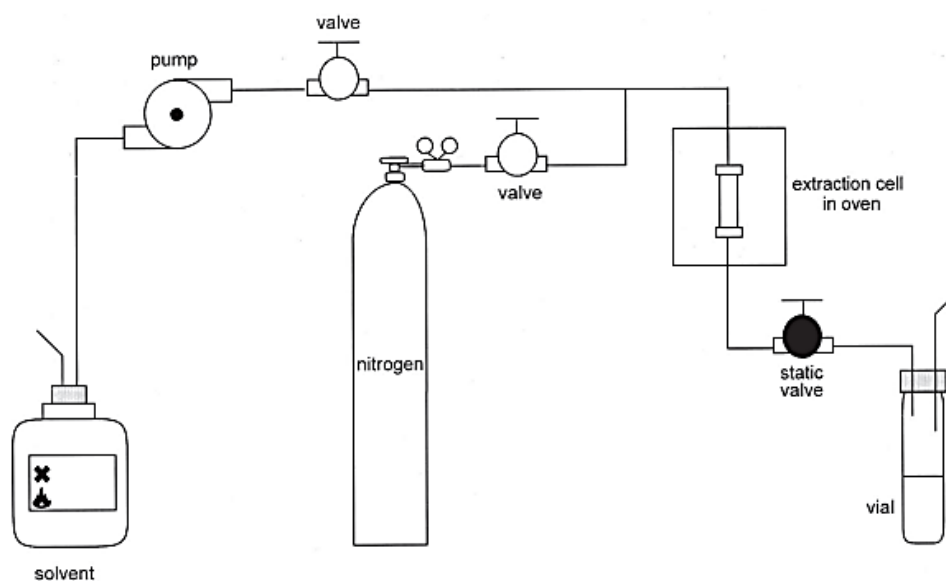


Figure 10 - Schematic view of accelerated solvent extraction system.

Source: (Giergielewicz-Mozajska, Da browski, & Namiesnik, 2001)

Accelerated solvent extraction was carried out on a Dionex ASE 150 (Thermo Scientific, USA), connected to a nitrogen bottle (pressurization gas).

For each assay, 0.25 g of freeze-dried biomass was weighed (in duplicate) and subject to grinding using a ball mill (Retsch, model MM400, Germany). The grinding was performed at 25 Hz, for 3 min and 30 seconds, using 4 metal spheres (AISI 316) of 1 cm diameter. To avoid aggregation of sample

particles, which interferes in extraction efficiency, it was added ~0.5 g of diatomaceous earth, an inert material. Hydrophilic cotton and cellulose filters were placed at the ends of the extraction cell (5 mL of internal volume), in order to avoid the drag of solid particles by the solvent. The preheating time was set to 1 min. The working pressure used was 10 Mpa (pre-established value for this equipment model) and the temperature was 120°C for 3 min (2 extraction cycles). The flush volume at the end of the extraction was 60% of cell volume and the purge time was set to 30s.

After each extraction, the solution containing the lipidic extract was concentrated and then gravimetrically measured, following the same procedure previously described for the Soxhlet extraction method (section 2.7.1.). The lipid percentage obtained by ASE was calculated using Equation 13.

The fatty acids profile was analyzed by gas-liquid chromatography, as described in section 2.5.7.

2.8. Lipid fractionation with urea complexes

The lipid fractionation using urea complexes allows the separation of the polyunsaturated lipid fraction, which include DHA, from the saturated and monounsaturated lipid fraction, with potential use as biodiesel. The fractionation process with urea complexes was performed according to the following protocol described by Moniz, et al. (2022), with modifications.

2.8.1. Saponification and ethylation

A volume of 595 mL of ethanol 96% (v/v) and 12.5 g of potassium hydroxide (KOH) were added to 5 g of freeze-dried biomass (in duplicate). The mixture was incubated in a stirring plate at 100 rpm, at room temperature, in nitrogen atmosphere, overnight.

Afterwards, 107 mL of distilled water were added, followed by 4 extractions using n-hexane (4x100 mL) in order to separate the unsaponifiable fraction. The hydroalcoholic phase, containing the soaps, was acidified to pH=1 by the addition of HCl 50% (v/v). Then, the free fatty acids were recovered by 4 extractions using n-hexane (4x50 mL). The solvent was then evaporated in a rotary vacuum evaporator (Büchi Rotavapor R-110, Switzerland).

The free fatty acids obtained were then ethylated according to Khozin-Goldberg, Bigogno, & Cohen (1999), with modifications, by adding a solution of ethanol and sulfuric acid (in concentration 49:1) and heating at 80°C for 1 hour. After cooling to room temperature, 100 mL of n-hexane and 100 mL of water were added and the upper hexane layer, containing the fatty acids ethyl esters (FAEE), was removed and dried using anhydrous sodium sulfate. The solvent was then evaporated in a rotary vacuum evaporator (Büchi Rotavapor R-110, Switzerland). Heptadecanoic acid (17:0) ester was added as internal standard and the ethyl esters were analyzed by gas-liquid chromatography. The quantities of individual FAEE obtained before crystallization were determined by comparing the peak area of each fatty acid with the peak area of the heptadecanoic acid (17:0), used as the internal standard, as previously shown in Equation 6.

2.8.2. Urea complexation

To the ethyl esters fraction obtained, a solution of 50 mL of ethanol and 1.6g of urea was added. This ethanol/urea ratio allowed a homogeneous and clear mixing of ethyl esters with urea. The urea

complexes were obtained by crystallization of the solution at 3 different temperatures (25°C, 4°C and -18°C) overnight, followed by filtration, in order to separate the urea complexing from the non-urea complexing fractions.

To both urea complexing and non-urea complexing fractions, a volume of 10 mL of n-hexane was added, followed by 10 mL of water (to separate the phases), in order to extract the ethyl esters. The hexane phases from both fractions (urea complexing and non-complexing) were collected and evaporated in a rotary vacuum evaporator (Büchi Rotavapor R-110, Switzerland). Heptadecanoic acid (17:0) ester was added as internal standard and the ethyl esters were analyzed by gas-liquid chromatography. The quantities of individual FAEE obtained after crystallization were determined, once again, as previously shown in Equation 6.

To evaluate the success of the fractionation process, recovery yields (expressed in percentage) were calculated, as shown in Equation 14, where $(m_{ethyl\ esters})_b$ is the initial ethyl esters mixture weight, before urea fractionation step, and $(m_{ethyl\ esters})_a$ is the weight of each ethyl esters fraction obtained after the urea fractionation (and removal, in the case of the urea complexing fraction).

$$\text{Recovery Yield} = \frac{(m_{ethyl\ esters})_a}{(m_{ethyl\ esters})_b} \times 100 \quad (14)$$

2.9. Characterization of monounsaturated and saturated fractions

As mentioned previously, for commercialization of biodiesel in the European Union its characteristics must be within the parameters presented in the standard EN 14214. Therefore, the monounsaturated and saturated fractions obtained after the lipid fractionation process (section 2.8.) were analyzed by gas-liquid chromatography, as described in 2.5.7., for fatty acids profile characterization. This analysis allowed the determination of various indexes to assess its potential use as biodiesel.

Average unsaturation determination was based on the fatty acids profile and calculated using Equation 15, where N is the number of double bounds of the unsaturated fatty acid and C_i is the fatty acid concentration in the total fatty acids, in mass fraction.

Through the calculation of the average unsaturation (AU), the parameters viscosity, specific gravity, cetane number and iodine value were obtained, by using Equations 16,17,18 and 19, determined by Kongruang, Roytrakul, & Sriariyanun (2020).

$$AU = \sum(N \times C_i) \quad (15)$$

$$\text{Viscosity} = -0.6316 AU + 5.2065 \quad (16)$$

$$\text{Specific Gravity} = 0.0055 AU + 0.8726 \quad (17)$$

$$\text{Cetane Number} = -6.6684 AU + 62.876 \quad (18)$$

$$\text{Iodine Value} = 74.373 AU + 12.71 \quad (19)$$

3. Results and Discussion

C. cohnii fermentations were performed according to the previously described Methodology, studying crude glycerol and sugarcane molasses as carbon sources. In this study, 3 cultivations were conducted and microalgal lipids produced were extracted from the biomass using urea complexes, in order to attain DHA and biodiesel fractions.

Besides the assays mentioned, that were analysed and described in this study, 2 another *C. cohnii* fermentations were carried out, yet the cultivations were interrupted due to contaminations or technical problems with the bioreactor used and for that reason the results will not be shown.

3.1. Assay I

In Assay I the carbon source used was crude glycerol and the fermentation process was carried out and monitored as previously described in the Methodology.

3.1.1. *C. cohnii* bioreactor fermentation

Dry cell weight and biomass productivity

Cell growth was monitored in real time by optical density at 470 nm and by flow cytometry. The evolution of the obtained optical density and the cell count performed by the flow cytometer is represented in the Figure 11. The vertical traits correspond to nutrient pulses added throughout fermentation, containing in its composition crude glycerol (GLY), yeast extract (YE) and corn steep liquor (CSL). The nutrient pulses initiate the fed-batch regime and they were added to the bioreactor whenever glycerol concentration in the broth decreased below 10 g L⁻¹ or the dissolved oxygen increased above 80%, except at the end of the fermentation. Therefore, the stationary phase could be extended to enhance lipid production.

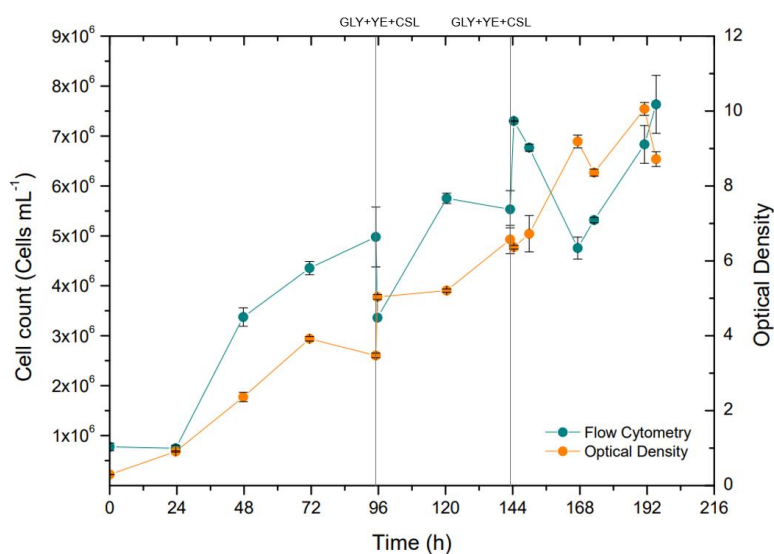


Figure 11 – *C. cohnii* cell count performed by flow cytometry and optical density (corrected) obtained in Assay I.

The optical density and cell count obtained allowed the calculation of *C. cohnii* biomass concentration, through the use of Equations 1 and 2, mentioned in sections 2.5.2. and 2.5.3. Figure 12 illustrates the evolution of *C. cohnii* biomass concentration over fermentation time.

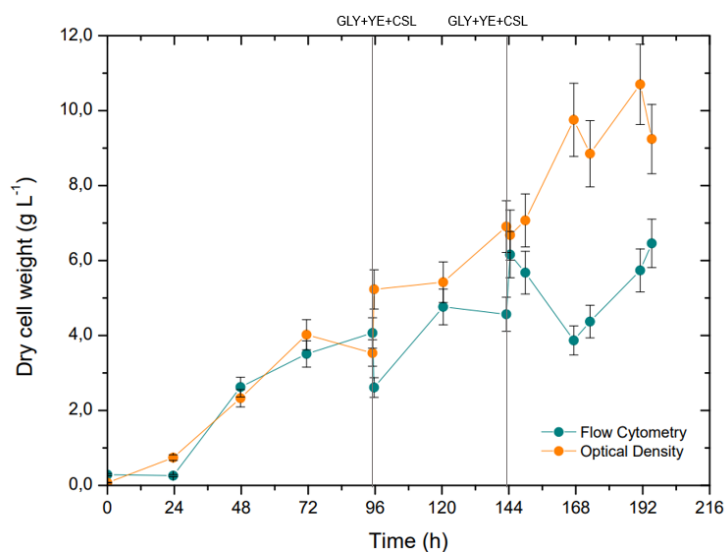


Figure 12 - Evolution of *C. cohnii* biomass concentration over time in Assay I.

It is important to notice that cell count through flow cytometry was only used as an additional method to monitor the relative growth of microalgae, given that DCW values obtained through the correlation for flow cytometry did not correspond to the DCW obtained by the given correlation for optical density (as observed in Figure 12). This may indicate that the correlation used (Equation 2, calculated in previous assays) may not be suitable for this assay's biomass. Therefore, the considered values in this study for DCW over time were the ones obtained through optical density. These values were used to calculate the natural logarithm profile of the biomass, illustrated in Figure 13.

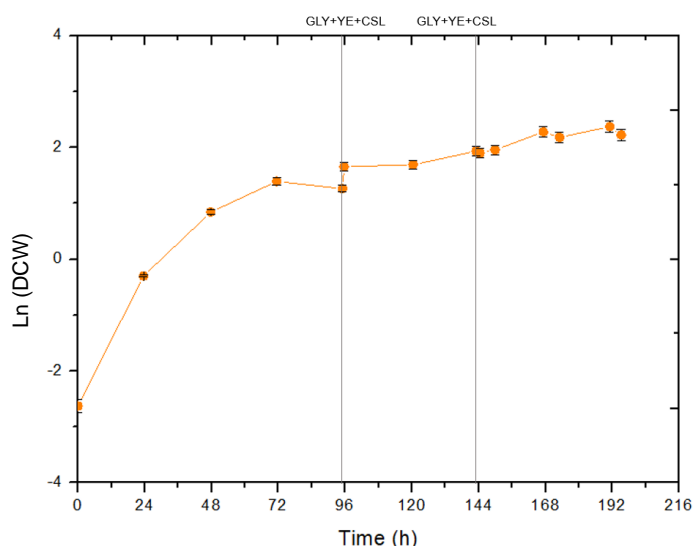


Figure 13 - Natural logarithm profile of the biomass over time in Assay I.

As observed in Figure 13, the *C. cohnii* culture presents an exponential growth (between 23.58h and 71.42h). The culture reached the exponential phase at $t = 23.58\text{h}$ and the stationary phase was attained at $t = 71.42\text{h}$, reaching at that time a biomass concentration of 4.02 g L^{-1} . The specific growth

rate in this assay was 0.035 h^{-1} (calculation shown in Annex III). As observed in Figure 12, the maximum *C. cohnii* biomass concentration was 10.70 g L^{-1} , attained at $t = 191.08 \text{ h}$ of fermentation. However, at the end of the assay ($t = 195.25 \text{ h}$) the biomass concentration was only 9.24 g L^{-1} , probably due to the decrease of carbon source concentration. The average productivity in biomass in this assay was $46.97 \text{ mg L}^{-1} \text{ h}^{-1}$.

It is possible to observe through Figures 12 and 13 that whenever a nutrient pulse was added, the biomass concentration increased, allowing prolongation of stationary phase and, consequently, resulting in major lipid production. At $t = 95.50 \text{ h}$ the first nutrient pulse was added to the bioreactor and biomass concentration improved from 3.53 g L^{-1} to 5.23 g L^{-1} . Again, at $t = 144.42 \text{ h}$, the second nutrient pulse allowed an increase in DCW from 6.68 g L^{-1} to 7.07 g L^{-1} .

In fact, DCW is one of the main factors affecting *C. cohnii* lipid productivity, so it is imperative that the highest concentrations of biomass are attained when conducting cultivations in bioreactor. In previous studies, reactors operating in fed-batch were used and high DCW was obtained. Safdar et al. (2017) obtained 15.8 g L^{-1} on medium containing glucose and NaNO_3 and De Swaaf, Sijtsma, & Pronk (2003) achieved 83 g L^{-1} of DCW when using ethanol and YE in the culture medium, both using the strain ATCC 30555. When comparing with this assay, the final DCW of 9.24 g L^{-1} attained was inferior to the values reported in literature, however it must be taken into account that carbon sources and *C. cohnii* strain used were different. Taborda et al. (2021) conducted assays in shake flasks and obtained 5.05 g L^{-1} DCW when using crude glycerol as carbon source, which presents as a lower value than the obtained in this assay. However, fed-batch fermentations in bioreactor allow higher DCW.

Carbon source consumption

The glycerol concentration over fermentation time is represented in Figure 14, as well as the speed rate and dissolved oxygen in the culture medium are illustrated in Figure 15. Since *C. cohnii* is an obligate aerobic organism, moderate agitation is needed for efficient oxygen supply and consequent carbon source consumption. These factors have significant impact in biomass and lipid production.

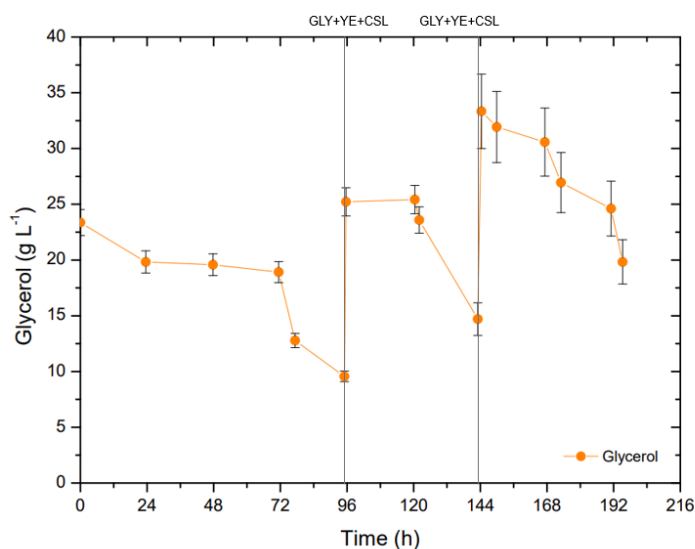


Figure 14 - Glycerol concentration in the culture medium over time in Assay I.

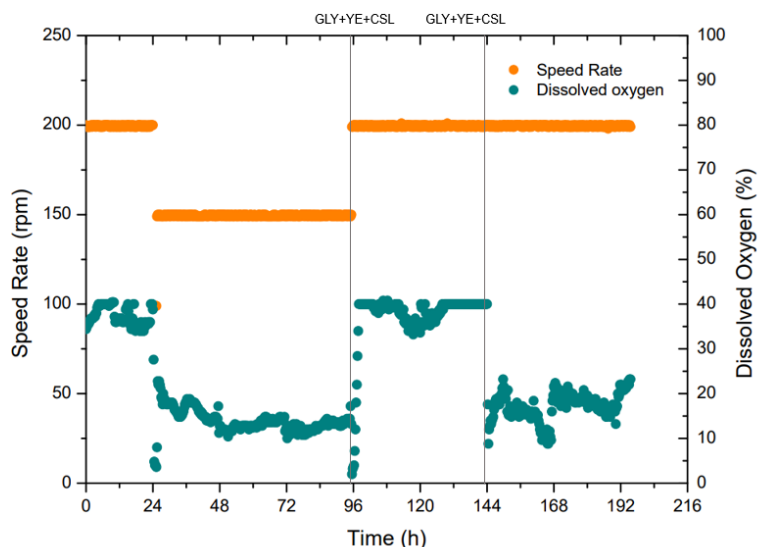


Figure 15 - Speed rate and dissolved oxygen over time in Assay I.

As observed in Figure 14, the initial glycerol concentration in the medium was 23.36 g L^{-1} . At fermentation time $t = 95.08\text{h}$, the glycerol concentration decreased to 9.56 g L^{-1} as well as the dissolved oxygen that reached 33% (Figure 15). This decrease is indicative that the cells were growing at this point, consuming the available carbon and oxygen in the medium, so a nutrient pulse was added, at $t = 95.50\text{h}$, and the speed rate was increased to 200 rpm, in order to improve oxygen availability. When adding the nutrient pulse, glycerol concentration increased to 25.22 g L^{-1} and the biomass concentration also increased, attaining 5.23 g L^{-1} , as observed in Figure 12. The same situation occurred at $t = 143.08\text{h}$, when glycerol concentration attained a value of 14.70 g L^{-1} . Another nutrient pulse was added, at $t = 144.42\text{h}$, and glycerol concentration increased to 33.34 g L^{-1} . From this point on, the biomass concentration presented little increase, since cells were at stationary phase and the excess carbon provided was used to produce storage lipids.

At the end of fermentation ($t = 195.25\text{h}$), glycerol concentration was 19.83 g L^{-1} . At this point, although the culture medium contained glycerol, the cells were not growing but were still metabolically active, since DO was 58%.

Total nitrogen content

Throughout fermentation, pulses of nutrients were added to the bioreactor in order to ensure that sufficient glycerol and other nutrients, such as nitrogen (provided by yeast extract and CSL in the culture medium), were available to *C. cohnii* cells. The total nitrogen content over fermentation time is represented in Figure 16.

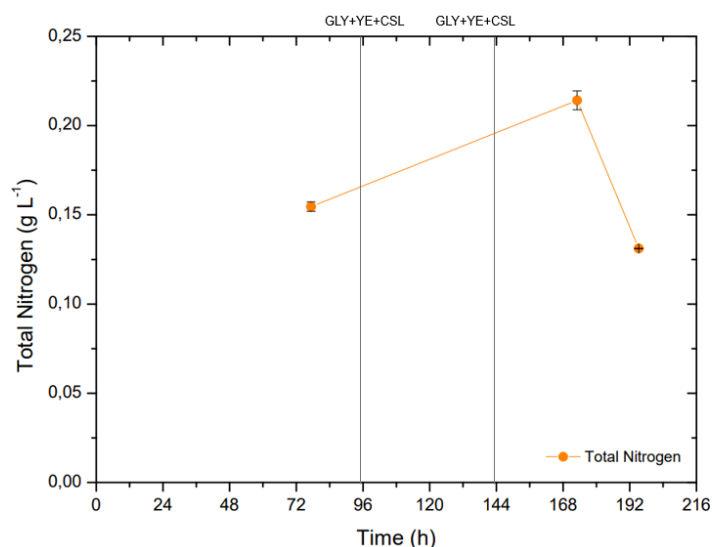


Figure 16 - Total nitrogen concentration in the culture medium over time in Assay I.

At $t = 77.33\text{h}$, a point that corresponds to the stationary phase of *C. cohnii* growth, the total nitrogen concentration was 0.15 g L^{-1} , indicating that nitrogen was being consumed for cellular division and proliferation (since the initial bioreactor medium contained 0.5 g L^{-1} YE and 5.5 g L^{-1} CSL). At $t = 173.08\text{h}$ the nitrogen content increased to 0.21 g L^{-1} due to addition of the nutrient pulse. At the end of the fermentation ($t = 195.25\text{h}$), the nitrogen content decreased to 0.13 g L^{-1} probably due to cell consumption of this nutrient. It is important to notice that was not possible to determine the total nitrogen content in all samples collected (only 3 samples were analysed). Therefore, it was not possible to carry out a detailed analysis of the nitrogen content from the data available.

Fatty acids profile analysis

In Table 3 the fatty acid profile of *C. cohnii* in Assay I is shown. The fatty acids composition was analysed when the microalga was in the stationary phase, so the data present in Table 3 corresponds to fermentation times in which the cells were in this growth phase.

Table 3 - Distribution of the most important fatty acids detected over fermentation time in Assay I, as percentage of total fatty acids (%(w/w) TFA). The obtained values resulted from an average of 2 duplicates.

	Time (h)	77.33	122.00	149.92	173.08	195.25
Fatty Acids	Capric (10:0)	0.73±0.00	0.53±0.00	0.57±0.01	0.5±0.05	0.61±0.11
	Lauric (12:0)	7.69±0.30	7.29±0.13	7.23±0.01	7.12±0.13	6.92±0.26
	Myristic (14:0)	20.38±0.81	20.40±0.39	20.11±0.02	20.65±0.09	20.92±0.01
	Myristoleic (14:1)	1.08±0.01	1.10±0.04	1.11±0.01	1.11±0.01	1.07±0.02
	Palmitic (16:0)	18.86±0.01	18.15±0.19	17.43±0.06	17.60±0.36	17.73±0.23
	Palmitoleic (16:1ω9)	2.80±0.01	3.05±0.01	3.01±0.03	2.97±0.14	2.83±0.02
	Stearic (18:0)	0.77±0.06	0.55±0.06	0.51±0.00	0.48±0.01	0.50±0.01
	Oleic (18:1ω9)	10.97±0.81	11.06±0.22	10.97±0.01	11.39±0.22	11.73±0.22
	Linoleic (18:2ω6)	0.16±0.00	0.13±0.01	0.39±0.01	0.32±0.01	0.26±0.02
	DPA (22:5ω3)	0.19±0.00	0.33±0.00	0.38±0.00	0.35±0.07	0.33±0.15
	DHA (22:6ω3)	36.86±0.57	37.79±0.39	38.15±0.04	37.46±0.51	36.96±0.28
	Others	0.11	0.08	0.14	0.04	0.14
	Saturated	48.43	46.92	45.84	46.36	46.67
Polyunsaturated	37.21	38.25	38.92	38.13	37.55	
Monounsaturated	14.85	15.22	15.10	15.47	15.63	

As observed in Table 3, DHA is by far the most abundant fatty acid resultant from *C. cohnii* metabolism, being the DHA proportion in TFA almost constant over the assay, accounting for about 38% (w/w) of TFA (as can be also observed in Figure 18, presented later in this section). At the end of fermentation ($t = 195.25\text{h}$), the DHA content was 36.96 % (w/w) of TFA. It is possible to observe that DHA is the major polyunsaturated fatty acid, present in meaningful quantities in the entire fermentation, which makes the purification of this compound easier. Other important fatty acids present include lauric (12:0), myristic (14:0), palmitic (16:0) and oleic (18:1 ω 9), that are present in higher percentages right after DHA, as noted in other studies (Mendes, et al., 2007). It is interesting to note that palmitoleic (16:1 ω 9) and linoleic (18:2 ω 6) acids account for more than 5% of the total fatty acid content of the profiles obtained by Safdar et al. (2017), yet are not even mentioned in other studies and are detected in relatively small amounts in this assay. Also, docosapentaenoic acid (22:5 ω 3) is absent in the same study mentioned but attained 0.33% (w/w) of TFA at the end of this fermentation. Other fatty acids detected in trace amounts are presented as “Others” in Table 3 and include arachidic (20:0), behenic (22:0) and α -linolenic (18:3 ω 3) acids. Considering all these observations, it can be concluded that the fatty acid profile of *C. cohnii* is highly variable and depends significantly upon strains, carbon sources, nitrogen sources and different stages of the cell’s growth cycle.

Along growth of *C. cohnii*, the fatty acid profile produced by the microalgae varies since this microorganism tends to decrease the production of short chain saturated fatty acids over time by synthesizing, from these, polyunsaturated fatty acids, that include DHA. According to data in Table 3, this result is observed, and more saturated fatty acids are detected in early fermentation time (48.43% (w/w) TFA) than at the end of the assay (46.67%(w/w) TFA). On the other hand, less polyunsaturated saturated fatty acids are detected in the beginning of the stationary phase (37.21% (w/w) TFA) than at a more final phase of the fermentation (38.13% (w/w) TFA at $t = 173.08\text{h}$), when the lipid production was at the maximum.

Through the obtained fatty acid profile of *C. cohnii* it was possible to calculate the TFA content, in percentage (w/w) of DCW, and TFA productivity over cultivation time. This data is shown in Figure 17.

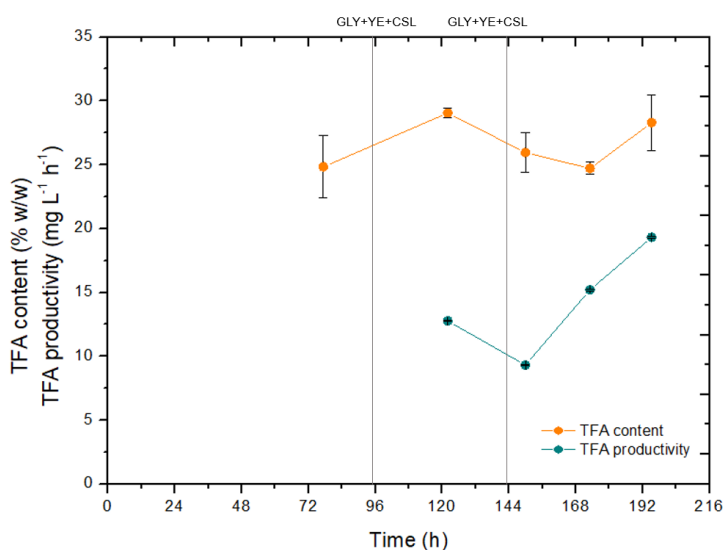


Figure 17 - Total fatty acid content and productivity in Assay I.

As observed in Figure 17, at the end of batch phase ($t = 77.33\text{h}$), the TFA content attained 24.84% (w/w) of DCW. The highest TFA content was 29.05% (w/w) of DCW, achieved at $t = 122.00\text{h}$, hours after the first nutrient pulse was added to the bioreactor. At the end of the fermentation ($t = 195.25\text{h}$), the TFA content reached 28.29% (w/w) of DCW, corresponding to a lipid productivity of $19.31\text{ mg L}^{-1}\text{ h}^{-1}$, the highest productivity achieved during this assay.

Figure 18 illustrates the evolution of DHA content in biomass (% w/w DCW), DHA proportion in TFA (% w/w TFA), other fatty acids content (% (w/w) DCW) and DHA productivity in Assay I.

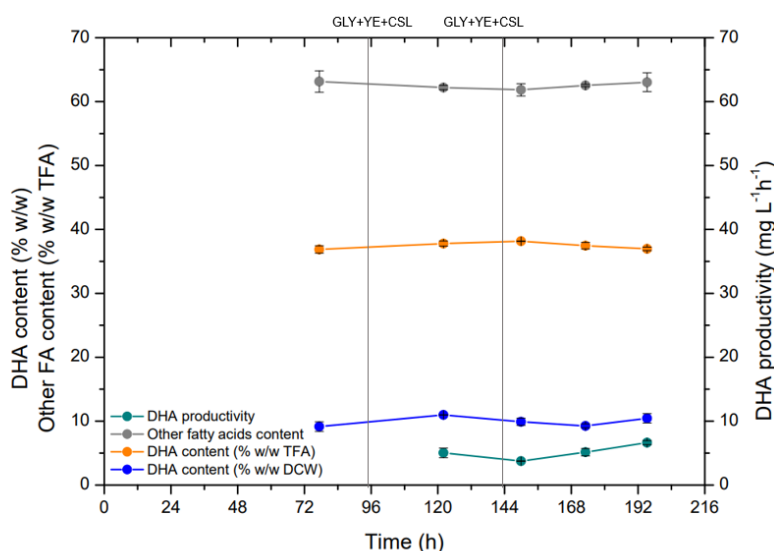


Figure 18 - DHA content and productivity and other fatty acid content in Assay I.

DHA content in biomass is almost constant throughout the fermentation, being the highest value of 10.98 % (w/w) of DCW, attained at $t = 122.00\text{h}$. As observed in Figure 18, also DHA proportion in TFA and DHA productivity were constant over time, being the final productivity in DHA of $6.64\text{ mg L}^{-1}\text{ h}^{-1}$. At the end of fermentation ($t = 195.25\text{h}$), the DHA content produced by *C. cohnii* was 10.46 % (w/w) of DCW and the DHA productivity reached the maximum value of $6.64\text{ mg L}^{-1}\text{ h}^{-1}$. The remaining fatty acids produced also remained stable over time, accounting for 62.5 % (w/w) of TFA.

When comparing to the literature, the results obtained in this assay were very satisfactory. Taborda et al. (2021) used crude glycerol as carbon source and attained a TFA content and productivity of 14.7 % (w/w) DCW and $3.19\text{ mg L}^{-1}\text{ h}^{-1}$, respectively. The DHA content and productivity obtained by Taborda et al. (2021) were 6.56 % (w/w) DCW and $1.42\text{ mg L}^{-1}\text{ h}^{-1}$, respectively. The results reported by these authors are lower than the ones obtained in Assay I, however the assays in the study mentioned were conducted in shake flasks and not in a bioreactor.

Flow Cytometry

Previous flow cytometry analysis was carried out using starter cultures before cultivation assays. In order to assess the feasibility of using flow cytometry to evaluate the physiological status of *C. cohnii*, in terms of membrane integrity and enzyme activity, cells in different conditions (healthy cells vs. dead cells) were stained and analysed by this technique. These controls were further used for comparison with data obtained during the microalgal cultivations conducted in this study (Assays I, II and III).

In order to analyse the cytograms obtained, the graph was divided into four quadrants, facilitating the analysis of cell viability and enzymatic activity. Therefore, the four quadrants will be referred to according to mathematical convention: the 1st quadrant lies in the top-right, the 2nd quadrant lies in the top-left, the 3rd quadrant lies in the bottom-left, and the 4th quadrant lies in the bottom-right.

The viability of using CFDA and PI was evaluated by verifying if the stained cells shifted clearly of quadrant in the graph, when under extreme conditions. To promote cell death and cell membrane damage, *C. cohnii* cells were heated in boiling water at 100°C for 15 min. A comparison was then made between cells in this extreme condition and cells that had not been manipulated in any way. Figure 19 illustrates the cytograms obtained for flow cytometric controls.

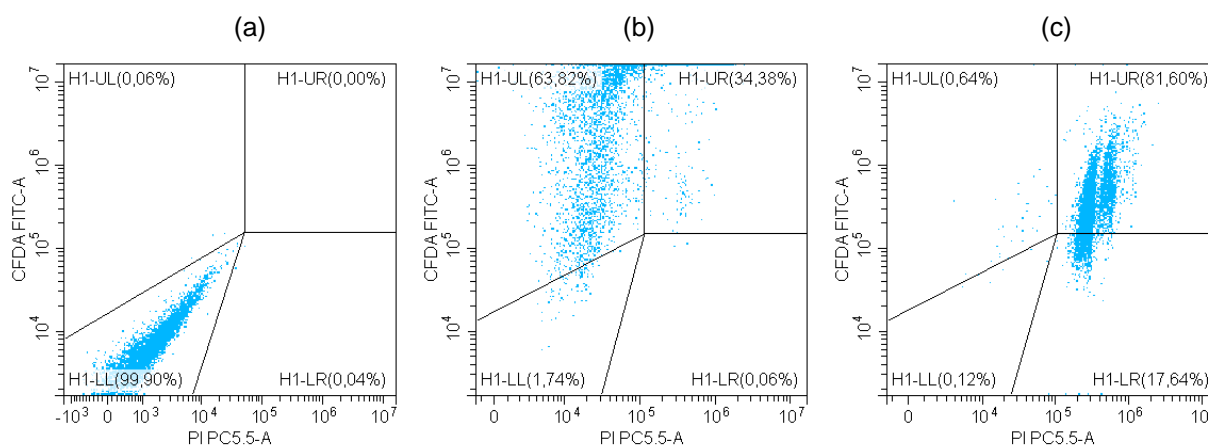


Figure 19 - Controls used for the CFDA (FITC-A) and PI (PC5.5-A) staining: (a) Unstained healthy culture (autofluorescence); (b) Healthy culture stained with both CFDA and PI; (c) Culture stained with CFDA and PI after boiling water bath.

Figure 19a shows the location of healthy unstained cells, which was kept constant over all the assays, in the 3rd quadrant. The healthy cells were then stained with CFDA and PI and the cytogram obtained is shown in Figure 19b. As observed, there is a significant number of cells in the 2nd quadrant (CFDA+/PI-), what indicates that most cells of this population presented enzymatic activity and intact cell membrane. In Figure 19c it is possible to observe that heat treatment increased the number of cells in the 1st (CFDA+/PI-) and 4th (CFDA-/PI+) quadrants, indicating that those cells were still active enzymatically, but the cell membranes got damaged.

According to these control experiments, double staining procedure with CFDA and PI coupled with flow cytometry allowed successful distinguish of *C. cohnii* subpopulations at different physiological states, in response to stressful environment conditions.

The cellular viability over time in Assay I was then analysed using this double staining method and the evolution of de cellular subpopulations is illustrated in Figure 20.

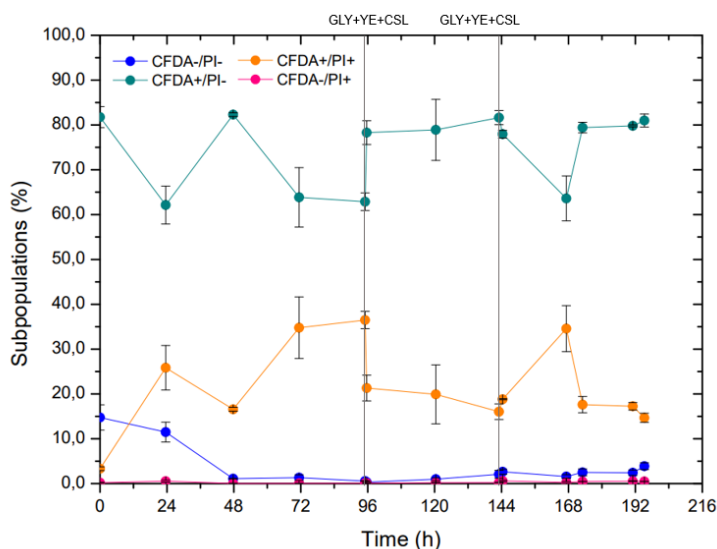


Figure 20 - *C. cohnii* cell subpopulations profiles for Assay I, after staining with CFDA and PI: subpopulation CFDA-/PI- includes cells with intact membrane and no enzymatic activity; subpopulation CFDA+/PI- includes cells with intact membrane and enzymatic activity; subpopulation CFDA+/PI+ includes cells with permeabilised membrane and enzymatic activity; subpopulation CFDA-/PI+ comprises cells with damaged membrane and no enzymatic activity.

As observed in Figure 20, the subpopulation CFDA+/PI- was predominant over the entire assay, indicating that most cells presented enzymatic activity and intact cell membrane (maximum value of 81.76% at $t = 0.00\text{h}$; minimum value of 62.13% at $t = 23.58\text{h}$), which demonstrates that the *C. cohnii* cells remain healthy during the assay. The subpopulation CFDA-/PI- with intact cellular membrane but with no enzymatic activity attained a maximum value of 14.75% at $t = 0.00\text{h}$ and a minimum value of 0.32% at $t = 95.67\text{h}$, which means that only a few cells presented no esterase activity during the assay. The subpopulation CFDA+/PI+, representing cells with enzymatic activity but permeabilized membrane, attained a maximum value of 36.48% at $t = 95.08\text{h}$ and a minimum value of 3.30% at $t = 0.00\text{h}$. It is possible to observe that the first nutrient pulse added to the bioreactor ($t = 95.67\text{h}$) generated the appearance of healthier cells, since the CFDA+/PI- population increased from 62.87% to 78.28% and the CFDA+/PI+ population decreased from 36.48% to 21.32%. Finally, the subpopulation CFDA-/PI+ rounded zero during the entire assay, so there were little cells with damaged cellular membrane and with no enzymatic activity (maximum value of 0.60% at $t = 144.42\text{h}$; minimum value of 0.03% at $t = 47.75\text{h}$).

These results demonstrate that during Assay I *C. cohnii* cells were not exposed to adverse conditions that could have compromised their enzymatic activity or cellular integrity.

3.1.2. *C. cohnii* biomass yield

The final DCW obtained in Assay I was 32.07g (after centrifugation and freeze-drying), measured gravimetrically and corresponding to the corrected value without moisture and ash, whose values were 2.94% and 4.74%, respectively. At the end of *C. cohnii* cultivation, the biomass concentration attained effectively was then 10.69 g L^{-1} , that corresponds to a slightly higher value than the one obtained through the correlation established for optical density (9.24 g L^{-1}).

3.1.3. Lipid extraction

The biomass obtained from the *C. cohnii* cultivation was used to carry out lipid extraction by accelerated solvent extraction and by Soxhlet conventional method, that, in this study, was considered the reference process for lipid quantification. For biomass obtained in Assay I, the yield in total lipids was determined (as described in section 2.7.1.), as well as the yield in TFA, DHA and fatty acids for biodiesel production (obtained through analysis by gas-liquid chromatography, described in section 2.5.7.). The obtained results are presented in Table 4.

Table 4 - Results obtained by ASE and Soxhlet extraction method, using hexane as solvent. The yields in total lipids, TFA, DHA and fatty acids for biodiesel production are presented in g/100g of dry biomass and without ash. The obtained values resulted from an average of 2 duplicates.

Lipid extraction method	Yield in Total Lipids	Yield in TFA	Yield in DHA	Yield in fatty acids for biodiesel production
Soxhlet	23.85±0.18	-	-	-
ASE	24.14±0.78	16.43±0.19	6.15±0.08	10.16±0.10

As observed in Table 4, the total lipids yield obtained by both extraction methods is similar. This is an advantage since it is possible to obtain an extraction yield through ASE similar to the one obtained through Soxhlet method, using a smaller amount of biomass, consuming less solvent and in less extraction time. However, the yields in TFA and DHA obtained by ASE (16.43% (w/w) DCW and 6.15% (w/w) DCW, respectively) present lower values than the percentages obtained by direct transmethylation of the biomass: 28.29% (w/w) DCW and 10.26% (w/w) DCW, for TFA content and DHA content in biomass, respectively (Figures 17 and 18). This indicates that ASE is not that effective in the recovery of the TFA present in biomass as direct transmethylation. Also, the higher percentages of yield in lipids relatively to the yield in TFA indicate that lipidic fractions resultant from ASE do not only contain fatty acids, but also other components such as pigments (carotenoids and chlorophylls), that may interfere and result in overestimated values.

For lipids extracted by Soxhlet from biomass obtained in Assay I it was not possible to determine the yield in TFA, DHA and fatty acids for biodiesel production, since profile evaluation of the obtained fatty acids was not performed, although it was carried out for Assays II and III.

The fatty acids profile obtained after analysis of lipids that resulted from ASE is shown in Figure 21.

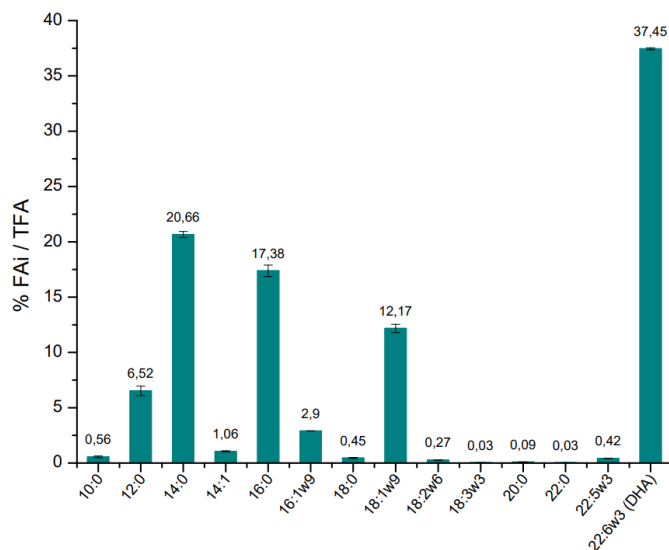


Figure 21 - Fatty acids profile of total lipids extracted by ASE from biomass obtained in Assay I. The obtained values resulted from an average of 2 duplicates.

It is possible to note that the profile presented in Figure 21 is very similar to the distribution of the most important fatty acids detected at the end of the fermentation, previously presented in Table 3, confirming the fatty acids profile.

3.1.4. Lipid fractionation with urea complexes

After *C. cohnii* cultivation, the fatty acids present in the collected biomass were subjected to ethylation, in order to obtain the correspondent FAEE, which were then fractionated, at different crystallization temperatures (-18°C, 4°C and 25°C), using urea complexes.

After crystallization with urea, the FAEE were separated in non-urea complexing and urea complexing fractions, according to the structure of these molecules. In fact, urea crystallizes in a hexagonal structure with channels of 8 to 12 Å diameter within the hexagonal crystals, whenever in presence of long straight-chain molecules. These channels are large enough to accommodate aliphatic chains of fatty acids. However, the presence of double bonds in the carbon chain increases the bulk of the molecule and reduces the likelihood of its complexation with urea, thus monoenes are more readily complexed as compared to dienes, which, in turn, are more readily complexed than trienes. As a result, urea complexes contain a high amount of saturated and monounsaturated fatty acids (Mendes, Lopes da Silva, & Reis, 2007).

Table 5 and Figure 22 show the FAEE profiles obtained before and after the separation process, using urea complexes, of biomass produced in Assay I.

Table 5 – *C. cohnii* FAEE % (w/w) in total fatty acid ethyl esters before and after crystallization with urea complexes of biomass obtained in Assay I. The obtained values resulted from an average of 2 duplicates.

FAEE	FAEE profile before urea crystallization	FAEE profile after urea crystallization					
		Non-urea complexing fraction			Urea complexing fraction		
		25°C	4°C	-18°C	25°C	4°C	-18°C
10:0	0.3±0.2	0.0±0.0	0.0±0.0	0.0±0.0	0.1±0.0	0.2±0.0	0.2±0.0
12:0	4.0±0.2	3.0±0.2	1.8±0.1	1.2±0.3	3.7±0.2	4.8±0.2	4.6±0.2
14:0	17.4±0.5	7.6±0.4	2.4±0.1	0.7±0.0	27.9±1.4	25.3±1.3	27.1±1.4
14:1	0.7±0.0	0.9±0.0	1.0±0.1	1.0±0.1	0.1±0.0	0.6±0.0	0.0±0.0
16:0	19.2±0.0	3.4±0.2	0.8±0.0	0.0±0.0	41.9±2.1	30.4±1.5	34.3±1.7
16:1ω9	2.7±0.1	2.5±0.1	2.1±0.1	2.0±0.1	1.7±0.1	3.0±0.2	2.6±0.1
18:0	0.7±0.0	0.0±0.0	0.0±0.0	0.0±0.0	1.5±0.1	1.1±0.1	1.2±0.0
18:1ω9	13.8±0.3	10.5±0.5	5.3±0.03	3.2±0.2	11.6±0.6	19.0±0.9	18.0±0.9
18:2ω6	0.2±0.0	0.3±0.0	0.3±0.0	0.3±0.0	0.1±0.0	0.2±0.0	0.2±0.0
22:5ω3	0.4±0.0	0.4±0.0	0.0±0.0	0.0±0.0	0.0±0.0	0.2±0.0	0.2±0.0
22:6ω3	40.6±0.3	71.8±3.6	86.3±4.3	91.6±4.6	11.4±0.6	15.1±0.8	11.6±0.6
Saturated	41.6	14.0	5.0	1.9	75.1	61.8	67.4
Monounsaturated	17.2	13.9	8.4	6.2	13.4	22.6	20.6
Polyunsaturated	41.0	72.5	86.3	91.6	11.4	15.3	11.8

As observed in Table 5, DHA ethyl ester (22:6ω3) was the highest FAEE obtained after ethylation and profile characterization of the fatty acids present in *C. cohnii* biomass, attaining a value of 40.6% (w/w) of total FAEE. Other fatty acids that presented significant concentrations were the palmitic (16:0), 19.2% (w/w) of total FAEE, myristic (14:0), 17.4% (w/w) of total FAEE, and oleic (18:1ω9), 13.8% (w/w) of total FAEE. The remaining FAEE were obtained in lower percentages.

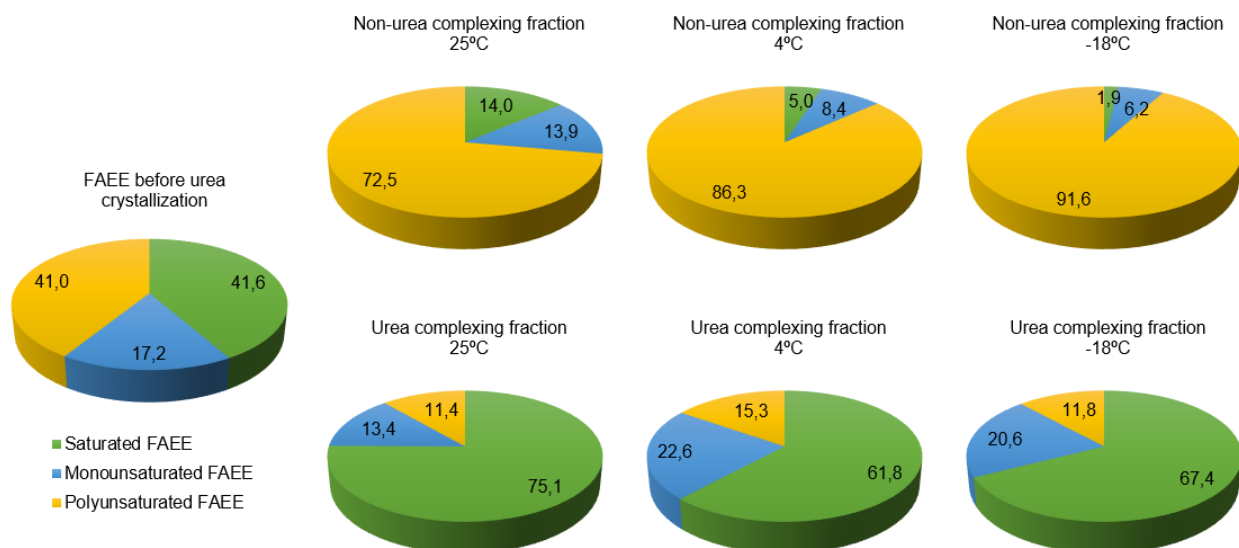


Figure 22 - Saturated, Monounsaturated and Polyunsaturated FAEE before and after urea crystallization of biomass obtained in Assay I, expressed in % (w/w) of total fatty acids ethyl esters.

According to Figure 22, the crystallization temperature that allowed the highest enrichment in PUFA ethyl esters was -18°C, that resulted in an increase from 41.0% (before urea complexation) to 91.6% (after urea complexation). As expected, the DHA proportion of total FAEE in the non-urea complexing fractions was much higher than in urea complexing fractions. It is possible to observe that DHA ethyl

ester was the dominant PUFA ethyl ester in the non-urea complexing fraction, being above 72% in all fractions, at different temperatures (Table 5). DHA ethyl ester percentage increased from 40.6% to 91.6%, after urea complexation at -18°C. These results also indicate that as the temperatures decrease from 25°C to -18°C, the DHA ethyl esters present a significant increase in the non-urea complexing fraction (71.8%, 86.3% and 91.6% of DHA ethyl esters, at 25°C, 4°C and -18°C, respectively) (Table 5). This increase was accompanied by a decrease of saturated and monounsaturated PUFA in this complexing fraction, whose values decreased from 14.0% to 1.9% (saturated FAEE) and 13.9% to 6.2% (monounsaturated FAEE), when the temperature ranged from -18°C to 25°C, respectively.

The proportions of saturated and monounsaturated FAEE in urea complexing fractions were higher at 25°C (75.1% + 13.4% = 88.5%), although the percentages obtained at 4°C and -18°C represented similar values (61.8% + 22.6% = 84.4% and 67.4% + 20.6% = 88.0%, at 4°C and -18°C, respectively) (Figure 22). The most prevalent saturated FAEE present in urea complexing fraction were myristic (14:0) and palmitic (16:0), that attained 27.9% and 41.9% of purity, respectively, after crystallization at 25°C. Stearic acid (18:0) was the only FAEE that was completely retained by urea molecules, although it is present at a low percentage in FAEE before crystallization. This FAEE attained percentages of 1.5%, 1.1% and 1.2% (at 25°C, 4°C and -18°C, respectively) in urea complexing fraction, but was not detected at all in the non-urea complexing fraction. The most prevalent monounsaturated FAEE in urea complexing fraction was oleic (16:1 ω 9) that attained 11.6% after crystallization at 25°C.

Concluding, the most effective separation of PUFA ethyl ester from saturated and monounsaturated FAEE was attained when performing urea crystallization at -18°C. This may be attributed to the lower urea solubility in aqueous ethanol, that allowed formation of more adduct between saturated FAEE and urea (Setywardhani, et al., 2015). At this temperature, a fraction with 91.6% purity of DHA ethyl ester was obtained, presenting a very satisfactory result, that accomplishes the purpose of this methodology. Also, a fraction rich in saturated and monosaturated FAEE was obtained, with potential use for biodiesel production.

3.1.5. Evaluation of the fraction for biodiesel production

As referred in section 1.2.2., biodiesel must meet strict parameters in order to be commercialized in European Union. Thus, the urea complexing fractions (rich in saturated and monounsaturated fatty acids) that were obtained after fractionation process at different temperatures, for biomass produced in Assay I, were then studied to assure they are appropriate and meet the parameters described in standard EN 14214 for biodiesel production.

Table 6 shows the theoretical estimated values for each fraction, calculated by equations mentioned in section 2.9. for the following parameters: viscosity, specific gravity, cetane number, iodine value and polyunsaturated ethyl esters content.

Table 6 - Theoretical estimate of FAEE quality for biodiesel production, according to EN 14214. The obtained values were determined through the Average Unsaturation (AU) calculation.

Parameter	Estimated values			Limit EN 14214
	25°C	4°C	-18°C	
Viscosity (mm ² s ⁻¹)	4.689	4.483	4.628	3.50 – 5.00
Specific Gravity (g cm ⁻³)	0.877	0.879	0.878	0.86 – 0.90
Cetane Number	57.408	55.234	56.768	>51.00
Iodine Value	73.696	97.941	80.836	<120.00
Polyunsaturated (≥4 double bonds) ethyl esters (% (w/w))	11.400	15.300	11.800	<1.00
AU	0.820	1.146	0.916	-

As observed in Table 6, all the estimated values for viscosity, specific gravity, cetane number and iodine value are within the regulations established by the European standard EN 14214. However, a considerable amount of polyunsaturated (≥4 double bonds) ethyl esters are still present in all FAEE urea complexing fractions. Therefore, an additional reaction step (for example, hydrogenation reaction) should be considered to reduce them to a level lower than 1% (w/w) and, consequently, allow the use of this lipidic fractions for biodiesel production.

3.2. Assay II

In Assay II the carbon source used was sugarcane molasses, that was previously hydrolysed, and the fermentation process was carried out and monitored as previously described in the Methodology.

3.2.1. *C. cohnii* bioreactor fermentation

Dry cell weight and biomass productivity

The progress of *C. cohnii* optical density and the cell count performed by the flow cytometer is represented in Figure 23. The vertical trait corresponds to the only nutrient pulse added throughout this fermentation, containing in its composition hydrolysed sugarcane molasses (SM), yeast extract (YE) and corn steep liquor (CSL).

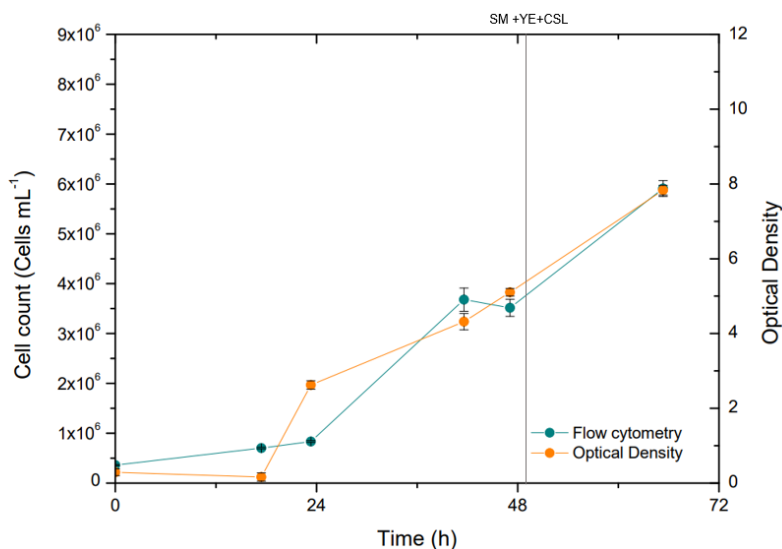


Figure 23 - *C. cohnii* cell count performed by flow cytometry and optical density (corrected) obtained in Assay II.

The data presented in Figure 23 was converted into *C. cohnii* biomass concentration, through the application of the correlations mentioned before. Figure 24 illustrates the evolution of DCW over time.

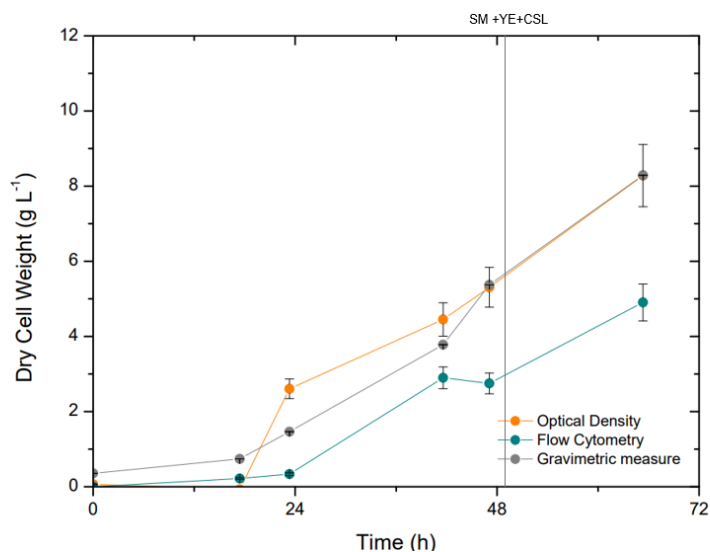


Figure 24 - Evolution of *C. cohnii* biomass concentration over fermentation time in Assay II.

Once again, as observed in Figure 24, flow cytometry underestimated the cell growth over time, thus, the considered values in this study for DCW were the ones obtained through optical density. These values were used to calculate the natural logarithm profile of the biomass, shown in Figure 25.

When observing Figure 24 it is possible to confirm that the biomass data obtained through optical density is very similar to the biomass growth profile obtained by gravimetric measure of the cells over time (this measure was only performed in this assay, when using sugarcane molasses as carbon source, as mentioned in the Methodology). However, the pellets of biomass obtained for this measure (after centrifugation and disposal of the residual medium in the sample) continued to present a dark colour, indicative of the presence of sugarcane molasses. This may indicate that the culture medium formulation interfered with the estimation of biomass concentration, that may be overestimated in this assay.

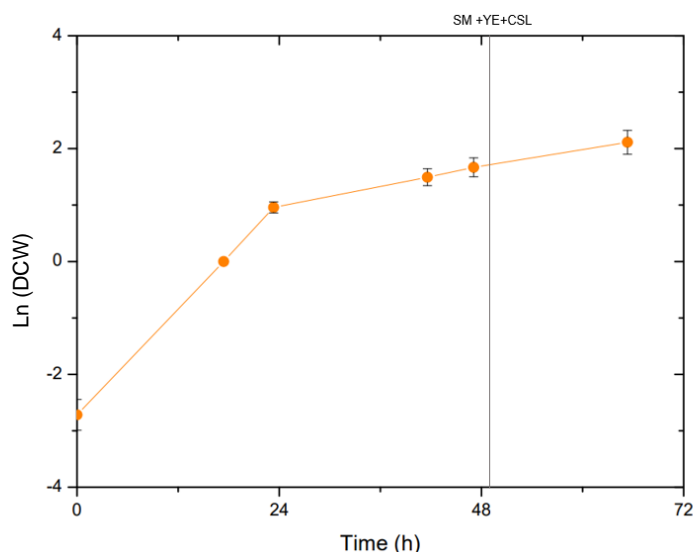


Figure 25 - Natural logarithm profile the biomass over time in Assay II.

As observed in Figure 25, the culture presents an exponential growth (between 0.0h and 23.33h), however, the produced biomass attained lower concentration than the biomass obtained in Assay I, probably because the fermentation time was shorter. No lag phase was observed in this assay, since *C. cohnii* preferentially consume glucose, being already adapted to the carbon source used. The specific growth rate in this assay was 0.1572 h^{-1} (calculated as shown in Annex III). At $t = 23.33\text{h}$, the stationary phase was attained, reaching at that time a biomass concentration of 2.61 g L^{-1} . As observed in Figure 24, the maximum *C. cohnii* biomass concentration was 8.28 g L^{-1} , attained at the end of the fermentation ($t = 65.33\text{h}$). The average productivity in biomass was $12.57 \text{ mg L}^{-1} \text{ h}^{-1}$.

In this assay only one nutrient pulse was added to the bioreactor, at $t = 49.17\text{h}$, and it is possible to observed through Figure 24 that the biomass concentration increased from 5.31 to 8.28 g L^{-1} after the pulse addition. This result indicates that at the last point of this cultivation the cells were still growing, since the biomass concentration was still improving. Therefore, if the fermentation had been extended and another nutrient pulse was added, the prolongation of the stationary phase would result in higher biomass production and, consequently, in major lipid production by *C. cohnii* cells. However, it was decided to stop the fermentation at this point since the profile of biomass concentration was similar to

the profile obtained in Assay I and a concentration of 8.28 g L^{-1} was already reached, what constitutes a reasonable amount.

When comparing these results with the ones obtained in Assay I, it is possible to conclude that the final biomass concentration attained when using sugarcane molasses is lower, since in Assay I the concentration obtained was 9.24 g L^{-1} (obtained by optical density correlation). The average productivity in biomass in this assay ($12.57 \text{ mg L}^{-1} \text{ h}^{-1}$) was lower than in Assay I ($46.97 \text{ mg L}^{-1} \text{ h}^{-1}$), probably because the fermentation time was shorter, and the stationary phase was still occurring when the culture was stopped. Taborda et al. (2021) conducted assays in shake flasks and obtained 3.91 g L^{-1} when using hydrolysed sugarcane molasses as carbon source, which presented a lower concentration value than the one obtained in this assay. Nevertheless, fermentations in bioreactor and fed-batch regime allow higher DCW.

Carbon source consumption

The glucose and fructose concentrations over time are represented in Figure 26, as well as the speed rate and dissolved oxygen in the culture medium are illustrated in Figure 27.

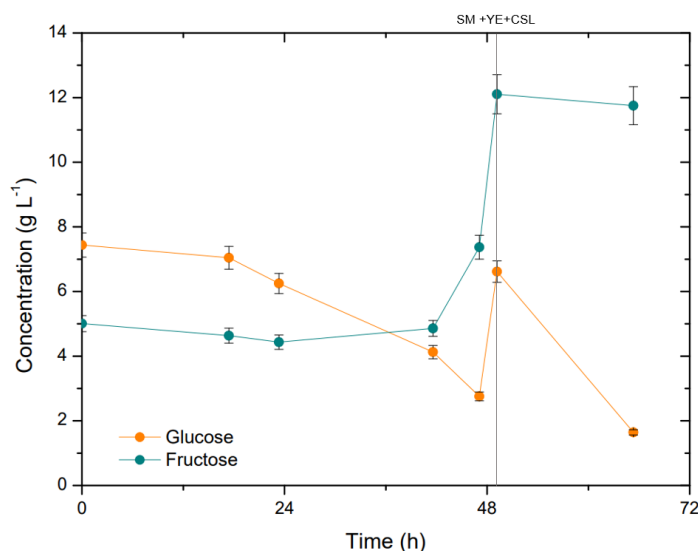


Figure 26 - Glucose and fructose concentrations in the culture medium over time in Assay II.

As observed in figure 26, the initial glucose concentration in the medium was only 7.44 g L^{-1} and the initial fructose concentration was 5.01 g L^{-1} . These concentrations were low given that an initial glucose concentration of 10 g L^{-1} was intended (20 g L^{-1} of total sugars). Thus, this carbon limitation may have compromised biomass growth and lipid accumulation. This low concentration of initial carbon sources may have occurred due to an excessive dilution of sugarcane molasses added to the bioreactor. As described in Methodology, sugarcane molasses is highly concentrated, and its sugar composition may vary along time.

It is also important to consider that the results presented in Figure 26 were obtained after conducting the fermentation, not allowing real-time quantification. Thus, in order to obtain an immediate quantitative notion of glucose concentration in the medium, rapid-contact strips for glucose detection were used to assess the glucose content in the medium. This method did not allow an exact quantification of glucose in the culture medium, only to detect the presence of this sugar.

According to Figure 26, the fructose concentration was constant over time, given that this sugar is not consumed by *C. cohnii*.

For carbon supply in this fermentation, it is possible to conclude that the hydrolysis of sucrose in glucose and fructose was complete, since there was no sucrose in the samples analysed, reason why this sugar is not represented in Figure 26. However, when there is complete hydrolysis of sucrose, it would be expected that the same concentration of glucose and fructose (50% glucose and 50% fructose) would be obtained at the starting point of fermentation, when the cells are inoculated, which, in fact, does not occur. The initial concentration of glucose in the culture medium is superior to the fructose concentration ($7.44 \text{ g L}^{-1} > 5.01 \text{ g L}^{-1}$). A possible explanation for this result may be related with the presence of CSL in the culture medium, whose composition contains free reducing sugars, such as glucose (Liggett & Koffler, 1948). Possibly there is interference of the sugars present in CSL, that do not include fructose, with the glucose that resulted from hydrolysis, resulting in a higher concentration of glucose in the culture medium.

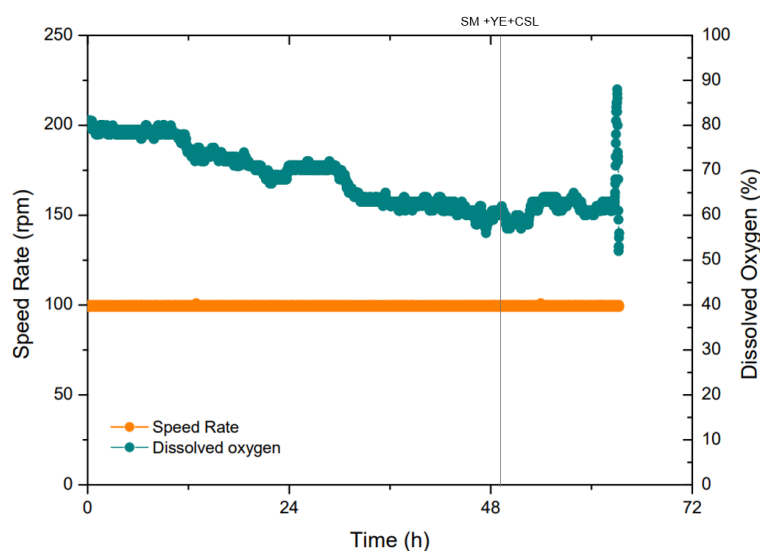


Figure 27 - Speed rate and dissolved oxygen over time in Assay II.

At fermentation time $t = 47.08\text{h}$, the glycerol concentration decreased to 2.76 g L^{-1} . This decrease is indicative that the cells were consuming the carbon present in the medium, although the dissolved oxygen was about 60% at this point, as observed in Figure 27. Therefore, at $t = 49.17\text{h}$ a nutrient pulse was added, in order to provide more glucose and nutrients to the cells. When adding the nutrient pulse, glucose concentration increased to 6.62 g L^{-1} and the biomass concentration also increased from 5.31 g L^{-1} to 8.28 g L^{-1} (last fermentation point, $t = 65.33\text{h}$), as observed in Figure 24. At the end of fermentation ($t = 65.33\text{h}$), glucose concentration was 1.64 g L^{-1} , what indicates that cells were exhausting the carbon source, that attained a very low concentration, compromising lipid production by the microalgae.

As observed in Figure 27, the speed rate was constant over all fermentation, rounding 100 rpm, and the dissolved oxygen decreased slowly over time, declining from an initial percentage of 81% to 52% at the end of the fermentation. Dissolved oxygen never reached values below 52% (lowest value verified at $t = 63.23\text{h}$). Since the cells were growing and consuming the glucose in the medium, the oxygen was

supposed to be consumed over time as well, what does not occur in this case, which could be due to a malfunctioning in the oxygen electrode.

The fermentation stopped at $t = 65.33\text{h}$ when 8.28 g L^{-1} of biomass were attained. Although a significant amount of biomass was produced, the production and accumulation of lipids by cells was not efficient (as discussed later in this section), probably due to the presence of little glucose in the medium. This lack of carbon induced a situation of stress in the cells that led to the consumption of the reserve lipids already accumulated, thus reducing the amount of reserve lipids in cells at the end of fermentation.

Total nitrogen content

In Assay II, a single nutrient pulse was added to the culture, in order to ensure that sufficient glucose and other nutrients, such as nitrogen (provided by YE and CSL in the culture medium), were available for the cells to grow. The total nitrogen content over fermentation is represented in Figure 28.

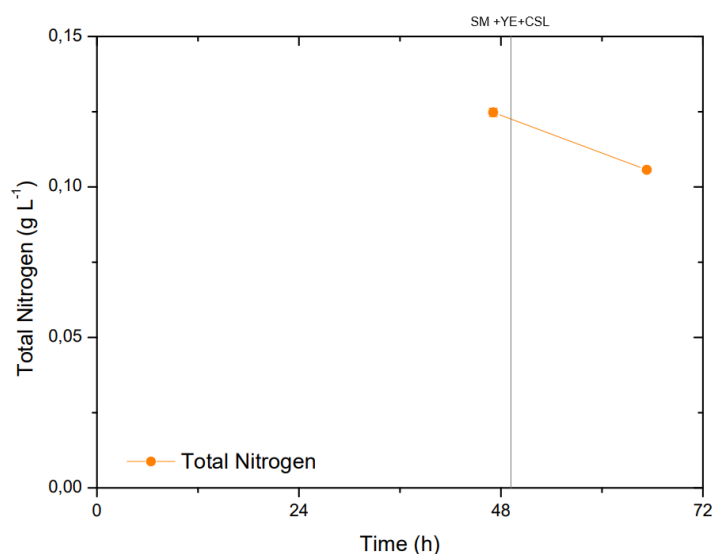


Figure 28 - Total nitrogen concentration in the culture medium over time in Assay II.

At $t = 47.08\text{h}$, a point that corresponds to the stationary phase of *C. cohnii* growth, the total nitrogen concentration was 0.125 g L^{-1} , what indicates that nitrogen is being consumed for cellular division and proliferation (since the initial bioreactor medium contained 0.5 g L^{-1} YE and 5.5 g L^{-1} CSL). Despite the addition of a nutrient pulse at $t = 49.17\text{h}$, at the end of the fermentation ($t = 65.33\text{h}$) the nitrogen content decreased to 0.106 g L^{-1} , indicating the consume of this nutrient by cells.

Fatty acids profile analysis

Table 7 contains the evolution of the fatty acid profile of *C. cohnii* in Assay II. Since this fermentation was shorter in time, as well as the stationary phase in *C. cohnii* growth, only two samples were collected during this assay, in order to evaluate the fatty acids production by cells.

Table 7 - Distribution of the most important fatty acids detected over fermentation time in Assay II, as percentage of total fatty acids (%(w/w) TFA). The obtained values resulted from an average of 2 duplicates.

	Time (h)	47.08	65.33
Fatty Acids	Capric (10:0)	0.00±0.00	0.52±0.74
	Lauric (12:0)	2.77±0.08	6.23±1.01
	Myristic (14:0)	17.14±0.25	21.03±1.36
	Myristoleic (14:1)	0.00±0.00	0.00±0.00
	Palmitic (16:0)	26.53±0.01	22.82±0.10
	Palmitoleic (16:1ω9)	0.96±0.02	1.63±0.17
	Stearic (18:0)	1.66±0.11	0.91±0.08
	Oleic (18:1ω9)	11.80±0.10	10.58±0.22
	Linoleic (18:2ω6)	1.63±0.35	1.03±0.00
	DPA (22:5ω3)	0.00±0.00	0.12±0.16
	DHA (22:6ω3)	37.10±0.35	34.64±0.54
	Others	0.00	0.48
Saturated	48.10	51.51	
Polyunsaturated	38.73	35.79	
Monounsaturated	12.76	12.21	

As noted in Assay I, over the cultivation of *C. cohnii* the production of short-chain saturated fatty acids decreased, given that there were synthesized, from these, polyunsaturated fatty acids, that include DHA. However, in Assay II the opposite was observed. In fact, as observed in Table 7, at $t = 47.08$ h, the percentage of polyunsaturated fatty acids presented a total of 38.73% (w/w) of TFA, that decreased to 35.79% (w/w) of TFA at the end of the fermentation. On the other hand, the percentage of short-chain saturated fatty acids increased from 48.10% (w/w) of TFA to 51.51% (w/w) of TFA. This may have occurred due to the lack of glucose in the culture medium, that was present in very low concentrations during the entire assay. The initial glucose present in the medium allowed the cells to grow and lipid production and accumulation, however, these lipids were consumed by cells whenever the carbon concentration decreased to almost 0 g L^{-1} . Thus, it is possible to explain the growth of biomass that was observed over time, which, however, did not imply an equivalent production and accumulation of lipids, that was the main objective of this assay.

Despite this, as observed in Table 7, DHA is still by far the most abundant fatty acid resultant from *C. cohnii* metabolism, being the DHA proportion in TFA 37.10% (w/w) at $t = 47.08$ h and 34.64% (w/w) at $t = 65.33$ h (as can also be observed in Figure 25).

In similarity to Assay I, other important fatty acids present include lauric (12:0), myristic (14:0), palmitic (16:0) and oleic (18:1ω9), that are present in higher percentages right after DHA, as noted in other studies as well. Also, palmitoleic (16:1ω9) and linoleic (18:2ω6) acids were detected in small amounts in this study, as in Assay I, although not even mentioned in other studies. Docosapentaenoic acid (22:5ω3) attained only 0.12% (w/w) of TFA at the end of this fermentation, not representing a very reliable value since the standard deviation obtained represents more than 100% of the percentage calculated of this fatty acid.

Considering all these observations, it is possible to conclude, once again, that the fatty acid profile of *C. cohnii* is highly variable and depends greatly upon strains, carbon sources, nitrogen sources, and different stages of its growth cycle. In this assay specifically, the glucose concentration was undoubtedly a limiting factor for the production and accumulation of lipids by the microalgae.

Through the fatty acid profile obtained in this assay, it was possible to calculate the TFA content, in % (w/w) of DCW, and TFA productivity over cultivation time. This data is shown in Figure 29.

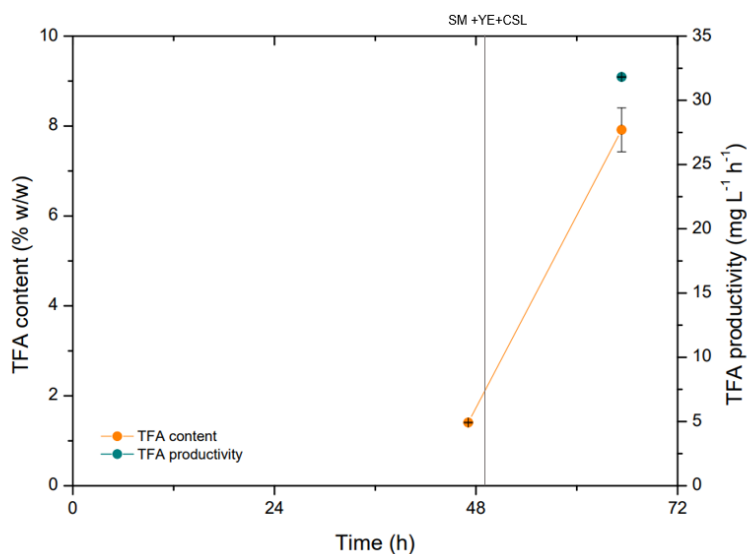


Figure 29 - Total fatty acid content and productivity in Assay II.

As observed in Figure 29, at the end of batch phase ($t = 47.08\text{h}$), the TFA content attained only 1.40% (w/w) of DCW. The highest TFA content was 7.92% (w/w) of DCW, achieved at the end of the fermentation ($t = 65.33\text{h}$), hours after the nutrient pulse was added to the bioreactor. At the end of the cultivation, a TFA productivity of $31.82\text{ mg L}^{-1}\text{ h}^{-1}$ was attained.

When using sugarcane molasses as carbon source, Taborda et al. (2021) attained a TFA content and productivity of 11.12 % (w/w) DCW and $2.00\text{ mg L}^{-1}\text{ h}^{-1}$, respectively. The TFA content obtained in the mentioned study was higher than the one obtained in Assay II, despite Taborda et al. (2021) conducted the cultivation in shake flasks and not in a bioreactor. However, a significantly lower productivity in TFA was reached in this study when comparing to Assay II, that reached a TFA productivity of $31.82\text{ mg L}^{-1}\text{ h}^{-1}$. These results point to the fact that the fermentation should definitely be extended, and more nutrient pulses should be provided to the culture in order to increase glucose concentration and improve lipid production and accumulation by cells.

Figure 30 illustrates the evolution of DHA content in biomass (% w/w DCW), DHA proportion in TFA, DHA content % (w/w) of DCW and DHA productivity in Assay II.

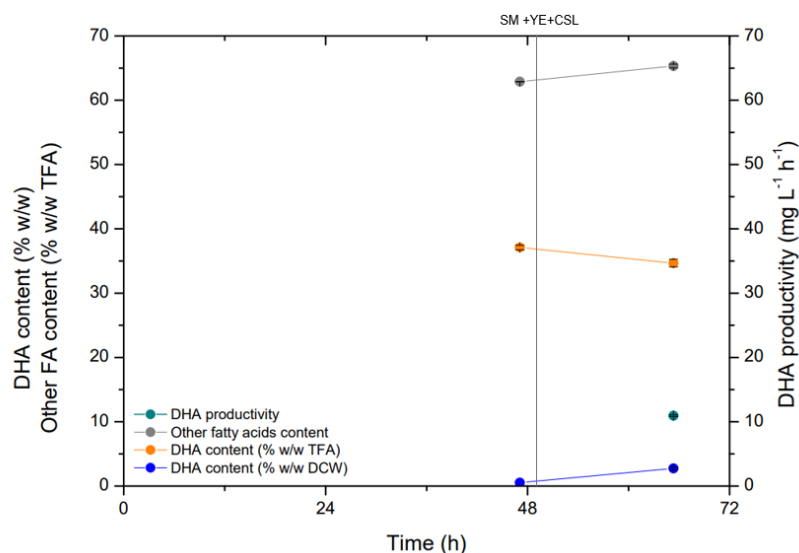


Figure 30 - DHA content and productivity and other fatty acid content in Assay II.

As observed in Figure 30, at the end of batch phase ($t = 47.08\text{h}$), the DHA content attained 0.52% (w/w) of DCW. The highest DHA content was 2.75% (w/w) of DCW, achieved at the end of the fermentation ($t = 65.33\text{h}$), hours after the nutrient pulse was added to the bioreactor. At this time, a DHA productivity of $10.94\text{ mg L}^{-1}\text{ h}^{-1}$ was attained. The remaining fatty acids produced remained stable in the stationary phase of *C. cohnii* growth, being around 62.90% (w/w) of TFA at $t = 47.08\text{h}$ and 65.32% (w/w) of TFA at the final point.

When comparing to the literature, Taborda et al. (2021) attained a DHA content and productivity of 5.51 % (w/w) DCW and $0.99\text{ mg L}^{-1}\text{ h}^{-1}$, respectively, when using sugarcane molasses as carbon source. The DHA content obtained in the mentioned study was higher than the one obtained in Assay II, despite Taborda et al. (2021) conducted the cultivation in shake flasks and not in a bioreactor. However, a significantly lower productivity in DHA was reached in this study when comparing to Assay II, that reached a DHA productivity of $10.94\text{ mg L}^{-1}\text{ h}^{-1}$.

In general, it is possible to verify that in Assay II the levels in TFA and DHA in the final biomass reached reduced values, but high productivities in TFA and DHA, what means that an extension of the assay would allow the achievement of better results, with a view to the objective of this work.

Flow Cytometry

According to the same control experiments described for Assay I, double staining procedure with CFDA and PI coupled with flow cytometry allowed successful distinguish of *C. cohnii* subpopulations at different physiological states, in response to stressful environment conditions.

The cellular viability over time in Assay II was then analysed using the double staining method with CFDA and PI and the evolution of cellular subpopulations is illustrated in Figure 31.

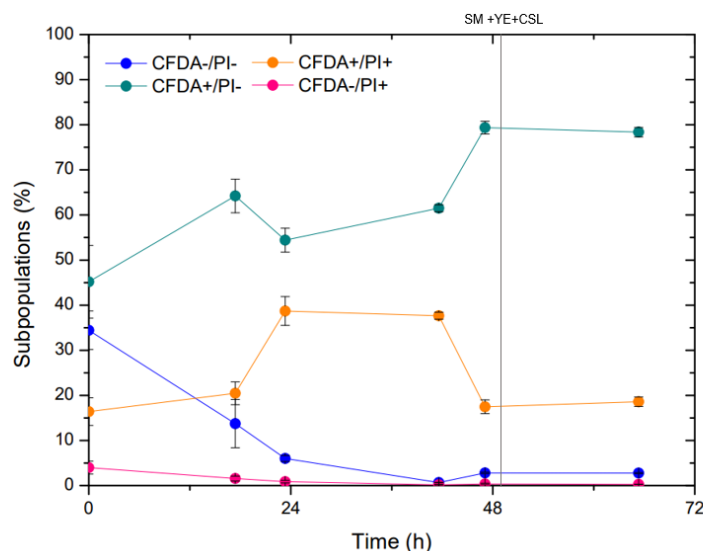


Figure 31 – *C. cohnii* cell subpopulations profiles for Assay II, after staining with CFDA and PI: subpopulation CFDA-/PI includes cells with intact membrane and no enzymatic activity; subpopulation CFDA+/PI- includes cells with intact membrane and enzymatic activity; subpopulation CFDA+/PI+ includes cells with permeabilised membrane and enzymatic activity; subpopulation CFDA-/PI+ comprises cells with damaged membrane and no enzymatic activity.

As observed in Figure 31, the subpopulation CFDA+/PI- was predominant over the entire assay, indicating that most cells presented enzymatic activity and intact cell membrane (maximum value of 79.36% at $t = 47.08\text{h}$; minimum value of 45.18% at $t = 0.00\text{h}$), which is a very satisfactory result demonstrating that the *C. cohnii* cells remain healthy during the assay. The subpopulation CFDA-/PI- with intact cellular membrane but with no enzymatic activity attained a maximum value of 34.43% at $t = 0.00\text{h}$ and a minimum value of 0.68% at $t = 41.58\text{h}$, which means that only a few cells presented no esterase activity during the assay. The subpopulation CFDA+/PI+, representing cells with enzymatic activity but permeabilized membrane, attained a maximum value of 38.70% at $t = 23.33\text{h}$ and a minimum value of 16.40% at $t = 0.00\text{h}$. It is possible to observe that the nutrient pulse added to the bioreactor ($t = 49.17\text{h}$) had no influence in the cell viability, since all four subpopulations presented no significant alterations in $t = 47.08\text{h}$ and $t = 65.33\text{h}$ (end of the cultivation). Finally, the subpopulation CFDA-/PI+ rounded zero during the entire assay, except at the beginning of the fermentation, so there were little cells with damaged cellular membrane and with no enzymatic activity (maximum value of 3.98% at $t = 0.00\text{h}$; minimum value of 0.27% at $t = 65.33\text{h}$).

These results demonstrate that *C. cohnii* cells were not exposed to adverse conditions, during Assay II, that could have compromised their enzymatic activity or cellular integrity. These results show that the cells were, generally, healthy during the entire assay, so the reduced lipid production occurred due to the lack of carbon in the bioreactor.

3.2.2. *C. cohnii* biomass yield

The final DCW obtained in Assay II was 23.53 g (after centrifugation and freeze-drying), measured gravimetrically and corresponding to the corrected value without moisture and ash, whose values were 0.19% and 4.23%, respectively. At the end of *C. cohnii* cultivation, the biomass concentration attained effectively was then 7.84 g L^{-1} , that corresponds to a slightly lower value than the one obtained through

the correlation established for optical density (8.28 g L^{-1}). This result may be related to the fact that sugarcane molasses is a substrate of very dark colour, which makes it difficult to read through optical density, leading to errors, as already mentioned previously.

3.2.3. Lipid extraction

The biomass obtained from the *C. cohnii* cultivation was used to carry out lipid extraction by accelerated solvent extraction and by Soxhlet conventional method. In Assay II, the yield in total lipids was determined (as described in section 2.7.1.), as well as the yield in TFA, DHA and fatty acids for biodiesel production (obtained through analysis by gas-liquid chromatography, described in section 2.5.7.). The obtained results are presented in Table 8.

Table 8 - Results obtained by ASE and Soxhlet extraction method, using hexane as solvent. The yields in total lipids, TFA, DHA and fatty acids for biodiesel production are presented in g/100g of dry biomass and without ash. The obtained values resulted from an average of 2 duplicates.

Lipid extraction method	Yield in Total Lipids	Yield in TFA	Yield in DHA	Yield in fatty acids for biodiesel production
Soxhlet	7.60±2.74	4.82±0.60	1.64±0.20	3.11±0.34
ASE	8.27±2.83	4.47±0.55	1.41±0.10	2.77±0.14

As observed in Table 8, the total lipids yields obtained by both extraction methods is similar, as well as the yield in TFA, DHA and in fatty acids for biodiesel production. This is an advantage since it is possible to obtain an extraction yield through ASE similar to the one obtained through Soxhlet method, using a smaller amount of biomass, consuming less solvent and in less extraction time.

Once again, the yields in TFA and in DHA obtained by Soxhlet (4.82% (w/w) DCW and 1.64% (w/w) DCW, respectively) and ASE (4.47% (w/w) DCW and 1.41% (w/w) DCW, respectively) present lower values than the percentages obtained by direct transmethylation of the biomass: 7.92% (w/w) DCW and 2.75% (w/w) DCW, for TFA content and DHA content in biomass, respectively (Figures 25 and 26). This result probably indicates that ASE and Soxhlet extraction methods are not as effective in the recovery of the total fatty acids present in biomass as direct transmethylation. Also, the higher percentages of yield in lipids relatively to the yield in TFA indicate that lipidic fractions resultant from ASE and Soxhlet extraction do not only contain fatty acids, but also other components such as pigments, that may interfere and result in overestimated values. Nevertheless, the lipid production in Assay II was much lower when comparing to Assay I, as already noticed with the previous results.

The fatty acids profile obtained after the analysis of the total lipids resulting from Soxhlet extraction and ASE is represented in figure 32.

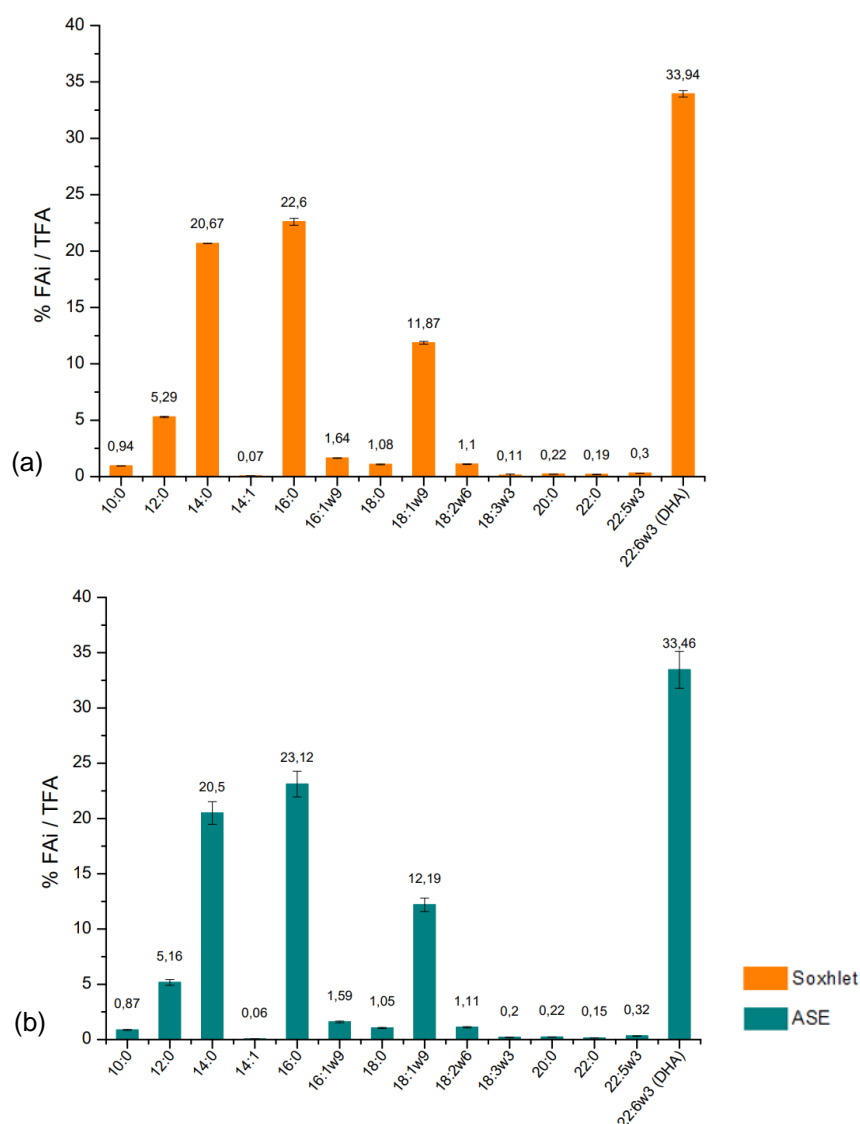


Figure 32 - Fatty acids profile of total lipids extracted in Assay II: (a) Soxhlet Extraction; (b) ASE. The obtained values resulted from an average of 2 duplicates.

It is possible to observe that the profiles presented in Figure 32 are analogous to the distribution of the most important fatty acids detected at the end of the fermentation, previously presented in Table 7. Besides, both fatty acids profiles presented in Figure 32, for total lipids resulted from Soxhlet extraction and ASE, are very similar taking into account the standard deviations. Therefore, it is possible to conclude that extraction by ASE allowed an efficient extraction of the fatty acids present in the biomass produced, when comparing to Soxhlet extraction.

In general, it is possible to conclude that cultivation of *C. cohnii* when using crude glycerol as carbon source was more effective and conducted to higher biomass concentration and lipid production than when performing the assay with sugarcane molasses. Therefore, as lipid production was reduced in this cultivation, fractionation using urea complexes was not performed for the biomass obtained in Assay II.

Also, since Assay II was conditioned by the lack of carbon in the growth medium, optimizing the fermentation using sugarcane molasses as carbon source is a suggestion for the future. However, this low-cost carbon source does not present itself as such a competitive resource when comparing to other

low-cost carbon sources, such as crude glycerol, since only 50% of its sugars are consumed by the microalgae. The fructose resultant from hydrolysis of sugarcane molasses is present in the culture medium during the entire fermentation given that *C. cohnii* does not consume it. Thus, an alternative approach, in order to use the totality of sugars present in hydrolysed sugarcane molasses would be to perform a mixed cultivation of *C. cohnii* and another microorganism with industrial relevance that would not interfere with the growth of the microalgae and whose preferable substrate is fructose. Therefore, a suggestion for future work would be the research of symbiotic microorganisms with the species *C. cohnii* whose preferred carbon source is fructose, not consuming glucose.

3.3. Assay III

In order to produce biomass to further study lipid fractionation under optimized conditions, a third assay was carried out. The carbon source used was crude glycerol, since it was the substrate that enabled a higher biomass and lipid production in the previous assays. The fermentation was carried out and monitored as previously described in the Methodology.

Also, the produced biomass was further used to improve the fractionation process, using urea complexes, in order to attain a more effective separation between non-urea complexing fraction (rich in polyunsaturated fatty acids, such as DHA) and urea complexing fraction (rich in saturated and monounsaturated fatty acids, for biodiesel production purposes).

3.3.1. *C. cohnii* bioreactor fermentation

Dry cell weight and biomass productivity

Cell growth of *C. cohnii* was carried out by optical density and cell count by flow cytometer as it is represented in Figure 33. The vertical traits correspond to the nutrient pulses added throughout this fermentation, containing in its composition crude glycerol (GLY), yeast extract (YE) and corn steep liquor (CSL). As in previous assays, the nutrient pulses were added whenever the residual glycerol concentration in the broth decreased below 10 g L⁻¹ or the dissolved oxygen increased above 80%.

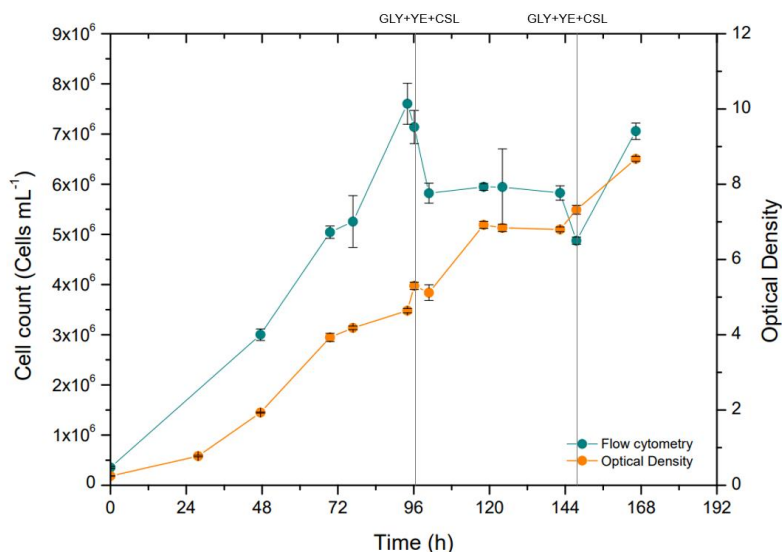


Figure 33 - *C. cohnii* cell count performed by flow cytometry and optical density (corrected) obtained in Assay III.

The data presented in Figure 33 was converted into *C. cohnii* biomass concentration, by using the correlations mentioned previously. Figure 34 shows the biomass concentration over the fermentation time.

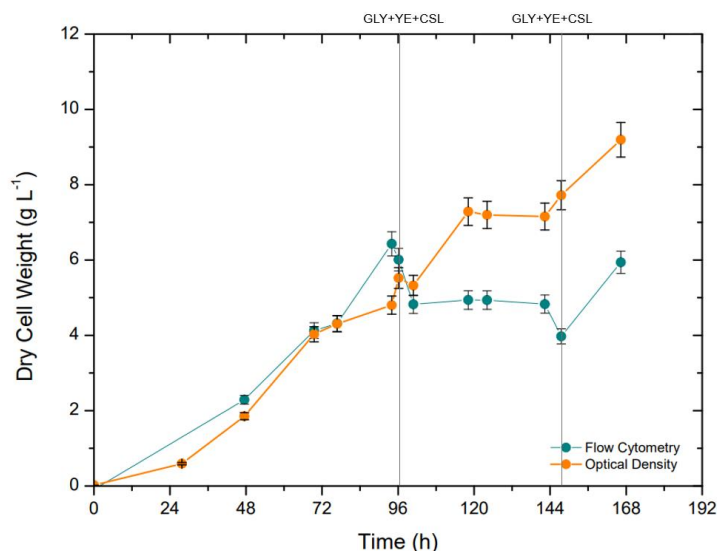


Figure 34 - Evolution of *C. cohnii* biomass concentration over fermentation time in Assay III.

Once again, as observed in Figure 34, after 72 h of fermentation, cell growth obtained by flow cytometry was underestimated when compared to optical density, thus, the considered values in this study for DCW were the ones obtained through optical density. These values were used to calculate the natural logarithm profile of the biomass, shown in Figure 35.

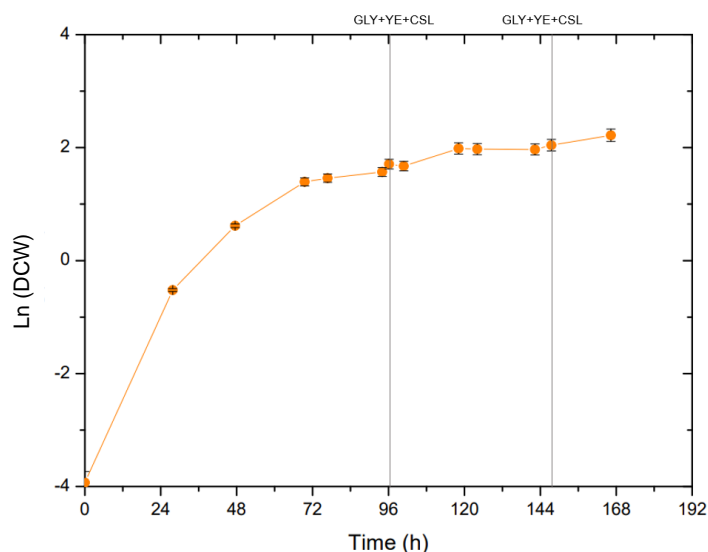


Figure 35 - Natural logarithm profile of the biomass over time in Assay III.

As observed in Figure 35, the *C. cohnii* culture presents an exponential growth. The culture entered the exponential phase at $t = 27.75\text{h}$. At $t = 69.50\text{h}$, the stationary phase was attained, reaching at that time a biomass concentration of 4.30 g L^{-1} . The specific growth rate calculated, as shown is Annex III, was 0.0457 h^{-1} . As observed in Figure 34, the maximum *C. cohnii* biomass concentration attained was at the end of the fermentation ($t = 166.33\text{h}$) and reached 9.19 g L^{-1} . The average productivity in biomass in this assay was $55.16\text{ mg L}^{-1}\text{ h}^{-1}$.

According to Figures 34 and 35, it is possible to observe that each time a nutrient pulse was added, the biomass concentration increased, allowing prolongation of stationary phase and, consequently, resulting in higher amounts of biomass and higher lipid production. The first nutrient pulse, added to the

bioreactor at $t = 96.16\text{h}$, led to an increase in biomass from 4.80 g L^{-1} ($t = 94.00\text{h}$) to 5.52 g L^{-1} ($t = 96.2\text{h}$) and the second one, added at $t = 146.33\text{h}$, allowed an improvement of biomass production from 7.15 g L^{-1} ($t = 142.33\text{h}$) to 7.72 g L^{-1} ($t = 147.50\text{h}$).

When comparing these results with the ones obtained in Assay I, it is possible to conclude that the final biomass concentration attained in Assay III is very similar, since in Assay I the concentration obtained was 9.24 g L^{-1} (obtained by optical density correlation). However, the average productivity in biomass in this assay ($55.16\text{ mg L}^{-1}\text{ h}^{-1}$) was higher than in Assay I ($46.97\text{ mg L}^{-1}\text{ h}^{-1}$), since Assay III was shorter in time than Assay I and yet allowed production of similar biomass concentration.

Carbon source consumption

The glycerol concentration over time is represented in Figure 36, as well as the speed rate and dissolved oxygen in the culture medium is illustrated in Figure 37.

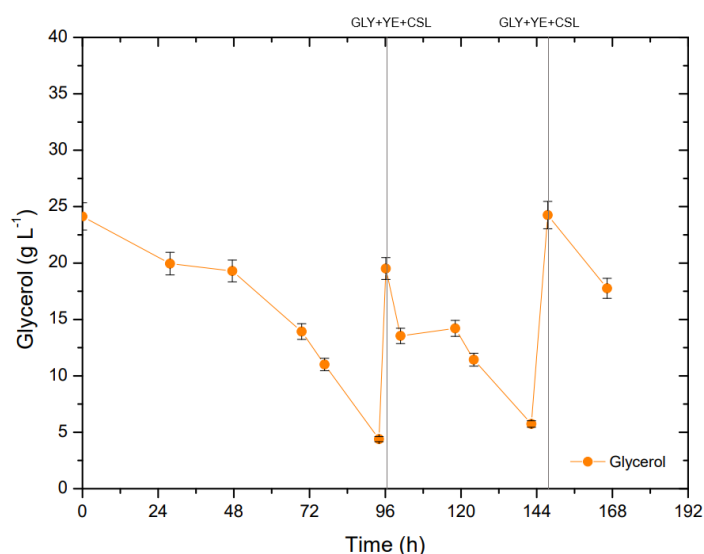


Figure 36 - Glycerol concentration in the culture medium over time in Assay III.

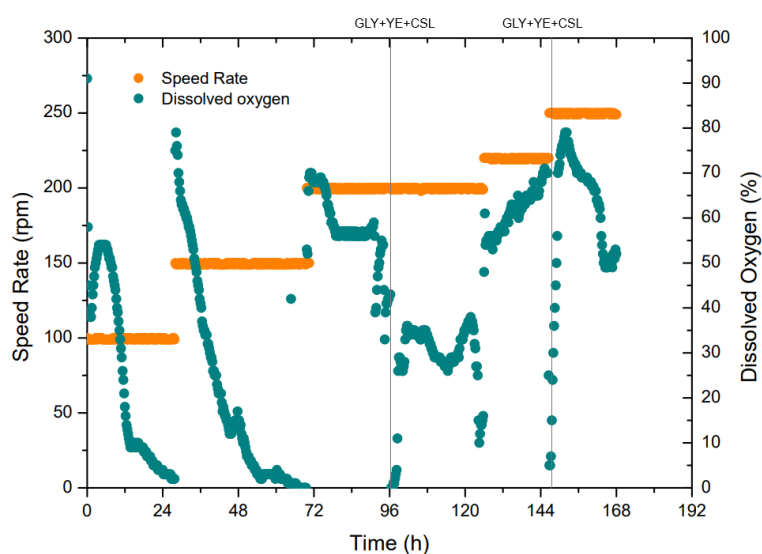


Figure 37 - Speed rate and dissolved oxygen over time in Assay III.

As observed in Figure 36, the initial glycerol concentration in the medium was 24.13 g L⁻¹. At fermentation time $t = 94.00\text{h}$, the glycerol concentration decreased to 4.39 g L⁻¹. This decrease is indicative that the cells were consuming the carbon present in the medium, so a nutrient pulse was added ($t = 96.17\text{h}$) in order to provide more glycerol and nutrients to the cells. When adding the nutrient pulse to the bioreactor, glycerol concentration increased to 19.52 g L⁻¹ and the biomass concentration also increased from this point, attaining 5.52 g L⁻¹, as observed previously in Figure 34. The same situation occurred at $t = 142.33\text{h}$, when the glycerol concentration attained a value of 5.74 g L⁻¹. Another nutrient pulse was added ($t = 146.33\text{h}$) and glycerol concentration increased to 24.25 g L⁻¹.

As observed in Figure 37, the assay started at a speed rate of 100 rpm, however the dissolved oxygen rapidly decreased to 2%, at $t = 27.75\text{h}$. Therefore, the speed rate was increased to 200 rpm, to increase oxygen availability, that went up to 75%. At $t = 66.50\text{h}$, there was no dissolved oxygen detected in the broth, so the speed rate was increased to 200 and the percentage of dissolved oxygen in the culture improved to 53%. When the first nutrient pulse was added ($t = 96.17\text{h}$), the dissolved oxygen was once again 0%, but this percentage increase to approximately 30% after some hours, what indicates that cells were adapting to the addition of glycerol and nutrients to the culture, as well as oxygen availability. At $t = 126.00\text{h}$, speed rate was increased to 220 rpm and again, at $t = 146.75\text{h}$, to 250 rpm, when the second nutrient pulse was added. It is important to stress *C. cohnii* cells are highly sensitive to agitation and the use of high-speed rates may cause cell damage.

At the end of the fermentation ($t = 166.33\text{h}$), glycerol was present in the culture medium at a concentration of 17.76 g L⁻¹. At this point, cells were still metabolically active and consuming carbon as dissolved oxygen was 52% at the end of the fermentation. *C. cohnii* cells were at stationary phase and the excess carbon provided was used to produce storage lipids. At the end of the fermentation there were favourable conditions for the cells to remain healthy, given that there was still carbon in the medium, the dissolved oxygen was adequate, and the biomass concentration was increasing. If the fermentation stops under adverse conditions, storage lipids are consumed by the cells and lipid production may decrease dramatically.

Total nitrogen content

In Assay III, pulses of nutrients were added to the bioreactor in order to ensure that sufficient glycerol and other nutrients, such as nitrogen (provided by yeast extract and CSL in the culture medium), were available for the cells to grow. The total nitrogen content over time is represented in Figure 38.

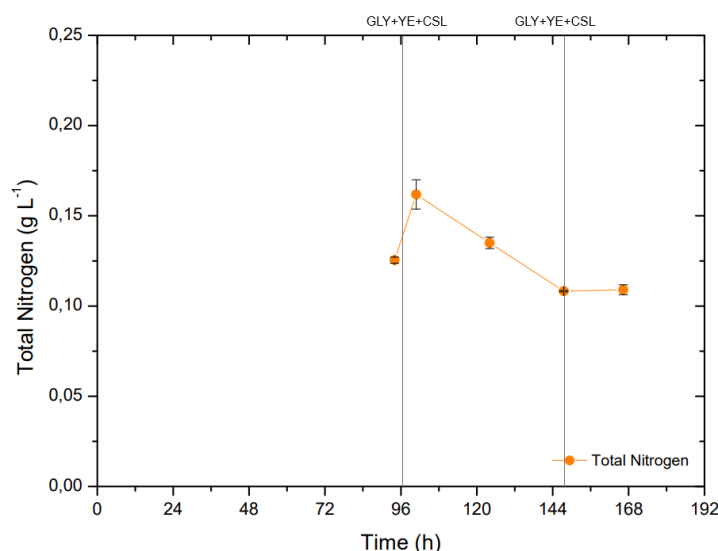


Figure 38 - Total nitrogen concentration in the culture medium over time in Assay III.

At $t = 94.00\text{h}$, a point that corresponds to the stationary phase of *C. cohnii* growth, the total nitrogen concentration was 0.13 g L^{-1} , what indicates that nitrogen is being consumed for cellular division and proliferation (since the initial bioreactor medium contained 0.5 g L^{-1} YE and 5.5 g L^{-1} CSL). At $t = 100.83\text{h}$ the nitrogen content increased to 0.16 g L^{-1} due to the nutrient pulse addiction. The total nitrogen suffered then a decrease, attaining a concentration of 0.11 g L^{-1} at $t = 147.5\text{h}$, that maintained constant until the end of the fermentation ($t = 166.33\text{h}$), despite the second nutrient pulse addiction at $t = 146.33\text{h}$. The fact that total nitrogen concentration in the broth did not increase when the pulse was added suggests that cells were under nitrogen starvation leading to instant consumption of nitrogen in the medium.

Fatty acids profile analysis

Table 9 shows the fatty acid profile of *C. cohnii* in Assay III. The fatty acids composition was analysed when the microalga was in the stationary phase, so the data present in Table 9 corresponds to fermentation times in which the cells were in this growth phase.

Table 9 - Distribution of the most important fatty acids detected over fermentation time in Assay III, as percentage of total fatty acids (%(w/w) TFA). The obtained values resulted from an average of 2 duplicates.

	Time (h)	94.00	100.83	124.08	147.50	166.33
Fatty Acids	Capric (10:0)	1.17±0.04	1.43±0.13	1.18±0.00	1.03±0.00	1.11±0.03
	Lauric (12:0)	9.46±0.10	9.48±0.48	9.67±0.12	8.99±0.02	8.61±0.07
	Myristic (14:0)	21.60±0.03	20.62±0.79	21.22±0.10	20.55±0.16	20.30±0.12
	Myristoleic (14:1)	1.68±0.01	1.56±0.08	1.57±0.03	1.55±0.00	1.45±0.01
	Palmitic (16:0)	17.74±0.10	17.29±0.18	16.76±0.31	15.66±0.09	15.33±0.22
	Palmitoleic (16:1ω9)	4.10±0.03	3.90±0.14	3.92±0.02	3.82±0.00	3.48±0.03
	Stearic (18:0)	0.62±0.02	0.77±0.25	0.48±0.02	0.43±0.00	0.47±0.00
	Oleic (18:1ω9)	11.79±0.17	12.31±1.29	11.10±0.13	11.28±0.08	11.17±0.34
	Linoleic (18:2ω6)	0.29±0.06	0.50±0.25	0.23±0.02	0.49±0.03	0.38±0.02
	DPA (22:5ω3)	0.24±0.01	0.21±0.01	0.29±0.01	0.34±0.00	0.37±0.00
	DHA (22:6ω3)	31.10±0.57	31.81±0.36	33.42±0.17	35.71±0.04	37.70±0.19
	Others	0.20	0.11	0.16	0.14	0.17
Saturated	50.59	49.59	49.31	46.6	45.82	
Polyunsaturated	31.63	32.52	33.94	36.54	38.45	
Monounsaturated	17.57	17.77	16.59	16.65	16.10	

According to data present in Table 9, and as already observed in the Assays I, *C. cohnii* tends to decrease the production of short-chain saturated fatty acids over time by synthesizing, from these, polyunsaturated fatty acids, that include DHA. According to data in Table 9, it is observed that more saturated fatty acids are detected in early fermentation time (50.59% (w/w) TFA) than at the end (45.82% (w/w) TFA). On the other hand, less polyunsaturated saturated fatty acids are detected in the beginning of the stationary phase (31.63% (w/w) TFA) than at the end of the fermentation (38.45% (w/w) TFA).

Also, it is possible to observe that DHA is the major polyunsaturated fatty acid, present in meaningful quantities in the entire fermentation, which makes the purification of this compound easier. DHA is the most abundant fatty acid resultant from *C. cohnii* metabolism, in similarity with the previous assays, being possible to notice that the DHA proportion in TFA fluctuates from 31.10% (w/w) TFA, at $t = 94.00\text{h}$, to 37.70% (w/w) TFA, at the end of the fermentation ($t = 166.33\text{h}$).

Other important fatty acids produced by the microalgae in this assay include lauric (12:0), myristic (14:0), palmitic (16:0) and oleic (18:1 ω 9), that are present in higher percentages right after DHA, as noted in Assay I and in other studies (Mendes, et al., 2007). It is also possible to observe that these fatty acids were produced in this assay in larger amounts than in Assay I, what may result in a richer fraction of saturated and monounsaturated fatty acids, for biodiesel production purposes. Also, and once again, palmitoleic (16:1 ω 9) and linoleic (18:2 ω 6) are detected in relatively small amounts in this assay. Docosapentaenoic acid (22:5 ω 3) attained 0.37% (w/w) of TFA at the end of this fermentation.

Through the fatty acid profile obtained in this assay, and presented in Table 3, it was possible to calculate the TFA content, in % (w/w) of DCW, and TFA productivity over cultivation time. This data is shown in Figure 39.

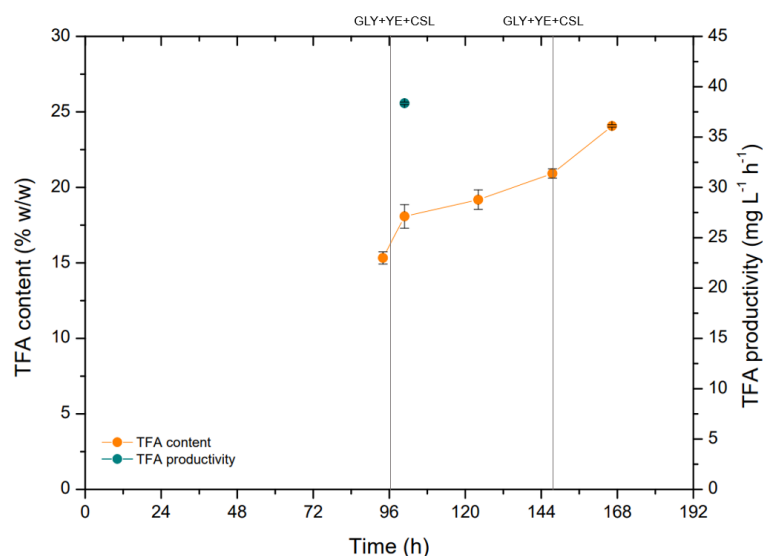


Figure 39 - Total fatty acid content and productivity in Assay III.

As observed in Figure 39, at the end of batch phase ($t = 94.00\text{h}$), the TFA content attained 15.33% (w/w) of DCW. The highest TFA content was 24.07% (w/w) of DCW, achieved at end of the cultivation ($t = 166.33\text{h}$). In general, TFA content increased progressively during the assay and presented an improve whenever a nutrient pulse was added. The first nutrient pulse, added to the bioreactor at $t = 96.16\text{h}$, conducted to an increase in TFA content from 15.33% (w/w) of DCW ($t = 94.00\text{h}$) to 18.08%

(w/w) of DCW ($t = 100.83\text{h}$) and the second one, added at $t = 146.33\text{h}$, allowed an improvement of TFA content from 19.18% (w/w) of DCW ($t = 124.08\text{h}$) to 20.92% (w/w) of DCW ($t = 147.50\text{h}$). The highest productivity in TFA attained was $38.36\text{ mg L}^{-1}\text{ h}^{-1}$ at $t = 100.83\text{h}$, right after the first nutrient pulse was added to the bioreactor. The final productivity in TFA was $10.52\text{ mg L}^{-1}\text{ h}^{-1}$.

Figure 40 illustrates the evolution of DHA content in biomass (% w/w DCW), DHA proportion in TFA, DHA content % (w/w) of DCW and DHA productivity in Assay III.

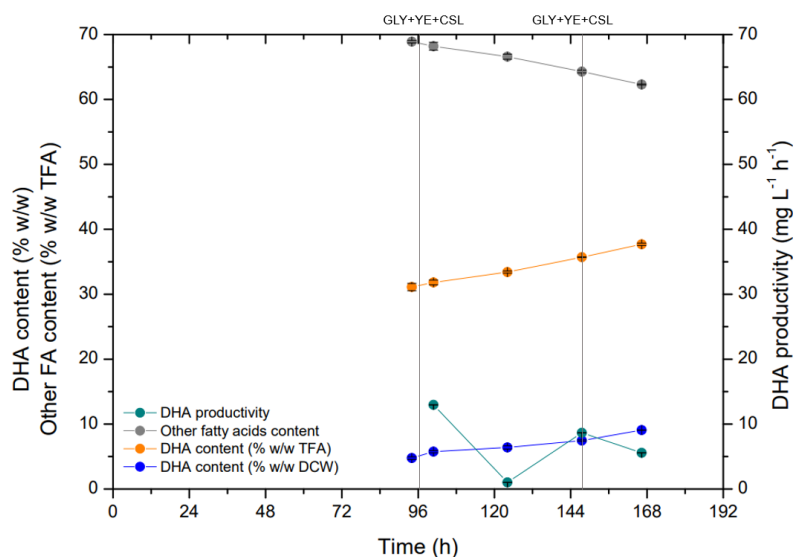


Figure 40 - DHA content and productivity and other fatty acid content in Assay II.

As observed in Figure 40, at the end of batch phase ($t = 94.00\text{h}$), the DHA content attained 4.77% (w/w) of DCW. The highest DHA content was 9.07% (w/w) of DCW, achieved at the end of the fermentation ($t = 166.33\text{h}$). It is possible to observe in Figure 40 that the DHA content in TFA and DCW increased over time, as already noticed. The highest productivity in DHA attained was $12.95\text{ mg L}^{-1}\text{ h}^{-1}$ at $t = 100.83\text{h}$, after the first nutrient pulse was added to the bioreactor, when the cells were at the beginning of the stationary phase.

The remaining fatty acids produced presented a decrease in its content over time when cells were in the stationary phase. These other fatty acids content decreased from 68.90% (w/w) of TFA, at $t = 94.00\text{h}$, to 62.30% (w/w) of TFA, at the final point ($t = 166.33\text{h}$).

When comparing the results obtained in this assay with Assay I, it is possible to conclude that in this assay a lower TFA content was obtained at the end of the fermentation (24.07% (w/w) of DCW), since in Assay I it was achieved a content of 28.29% (w/w) of DCW. Also, a lower DHA content was achieved (9.07% (w/w) of DCW) when comparing to Assay I (10.46% (w/w) of DCW). However, when comparing to Assay I, in this assay a higher proportion of polyunsaturated fatty acids in TFA was attained at the end of the fermentation (38.45% (w/w) of TFA) and a lower proportion of saturated and monounsaturated fatty acids was obtained (45.82% (w/w) of TFA and 16.10% (w/w) of TFA, respectively), what may facilitate DHA purification.

Flow Cytometry

According to the same control experiments described for Assay I, double staining procedure with CFDA and PI coupled with flow cytometry allowed successful distinguish of *C. cohnii* subpopulations at different physiological states, in response to stressful environment conditions.

The cellular viability over time in Assay III was analysed using this double staining method and the evolution of de cellular subpopulations is illustrated in Figure 41.

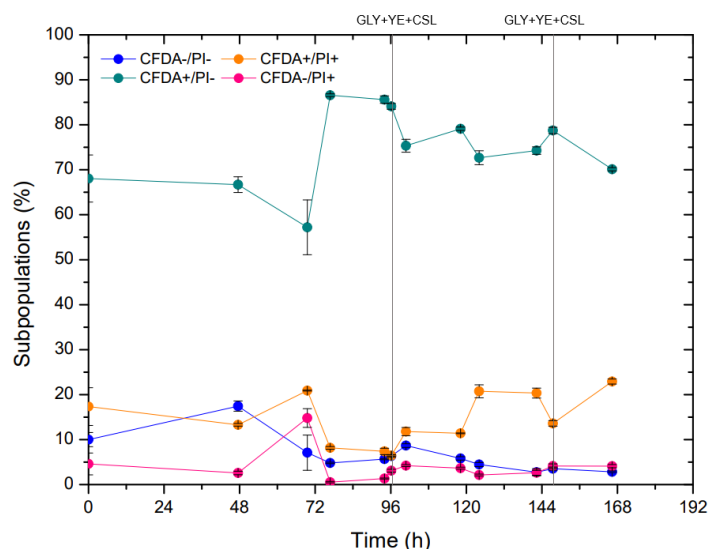


Figure 41 - *C. cohnii* cell subpopulations profiles for Assay III, after staining with CFDA and PI: subpopulation CFDA-/PI- includes cells with intact membrane and no enzymatic activity; subpopulation CFDA+/PI- includes cells with intact membrane and enzymatic activity; subpopulation CFDA+/PI+ includes cells with permeabilised membrane and enzymatic activity; subpopulation CFDA-/PI+ comprises cells with damaged membrane and no enzymatic activity.

As observed in Figure 41, the subpopulation CFDA+/PI- was predominant during the entire assay, indicating that most cells presented enzymatic activity and intact cell membrane (minimum value of 57.21% at $t = 69.50\text{h}$; maximum value of 85.61% at $t = 94.00\text{h}$), demonstrating that the *C. cohnii* cells remain healthy during the assay. The subpopulation CFDA-/PI- with intact cellular membrane but with no enzymatic activity attained a maximum value of 17.45% at $t = 47.5\text{h}$ and a minimum value of 2.75% at $t = 142.33\text{h}$, which means that a few cells presented no esterase activity during the assay. The subpopulation CFDA+/PI+, representing cells with enzymatic activity but permeabilized membrane, attained a maximum value of 22.93% at the end of the cultivation ($t = 166.33\text{h}$) and a minimum value of 8.16% at $t = 76.75\text{h}$. Finally, the subpopulation CFDA-/PI+ in this assay attained low values during the entire assay, so a few cells presented damaged cellular membrane and with no enzymatic activity during the cultivation. The maximum value for this subpopulation was 14.80% (at $t = 69.50\text{h}$), probably because of the decreasing in glycerol that was observed at this point, that may have compromised the integrity of cells. Also, as mentioned above, at $t = 69.50\text{h}$, the CFDA+/PI- subpopulation was present in 57.21%, what still represents a significative amount of healthy and intact cells.

Is possible to conclude that there were more damaged cells during this assay than in the previous ones, what might be an explanation for the less lipid production by *C. cohnii* in Assay III when comparing to Assay I. However, this lower lipid production was not significant. And since Assay III was shorter in

time, a prolongation of the cultivation, through adding another nutrient pulse, might have resulted in higher biomass production and, thus, more lipid accumulation, as already suggested.

Therefore, these results demonstrate that *C. cohnii* cells were not exposed to severe conditions, during Assay III, that could have compromised their enzymatic activity or cellular integrity.

3.3.2. Lipid extraction

The biomass obtained from the *C. cohnii* cultivation was then used to carry out lipid extraction by accelerated solvent extraction and by Soxhlet conventional method. In Assay III, the yield in total lipids was determined (as described in section 2.7.1.), as well as the yield in TFA, DHA and fatty acids intended for biodiesel production (obtained through analysis by gas-liquid chromatography, described in section 2.5.7.). The obtained results are presented in Table 10.

Table 10 - Results obtained by ASE and Soxhlet extraction method, using hexane as solvent. The yields in total lipids, TFA, DHA and fatty acids for biodiesel production are presented in g/100g of dry biomass and without ash. The obtained values resulted from an average of 2 duplicates.

Lipid extraction method	Yield in Total Lipids	Yield in TFA	Yield in DHA	Yield in fatty acids for biodiesel production
Soxhlet	26.63±1.58	10.01±1.11	3.62±0.45	32.32±0.66
ASE	24.17±0.57	12.26±0.80	4.55±0.32	31.83±0.54

As observed in Table 10, the total lipids yield obtained by Soxhlet extraction (26.63% (w/w) DCW) was slightly higher than by ASE (24.17% (w/w) DCW), but a standard deviation of 1.58 may be considered. Nevertheless, this presents as a positive result since it is possible to obtain an extraction yield through ASE equivalent to the one obtained through Soxhlet method, using a smaller amount of biomass, consuming less solvent and in less extraction time. It is also possible to observe that the total lipids yield obtained by ASE (24.17% (w/w) DCW) in this assay is similar to the one obtained in Assay I (23.85% (w/w) DCW for Soxhlet and 24.14% (w/w) DCW for ASE).

Once again, it was observed that the yields in TFA and DHA obtained by Soxhlet extraction (10.10% (w/w) DCW and 3.62% (w/w) DCW, respectively) and by ASE (12.26% (w/w) DCW and 4.55% (w/w) DCW, respectively) present lower values than the percentages obtained by direct transmethylation of the biomass: 24.07% (w/w) DCW and 9.07% (w/w) DCW, for TFA content and DHA content in biomass, respectively (Figures 39 and 40). This result may indicate that ASE and Soxhlet extraction methods are not as effective in the recovery of the total fatty acids present in biomass as direct transmethylation. Also, the higher percentages of yield in lipids relatively to the yield in TFA indicate that lipidic fractions resultant from ASE and Soxhlet extraction do not only contain fatty acids, but also other components such as pigments (carotenoids and chlorophylls), that may interfere and result in overestimated values.

The fatty acids profile obtained after the analysis of the total lipids resulting from Soxhlet extraction and ASE is represented in Figure 42.

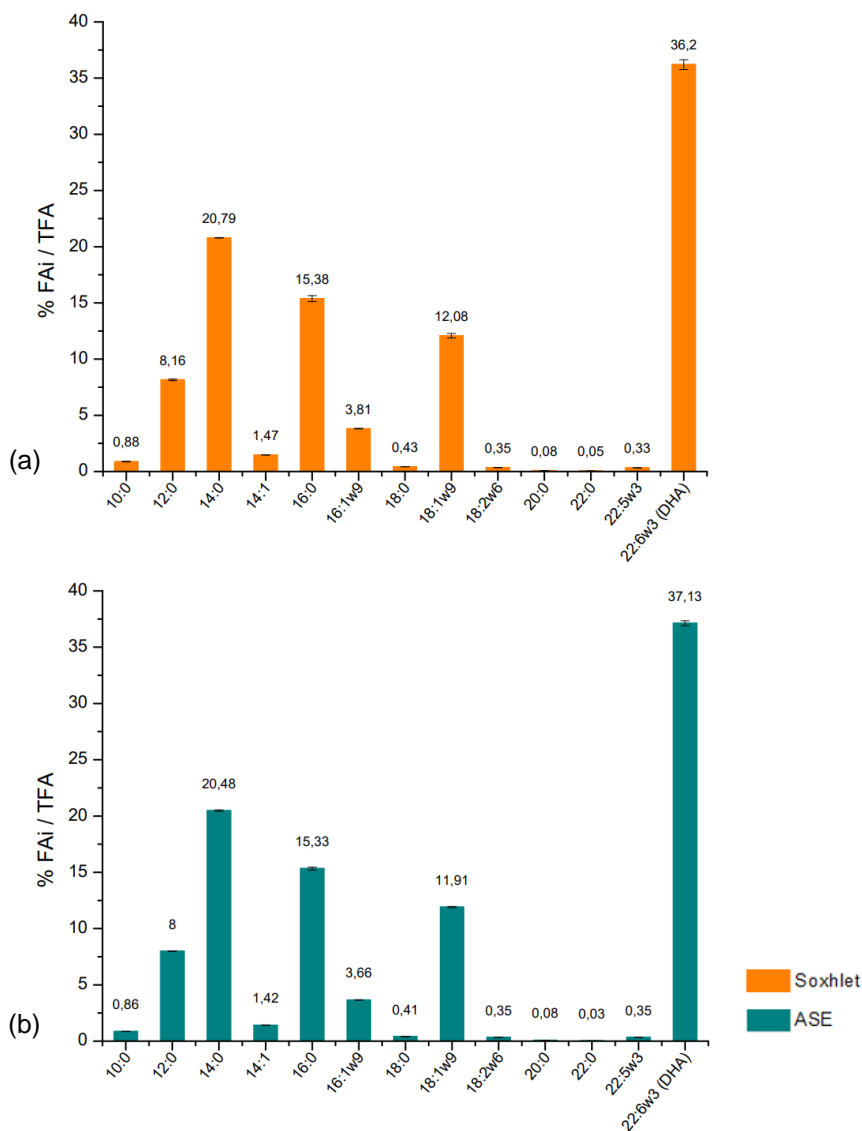


Figure 42 - Fatty acids profile of total lipids extracted in Assay III: (a) Soxhlet Extraction; (b) ASE. The obtained values resulted from an average of 2 duplicates.

It is possible to note that both profiles presented in Figure 42 are similar to the distribution of the most important fatty acids detected at the end of the fermentation, previously presented in Table 9. Besides, both fatty acids profiles presented in Figure 42, for total lipids resulted from Soxhlet extraction and ASE, are analogous to each other. Therefore, it is possible to conclude that extraction by ASE allowed an efficient extraction of the fatty acids present in the biomass produced, when comparing to Soxhlet extraction.

3.3.3. Lipid fractionation with urea complexes

After *C. cohnii* cultivation, the fatty acids present in the collected biomass were subjected to ethylation, in order to obtain the correspondent FAEE, which were then fractionated, using urea complexes, at a crystallization temperature of -18°C, since it was the temperature used in Assay I that resulted in best separation results. Table 11 and Figure 43 show the FAEE profiles obtained before and after the purification/concentration process using urea complexes.

Table 11 - *C. cohnii* FAEE % (w/w) in total fatty acid ethyl esters before and after crystallization with urea complexes of biomass obtained in Assay III. The obtained values resulted from an average of 3 triplicates.

	FAEE profile before urea crystallization	FAEE profile after urea crystallization	
		Non-urea complexing fraction -18°C	Urea complexing fraction -18°C
FAEE			
10:0	0.46±0.03	0.67±0.02	0.11±0.15
12:0	6.28±0.03	5.01±0.23	7.25±0.10
14:0	20.07±0.17	4.56±0.82	35.15±0.23
14:1	1.23±0.02	1.79±0.03	0.00±0.00
16:0	18.40±0.25	0.87±0.21	34.31±0.12
16:1ω9	3.72±0.03	4.81±0.11	2.55±0.03
18:0	0.55±0.03	0.05±0.08	1.08±0.06
18:1ω9	13.95±0.26	11.11±0.56	16.93±0.24
18:2ω6	0.30±0.01	0.52±0.01	0.09±0.01
22:5ω3	0.39±0.13	0.71±0.01	0.00±0.00
22:6ω3	34.64±0.83	69.91±1.56	2.54±0.01
Saturated	45.76	11.16	77.90
Monounsaturated	18.90	17.71	19.48
Polyunsaturated	35.33	71.14	2.63

As observed in Table 11, DHA ethyl ester (22:6ω3) was the highest FAEE obtained after ethylation and profile characterization of the fatty acids present in *C. cohnii* biomass, attaining a value of 36.64% (w/w) of total FAEE. Although this proportion in DHA is reasonable, it represents a lower percentage of ethyl esters than the obtained in Assay I. Other fatty acids that presented significant concentrations were the palmitic (16:0), 18.40% (w/w) of total FAEE, myristic (14:0), 20.07% (w/w) of total FAEE, and oleic (18:1ω9), 13.95% (w/w) of total FAEE. The remaining FAEE were obtained in lower percentages.

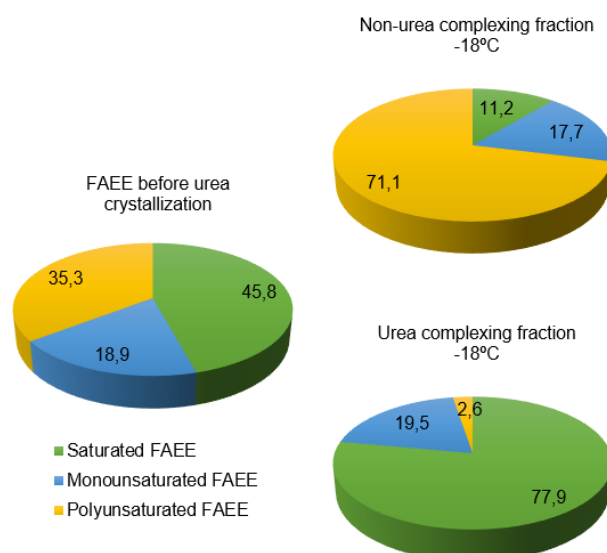


Figure 43 - Saturated, Monounsaturated and Polyunsaturated FAEE before and after urea crystallization of biomass obtained in Assay III, expressed in % (w/w) of total fatty acids ethyl esters.

According to Figure 43, the crystallization at -18°C using urea complexes allowed an efficient separation of PUFA ethyl esters from the remaining FAEE, since an increase from 35.3% (before urea complexation) to 71.1% (after urea complexation) was observed. Also, as expected, the DHA proportion of total FAEE in the non-urea complexing fractions was much higher than in urea complexing fractions.

It is possible to observe that DHA ethyl ester was the dominant PUFA ethyl ester in the non-urea complexing fraction, being 69.91% (w/w) of FAEE, as shown in Table 11. Although when performing crystallization at -18°C in Assay I the percentage of DHA obtained in the non-complexing fraction was higher (91.6% (w/w) of FAEE), we can verify that the separation was quite efficient in this assay, since the presence of PUFA ethyl esters in urea complexing fraction was only 2.6% (w/w) of FAEE, as observed in Figure 43.

The proportion of saturated FAEE in urea complexing fraction attained 77.9% (w/w) of FAEE and only 11.2% (w/w) of FAEE was detected in non-urea complexing fraction. The separation of saturated FAEE shows improvement in relation to Assay I. The most prevalent saturated FAEE present in urea complexing fraction were myristic (14:0) and palmitic (16:0), that attained 35.15% and 34.31% of purity, respectively, after crystallization at -18°C.

The monounsaturated FAEE in urea complexing fraction attained 19.5% (w/w) of FAEE, which is also a positive result. However, the separation of these FAEE was less effective, since a percentage of 11.2% (w/w) of FAEE was detected in the non-urea complexing fraction. The most prevalent monounsaturated FAEE in urea complexing fraction was oleic (18:1 ω 9) accounting for 16.93% after crystallization.

In order to assess if this fractionation process is effective and to evaluate the recovery of ethyl esters in the fractions obtained after crystallization using urea complexes, recovery yields have been calculated, as mentioned in section 2.8.2. Figure 44 shows the recovery yields, defined as the ratio between the initial ethyl esters mixture weight, before the urea fractionation step, and the weight of each EE fraction obtained after the urea fractionation (and removal, in case of the urea complexing fraction).

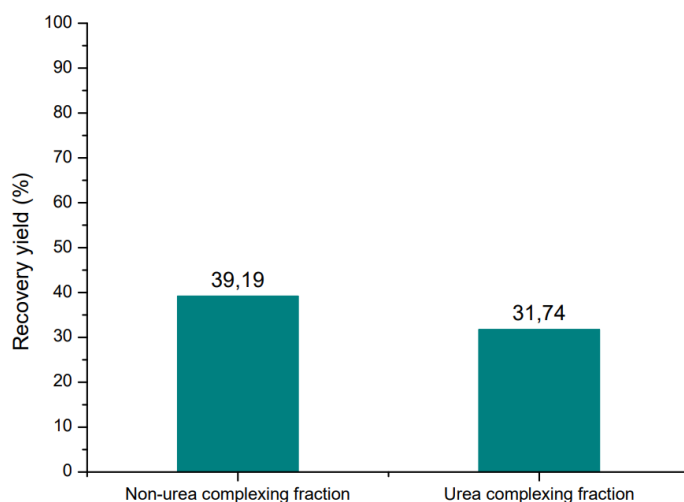


Figure 44 - Recovery yields for the final FAEE fractions, obtained after urea crystallization at -18°C in Assay III, relatively to the initial ethyl esters mixture before urea addition.

According to Figure 44, it is possible to conclude that, the recovery yield, for the sum of both fractions, presented a value around 70%, what indicates that there was a 30% loss of FAEE during the process. This loss may occur during the filtration step (performed to separate urea complexing fraction from non-urea fraction), considering that the fatty acids may be retained in the filter. Also, in case of the

urea complexing fraction, the FAEE may not be totally removed and solubilized in hexane, remaining in the urea.

Concluding, the fractionation process using urea complexes at a crystallization temperature of -18°C was effective for the separation PUFA ethyl ester from saturated and monounsaturated FAEE in this assay. A fraction with 69.91% purity of DHA ethyl ester was obtained, presenting a very satisfactory result, that accomplishes the purpose of this methodology. Also, a fraction rich in saturated and monosaturated FAEE was obtained. Thus, the non-urea complexing fraction, rich in polyunsaturated FAEE including DHA, may be directed to food, pharmaceutical and cosmetic industries (although additional studies must be accomplished to confirm the suitability for human consumption), while the urea complexing fraction may be directed to biodiesel purposes, after a hydrogenation step. With this approach, all compounds in *C. cohnii* are valorised, and no waste is generated.

However, the totality of FAEE resultant from ethylation of biomass was not yet fully fractionated. In future, for attainment of richer fractions and more efficient recovery of all FAEE, an alternative step for the separation of urea complexing fraction from non-urea complexing fraction must be studied or, for example, more washes using n-hexane must be performed.

3.3.4. Evaluation of the fraction for biodiesel production

As referred in section 1.2.2., biodiesel must meet strict parameters in order to be commercialized in European Union. Thus, the urea complexing fraction (rich in saturated and monounsaturated fatty acids) that was obtained after fractionation process at -18°C , for biomass obtained in Assay III, was then studied to assure they are appropriate and meet the parameters described in standard EN 14214 for biodiesel production.

Table 12 shows the theoretical estimated values for this fraction, calculated by equations mentioned in section 2.9., for the following parameters: viscosity, specific gravity, cetane number, iodine value and polyunsaturated ethyl esters content.

Table 12 - Theoretical estimate of FAEE quality for biodiesel production, according to EN 14214. The obtained values were determined through the Average Unsaturation (AU) calculation.

Parameter	Estimated values	Limit EN 14214
	-18°C	
Viscosity ($\text{mm}^2 \text{s}^{-1}$)	4.986	3.50 – 5.00
Specific Gravity (g cm^{-3})	0.875	0.86 – 0.90
Cetane Number	60.549	>51.00
Iodine Value	38.666	<120.00
Polyunsaturated (≥ 4 double bonds) ethyl esters (% (w/w))	2.540	<1.00
AU	0.349	-

As observed in Table 12, all the estimated values for viscosity, specific gravity, cetane number and iodine value are within the regulations established by the European standard EN 14214. However, an amount of polyunsaturated (≥ 4 double bonds) ethyl esters are still present in all FAEE urea complexing fractions. It is important to notice that the polyunsaturated ethyl esters still present in this urea complexing fraction (2.54% (w/w)) are even lower than the percentages that remained in fractions obtained in Assay I, what constitutes an improvement in process (11.4% (w/w), 15.3% (w/w) and 11.8%

(w/w) for fractions obtained at 25°C, 4°C and -18°C, respectively). However, it is still needed an additional reaction step (for example, hydrogenation reaction) to reduce the presence of polyunsaturated ethyl esters to a level lower than 1% (w/w) and, consequently, allow the use of this lipidic fractions for biodiesel production.

3.4. Discussion of results obtained in this study

Efforts to explore alternative sources of DHA have been made in the last decade, including large-scale production of oilseed microalgae and protists, capable of synthesising this polyunsaturated fatty acid (Gong, et al., 2015). The heterotrophic microalga *C. cohnii* has been widely studied for industrial production of DHA since it can accumulate it at high concentrations within the cells. Also, in order to reduce the costs of this microalga biomass production and, consequently, turn this process into a competitive alternative for the traditional methods currently used for DHA production, several low-cost carbon sources have been studied. Therefore, to discuss with more detail the relevance of the results obtained in the present study, a compilation has been made with the most relevant studies reporting *C. cohnii* cultivations for DHA production. Table 13 presents a summary of the conditions and results reported in previous studies, described in the literature, in which *C. cohnii* cultivations were conducted with a view to DHA production, as well as the results attained in the present study (Assays I, II and III).

As observed in Table 13, De Swaaf, Sijtsma, & Pronk (2003) achieved 83.35 g L⁻¹ of DCW, the highest biomass concentration biomass reported at time, when conducted a fermentation using glucose, ethanol and YE in the culture medium, in a 2L fed-batch bioreactor cultivation. Safdar et al. (2017), using the same strain ATCC 30555, attained a lower biomass concentration of 15.80 g L⁻¹ on a medium containing glucose and NaNO₃, when performing a 5L batch bioreactor cultivation. These results present higher DCW than the biomass concentration attained in all assays performed in the present study. However, De Swaaf, Sijtsma, & Pronk (2003) and Safdar et al. (2017) both used pure substrates in the cultivation. Also, glucose and yeast extract are the preferential carbon and nitrogen sources used for production of DHA through *C. cohnii* fermentation, however these substrates present themselves as very expensive resources. In large-scale production, the use of these substrates would not be feasible.

Mendes et al. (2007) used carob pulp syrup as carbon source to grow *C. cohnii* CCMP 316 and reported final biomass concentrations of 42.0 g L⁻¹, 9.2% w/w of TFA, 38.5 mg L⁻¹ h⁻¹ of lipid productivity and 18.5 mg L⁻¹ h⁻¹ DHA productivity (Table 13). The results reported by Mendes et al. (2007) are higher than those obtained in all assays of the present study. However, Mendes et al. (2007) may have achieved higher results in terms of lipid and DHA productivities due to the use of yeast extract as nitrogen source, that contains all the nutrients required for heterotrophic growth, although it is a very expensive and industrially lead to a significant increase of economic costs.

Gong et al. (2015) and Isleten-Hosoglu & Elibol (2017) conducted cultivations for DHA production in shake flasks, both using *C. cohnii* ATCC 30772, the same strain used in the present study. Gong et al. (2015) used rapeseed meal hydrolysate and waste molasses in the culture medium and obtained 2.90 g L⁻¹ biomass concentration, 27.70% w/w of TFA, 4.70 mg L⁻¹ h⁻¹ of lipid productivity and 0.50 mg L⁻¹ h⁻¹ DHA productivity. These results are lower than the ones obtained in Assay I, however Gong et al. (2015) reported higher TFA content than the one attained in Assay II in the present study, where the same low-cost substrate was used (sugarcane molasses). Thus, the presence of rapeseed meal hydrolysate improved lipid production by the microalgae. Isleten-Hosoglu & Elibol (2017) used cheese whey and CSL as carbon source and reported 28.7% w/w of TFA, that was a similar value to the one reported in the present study, in Assay I.

Table 13 - Summary table of the conditions and results obtained in previous studies, reported in the literature, in which *C. cohnii* cultivations were conducted with a view to DHA production and the results attained in the present study (Assays I, II and III).

Strain	Substrate	Cultivation system	Biomass concentration (g L ⁻¹)	TFA content (% w/w)	TFA productivity (mg L ⁻¹ h ⁻¹)	DHA productivity (mg L ⁻¹ h ⁻¹)	Reference
<i>C. cohnii</i> ATCC 30555	Glucose, ethanol and YE	2L bioreactor fed-batch cultivation	83.35	7.12	-	53.00	De Swaaf, Sijtsma, & Pronk (2003)
<i>C. cohnii</i> CCMP 316	Carob pulp syrup and YE	2L bioreactor fed-batch cultivation	42.00	9.20	38.50	18.50	Mendes et al. (2007)
<i>C. cohnii</i> ATCC 30772	Rapeseed meal hydrolysate and waste molasses	250 mL shake flasks	2.90	27.70	4.70	0.50	Gong et al. (2015)
<i>C. cohnii</i> ATCC 30555	Glucose and NaNO ₃	5L bioreactor batch cultivation	15.82	21.40	21.73	8.08	Safdar et al. (2017)
<i>C. cohnii</i> ATCC 30772	Cheese whey and CSL	250 mL shake flasks	-	28.7	-	-	Isleten-Hosoglu & Elibol (2017)
<i>C. cohnii</i> ATCC 30772	Crude glycerol and YE	500 mL shake flasks	5.05	14.7	3.19	1.42	Taborda et al. (2021)
	Sugarcane molasses and YE	500 mL shake flasks	3.91	11.12	2.00	0.99	
<i>C. cohnii</i> ATCC 30772	Crude glycerol and CSL	7L bioreactor batch cultivation	5.34	24.6	8.05	1.6	Moniz et al. (2021)
<i>C. cohnii</i> ATCC 30772	Crude glycerol and CSL	2L bioreactor fed-batch cultivation	10.69	28.29	19.31	6.64	Assay I
	Sugarcane molasses and CSL	2L bioreactor fed-batch cultivation	7.84	7.92	31.82	10.94	Assay II
	Crude glycerol and CSL	2L bioreactor fed-batch cultivation	9.19	24.07	10.52	5.57	Assay III

Taborda et al. (2021) used, for the first time, raw glycerol to grow *C. cohnii* ATCC 30772, and conducted cultivations in shake flasks. The authors studied several pure carbon sources (glucose, acetate and glycerol) and complex substrates (sugarcane molasses, raw glycerol, and industry vinegar effluent) in culture medium for biomass and lipid production. It was concluded that the complex substrate that led to the highest TFA content, TFA productivity and DHA productivity was crude glycerol (14.7% (w/w), 3.19 mg L⁻¹ h⁻¹ and 1.42 mg L⁻¹ h⁻¹, respectively), which demonstrated better results even than pure glycerol. Also, in this cultivation 5.05 g L⁻¹ of biomass concentration was attained. As expected, the results obtained in the present study when using crude glycerol (Assays I and II), were higher than the ones reported by Taborda et al. (2021), since they were conducted in a bioreactor, in fed-batch regime. In fact, cultivations in shake flasks are not as productive as bioreactor assays since they are usually exposed to adverse conditions, such as oxygen limitation or uncontrolled medium pH, which are overcome in a bioreactor (as used in this work) due to a higher mass transference, as a result of a better aeration, agitation and mixing, and medium pH automatic control.

On the other hand, when using sugarcane molasses, the results obtained by Taborda et al. (2021) for biomass concentration, TFA content, TFA productivity and DHA productivity were 3.91 g L⁻¹, 11.12% (w/w), 2.00 mg L⁻¹ h⁻¹ and 0.99 mg L⁻¹ h⁻¹. The TFA content obtained in the mentioned study was higher than the one obtained in Assay II, despite Taborda et al. (2021) conducted the cultivation in shake flasks and not in a bioreactor. However, a significantly lower productivity in TFA was reached in this study when comparing to Assay II, that reached a TFA productivity of 31.82 mg L⁻¹ h⁻¹. As previously reported, the lower TFA content attained in Assay II occurred due to lack of glucose in the medium. The high productivity value attained is evidence that addition of more nutrient pulses, in order to extend the assay, would result in an improvement in biomass and lipid production.

Moniz et al. (2021) used previously distilled crude glycerol, a by-product of biodiesel industry, and CSL, a by-product from starch industry, as carbon and nitrogen sources, respectively, in the culture medium in order to cultivate *C. cohnii* ATCC 30772 in a 7L batch bioreactor cultivation. It is important to notice that the same substrates and *C. cohnii* strain were used in the mentioned study and in Assays I and II, however, Moniz et al. (2021) operated in a batch regime. At the end of the fermentation, the authors registered a biomass concentration, TFA content, TFA productivity and DHA productivity of 5.34 g L⁻¹, 24.60% (w/w), 8.05 mg L⁻¹ h⁻¹ and 1.6 mg L⁻¹ h⁻¹, respectively. In the present study, both Assays I and II presented better results than the ones reported in this study. As expected, under fed-batch regime, the lipid productivity increased relatively to the lipid productivity reported for *C. cohnii* batch cultivation, which highlights the benefits of using fed-batch cultivations for lipid production, since the addition of nutrient pulses improves microalgal biomass and lipid production and accumulation, when compared to batch cultivations.

In general, crude glycerol is the low-cost carbon source that presents best results for biomass production and consequent lipid and DHA production by *C. cohnii*, as concluded in several studies already reported and, in this study, in Assays I and II. Berzins et al. (2022) investigated *C. cohnii* CCMP 316 growth and DHA production using glucose, ethanol, and glycerol as carbon sources, and presented mathematical modelling results that demonstrated that glycerol had the best experimentally observed carbon transformation rate into biomass, reaching a value that was closest to the upper limit of

theoretical theory. The authors concluded that crude glycerol was readily consumed by this microalga, making this feedstock an attractive substrate for DHA production from this microalga, which corroborated the results reported in the present work.

Using low-cost carbon and nitrogen sources, such as crude glycerol and CSL, for *C. cohnii* lipid and DHA production, can represent up to 84% in cost savings, relative to conventional carbon and nitrogen sources, such as glucose and yeast extract (Moniz, et al., 2021). In fact, the culture medium cost can account for up to 30% of the total production costs in commercial fermentations (Rivas, et al., 2004). This means that efforts must be made to reduce the medium cost, by using low-cost substrates as industrial byproducts. This approach not only contributes to reducing the overall bioprocess costs, but also contributes to a circular economy-based society, which is based on three principles: eliminate waste and pollution, circulate products and materials (at their highest value) and regenerate nature (Ellen MacArthur Foundation, 2022).

Next step in the present study, after *C. cohnii* cultivation for biomass and lipid production, was biomass saponification and lipid fractionation using urea complexes. This method has been successfully used to concentrate PUFA in diverse lipidic materials, including vegetable and fish microalgal oils (Magallanes, et al., 2019). The use of non-toxic and environmentally friendly chemicals was a major concern of this research, since the non-urea complexing fraction, rich in PUFA, was intended for human consumption. Thus, since ethanol is less toxic than methanol, the free fatty acids obtained after saponification were converted into FAEE before urea complexation.

Trough the present study, it was possible to verify that the most effective separation of PUFA ethyl ester from saturated and monounsaturated FAEE was attained when performing urea crystallization at -18°C. At this temperature, a fraction with 91.6% purity of DHA ethyl ester was obtained in Assay I and a fraction with 69.91% purity of DHA ethyl ester was attained in Assay III. This fractions, rich in polyunsaturated FAEE including DHA, may then be directed to food, pharmaceutical and cosmetic industries, although additional studies must be accomplished to confirm the suitability for human consumption. Furthermore, the urea complexing fraction may be directed to biodiesel purposes, after a hydrogenation step. With this approach, all compounds in *C. cohnii* are valorised, no waste is generated and, once again, the principles of circular economy are respected.

4. Conclusions and future prospects

The present work aimed to study the implementation of a simple and sustainable process, which supports the circular economy, to produce docosahexaenoic acid (DHA) and biodiesel, from biomass biorefinery of the microalgae *Cryptocodinium cohnii*. For that purpose, high density cell cultures of *C. cohnii* were produced, with high content in intracellular lipids, by conducting several fermentations using different low-cost substrates (crude glycerol, sugarcane molasses and CSL) to study their viability and potential application for industrial lipid production. It also aimed to study fractionation process, using urea complexes, of fatty acids present in the microalgal biomass produced, as an efficient method to separate the lipidic fractions with different degrees of saturation: a polyunsaturated fatty acid fraction, rich in DHA, that can be used for pharmaceutical, nutraceutical and food purposes, and a lipid fraction rich in saturated and monounsaturated fatty acids, for biodiesel purposes.

In the present study, three assays were conducted, in a 7L benchtop bioreactor operating in fed-batch regime, using different nutrient sources: crude glycerol, sugarcane molasses and CSL, all industrial by-products. It was possible to conclude that crude glycerol was the most suitable carbon source used for *C. cohnii* fermentation, presenting better results in terms of biomass production and consequent fatty acids accumulation, such as DHA. In Assay I, using crude glycerol and CSL as low-cost nutrient sources, 10.69 g L⁻¹ of biomass were produced and a TFA content of 28.29% (w/w), TFA productivity of 19.31 mg L⁻¹ h⁻¹ and DHA productivity of 6.64 mg L⁻¹ h⁻¹ were attained, what indicates productive and reasonable results when comparing to previous studies already reported in this research area. Operating in fed-batch regime, by adding nutrient pulses of crude glycerol, YE and CSL, allowed, effectively, a prolongation of the stationary phase, what resulted in higher amounts of biomass and in an increase in lipid accumulation.

On the other hand, in Assay II, when using sugarcane molasses as carbon source, the results were not that productive since it was only obtained a biomass concentration of 7.84 g L⁻¹ and TFA content of 7.92% (w/w), representing lower results when comparing to the other assays performed in this study and when comparing to other studies reported in the literature. This result occurred due to lack of glucose in the medium, that induced a situation of stress in the cells and led to the consumption of the reserve lipids already accumulated, thus reducing the amount of reserve lipids in cells at the end of fermentation. However, higher TFA productivity of 31.82 mg L⁻¹ h⁻¹ and DHA productivity of 10.94 mg L⁻¹ h⁻¹ were attained, evidencing that addition of more nutrient pulses, in order to extend the cultivation, would result in an improvement in biomass and lipid production. These results demonstrate that *C. cohnii* grows in the presence of glucose from sugarcane molasses hydrolysis, however, it must be provided higher glucose concentration in the culture medium. Thus, a new bioreactor fermentation, operating in fed-batch, should be conducted in the future, to evaluate if sugarcane molasses is in fact a promising low-cost carbon source.

Also, culture monitoring through flow cytometry allowed to conclude that industrial cultivation of *C. cohnii* using low-cost substrates, is not only possible but has little to no impact in the growth of the cells, since it was possible to observe that cells remained healthy, presenting enzymatic activity and intact cell membrane during the assays conducted.

Lipid extraction from microalgal biomass produced was carried out through ASE and conventional Soxhlet extraction, that in the present study was considered the reference process for lipid quantification. In general, for each assay conducted, the total lipids yield obtained by Soxhlet extraction and ASE presented similar values. This is an advantage given that ASE allowed to achieve high extraction yields using a smaller amount of biomass, consuming less solvent and in less extraction time, being an eco-friendlier extraction method.

Microalgal biomass resultant from Assays I and III was subjected to a saponification and ethylation process, to obtain FAEE, which were then fractionated using urea complexes. The crystallization with urea allowed separation of two different fractions, according to FAEE structure: non-urea complexing fraction (rich in DHA) and urea complexing fraction (rich in saturated and monounsaturated FAEE, for biodiesel purposes). Results reported in the present study allowed to conclude that the most effective separation of PUFA ethyl ester from saturated and monounsaturated FAEE was attained when performing urea crystallization at -18°C . At this temperature, a fraction with 91.6% purity of DHA ethyl ester was obtained in Assay I and a fraction with 69.91% purity of DHA ethyl ester was attained in Assay III. However, the recovery yield, for the sum of both fractions, presented a value around 70%, what indicates that there was a 30% loss of FAEE during the process. These losses may occur during the filtration step (performed to separate urea complexing fraction from non-urea fraction), since the fatty acids may be retained in the filter. Also, in case of the urea complexing fraction, the FAEE may not be totally removed and solubilized in hexane, remaining in the urea. Thus, further studied must be carried out in future, to attain higher DHA purity, turning this process more effective and more sustainable environmental and economically. For example, for attainment of richer fractions and more efficient recovery of all FAEE, an alternative step for the separation of urea complexing fraction from non-urea complexing fraction must be studied or, for example, more washes using n-hexane must be performed.

The urea complexing fractions, rich in saturated and monounsaturated FAEE, resultant from fractionation process of biomass produced in Assays I and III, were then evaluated from a theoretical approach to assure its viability and to verify if they meet the parameters described in standard EN 14214 for biodiesel production. Theoretical estimated values for parameters such as viscosity, cetane number, iodine value and polyunsaturated ethyl esters content were calculated using correlations previously established and described in the literature. It was possible to conclude that the calculated parameters were in line with the EU standards, except for the polyunsaturated ethyl esters content, that were present in a higher percentage than the limit established by EN 14214. Therefore, an additional reaction step must be performed, for example, hydrogenation reaction, to reduce the presence of polyunsaturated ethyl esters to a level lower than 1% (w/w) and, consequently, allow the use of this lipidic fractions for biodiesel production.

The implementation of biorefineries based on heterotrophic microalgae, for added-value products and biofuels production, regarding the treatment of effluents or waste, is a very important step for the development of an economically sustainable process, from an environmental and economic point of view. For this reason, it is very important to explore the integration of new efficient technologies for the cultivation of microalgae, extraction of biocompounds and purification of microalgae lipids, emphasizing the need to recycle by-products and waste generated throughout the process. The development of

heterotrophic microalgae cultivation processes to produce ω -3 compounds can provide a biotechnological alternative to produce added-value products that would otherwise be produced unsustainably from other living resources, such as marine fish.

Concluding, this work presents a novel process for *C. cohnii* biomass and lipid production using low-cost nutrients, such as crude glycerol, sugarcane molasses and CSL, followed by microalgal lipid fractionation, to obtain DHA ethyl esters, that can be used in food, pharmaceutical and cosmetic industries. Also, this process conducts to the production of saturated and monounsaturated FAEE that are appropriate for conversion into biodiesel, after a hydrogenation step. Although several studies, including the present one, have shown that urea complexation can be an effective and economic method of fractionating and purifying oils, further research is needed to ensure that this process is technically, environmentally and economically sustainable when applied to microalgae lipids. Also, additional studies must be accomplished to confirm the suitability of the purified DHA, that results from this process, for human consumption. Therefore, future research in this field is very important, for optimization of the biorefinery of *C. cohnii*, for valorisation of all microalgal lipid fractions produced and reduction of the overall costs of microalgal lipid heterotrophic production, thus fulfilling the principles of a circular economy. Also, although innovative, this approach still presents several challenges and obstacles to overcome. Some of the main disadvantages are microbial contaminations, that lead to production of unsuitable biomass for commercial applications and the existence of limitations in mass transfers, due to reduced aeration rate of bioreactors, which can cause cellular stress that can lead to reduction in process yield.

Nevertheless, this study represents a pioneering and environmentally friendly method for producing DHA and biodiesel from *C. cohnii*, increasing the potential revenue generated by the entire process. Thus, to assess the practical and economic feasibility of microalgae lipid fractionation scale-up, large-scale *C. cohnii* fermentations should be conducted in the future.

References

- American Chemistry for Life. (2020, janeiro 27). *Molecule of the Week Archive: Docosahexaenoic acid*. Retrieved agosto 26, 2022, from <https://www.acs.org/content/acs/en/molecule-of-the-week/archive/d/docosahexaenoic-acid.html>
- Asimakopoulou, G., Karnaouri, A., Staikos, S., Stefanidis, S. D., Kalogiannis, K. G., Lappas, A. A., & Topakas, E. (2021). Production of Omega-3 Fatty Acids from the Microalga *Cryptocodinium cohnii* by Utilizing Both Pentose and Hexose Sugars from Agricultural Residues. *Fermentation*. doi:10.3390/fermentation7040219
- Beam, C. A., & Himes, M. (1982). Distribution of the Members of the *Cryptocodinium cohnii* (Dinophyceae) Species Complex. *The Journal of Protozoology*. doi:10.1111/j.1550-7408.1982.tb02874.x
- Berzins, K., Muiznieks, R., R. Baumanis, M., Strazdina, I., Shvirksts, K., Prikule, S., Stalidzans, E. (2022). Kinetic and Stoichiometric Modeling-Based Analysis of Docosahexaenoic Acid (DHA) Production Potential by *Cryptocodinium cohnii* from Glycerol, Glucose and Ethanol. *marine drugs*. doi:10.3390/md20020115
- Brunschwig, C., Mossavou, W., & Blin, J. (2012). Use of bioethanol for biodiesel production. *Progress in Energy and Combustion Science*. doi:10.1016/j.pecs.2011.11.001
- Cardoso, L., Campos de Almeida, F. N., Souza, G. K., Asanome, I. Y., & Pereira, N. C. (2019). Synthesis and optimization of ethyl esters from fish oil waste for biodiesel production. *Renewable Energy*. doi:10.1016/j.renene.2018.10.081
- Castej6, N., Luna, P., & Senorans, F. J. (2021). Microencapsulation by spray drying of omega-3 lipids extracted from oilseeds and microalgae: Effect on polyunsaturated fatty acid composition. *Food Science and Technology*. doi:10.1016/j.lwt.2021.111789
- CD Creative Diagnostics. (2022). *Flow Cytometry Guide*. Retrieved august 17, 2022, from <https://www.creative-diagnostics.com/flow-cytometry-guide.htm>
- Chisti, Y. (2007). Biodiesel from microalgae. *Biotechnology Advances*. doi:10.1016/j.biotechadv.2007.02.001
- Danielsen, S., Beech, H., Wang, S., El-Zaatari, B., Wang, X., Sapir, L., Rubinstein, M. (2021). Molecular Characterization of Polymer Networks. *Chemical Reviews*. doi:10.1021/acs.chemrev.0c01304
- De Swaaf, M., Sijtsma, L., & Pronk, J. (2003). Fed-batch cultivation of the docosahexaenoic acid producing marine alga *Cryptocodinium cohnii* on ethanol. *Applied microbiology and biotechnology*. doi:10.1007/s00253-002-1118-1
- Ellen MacArthur Foundation. (2022). Retrieved setembro 22, 2022, from <https://ellenmacarthurfoundation.org/topics/circular-economy-introduction/overview>
- Fargione, J., Hill, J., Tilman, D., Polasky, S., & Hawthorne, P. (2008). Land Clearing and the Biofuel Carbon Debt. *Science*. doi:10.1126/science.1152747
- Giergielewicz-Mozajska, H., Da browski, L., & Namiesnik, J. (2001). Accelerated Solvent Extraction (ASE) in the Analysis of Environmental Solid Samples - Some Aspects of Theory and Practice. *Critical Reviews in Analytical Chemistry*. doi:10.1080/20014091076712
- Gong, Y., Liu, J., Jiang, M., Liang, Z., Jin, H., & Hu, X. (2015). Improvement of omega-3 docosahexaenoic acid production by marine dinoflagellate *Cryptocodinium cohnii* using rapeseed meal hydrolysate and waste molasses as feedstock. *PLoS ONE*. doi:10.1371/journal.pone.0125368
- Ho, D. P., Ngo, H. H., & Guo, W. (2014). A mini review on renewable sources for biofuel. *Bioresource Technology*. doi:10.1016/j.biortech.2014.07.022

- Horrocks, L. A., & Yeo, Y. K. (1999). Health benefits of Docosahexaenoic Acid (DHA). *Pharmacological Research*. doi:https://doi.org/10.1006/phrs.1999.0495
- Hu, S., Luo, X., Wan, C., & Li, Y. (2012). Characterization of Crude Glycerol from Biodiesel Plants. *Journal of Agricultural and Food Chemistry*. doi:10.1021/jf3008629
- Islam, M. A., Heimann, K., & Brown, R. J. (2017). Microalgae biodiesel: Current status and future needs for engine performance and emission. *Renewable and Sustainable Energy Reviews*. doi:http://dx.doi.org/10.1016/j.rser.2017.05.041
- Isleten-Hosoglu, M., & Elibol, M. (2017). Bioutilization of Cheese Whey and Corn Steep Liquor by Heterotrophic Microalgae *Cryptocodinium cohnii* for Biomass and Lipid Production. *Academic Food Journal/ Akademik GIDA*. doi:10.24323/akademik-gida.345256
- Isleten-Hosoglu, M., & Elibol, M. (2017). Improvement of medium composition and cultivation conditions for growth and lipid production by *Cryptocodinium cohnii*. *Romanian Biotechnological Letters*.
- Khozin-Goldberg, I., Bigogno, C., & Cohen, z. (1999). Salicylhydroxamic acid inhibits $\Delta 6$ desaturation in the microalga *Porphyridium cruentum*. *Biochimica et Biophysica Acta*. doi:10.1016/S1388-1981(99)00107-9
- Kongruang, S., Roytrakul, S., & Sriariyanun, M. (2020). Renewable Biodiesel Production from Oliaginous Yeast Biomass Using Industrial Wastes. *E3S Web of Conferences - 2019 Research, Invention and Inovative Congress*. doi:10.1051/e3sconf/202014103010
- Kumar , G., Shekh, A., Jakhu, S., Sharma, Y., Kapoor, R., & Sharma, T. (2020). Bioengineering of Microalgae: Recent Advances, Perspectives, and Regulatory Challenges for Industrial Application. *Frontiers in Bioengineering and Biotechnology*. doi:10.3389/fbioe.2020.00914
- Leoneti, A. B., Aragão-Leoneti, V., & Oliveira, S. V. (2012). Glycerol as a by-product of biodiesel production in Brazil: Alternatives for the use of unrefined glycerol. *Renewable Energy*. doi:10.1016/j.renene.2012.02.032
- Lepage, G., & Roy, C. C. (1986). Direct transesterification of all classes of lipis in one-step reaction. *Journal of Lipid Research*.
- Li, Q., Du, W., & Liu, D. (2008). Perspectives of microbial oils for biodiesel production. *Applied Microbiology and Biotechnology*. doi:10.1007/s00253-008-1625-9
- Liggett, R. W., & Koffler, H. (1948). Corn steep liquor in microbiology. *Bacteriological reviews*.
- Lim, P. Y. (1992). Determination fo chemical properties of meat: Protein determination by Kjeldahl method. *Laboratory Manual on Analytical Methods and Procedures for Fish and Fish Products*.
- Lopes da Silva, T., Moniz, P., & Reis, A. (2020). A Face Escura da Biotecnologia de Microalgas: A Biorrefinaria de microalgas heterotróficas direcionada para a produção de lípidos ricos em compostos Ω -3 e biocombustíveis. *CIES 2020: XVII Congresso Ibérico y XIII Congresso Iberoamericano de Energía Solar* . doi:10.34637/cies2020.1.4078
- Lopes da Silva, T., Moniz, P., Silva, C., & Reis, A. (2019). The Dark Side of Microalgae Biotechnology: A Heterotrophic Biorefinery Platform Directed to ω -3 Rich Lipid Production. *Microorganisms*. doi:10.3390/microorganisms7120670
- Lopes da Silva, T., Moniz, P., Silva, C., & Reis, A. (2021). The Role of Heterotrophic Microalgae in Waste Conversion to Biofuels and Bioproducts. *Processes*. doi:10.3390/pr9071090
- Lopes da Silva, T., Reis, A., Hewitt, C., & Roseiro, J. C. (2004). Citometria de Fluxo - Funcionalidade celular on-line em bioprocessos. *Boletim de Biotecnologia*.
- Luque de Castro, M. D., & Priego-Capote, F. (2010). Soxhlet extraction: Past and Present panacea. *Journal of Chromatography A*. doi:10.1016/j.chroma.2009.11.027

- Ma, F., & Hanna, M. (1999). Biodiesel Production: a review. *Bioresource Technology*. doi:10.1016/S0960-8524(99)00025-5
- Magallanes, L., Tarditto, L., Grosso, N., Pramparo, M., & Gayol, M. (2019). Highly concentrated omega-3 fatty acid ethyl esters by urea complexation and molecular distillation. *Journal of the science of food and agriculture*. doi:10.1002/jsfa.9258
- Mendes, A., Guerra, P., Madeira, V., Ruano, F., Lopes da Silva, T., & Reis, A. (2007). Study of docosahexaenoic acid production by the heterotrophic microalga *Cryptocodinium cohnii* CCMP 316 using carob pulp as a promising carbon source. *World Journal of Microbiology and Biotechnology*. doi:10.1007/s11274-007-9349-z
- Mendes, A., Lopes da Silva, T., & Reis, A. (2007). DHA Concentration and Purification from the Marine Heterotrophic Microalga *Cryptocodinium cohnii* CCMP 316 by Winterization and Urea Complexation. *DHA from Cryptocodinium cohnii, Food Technology and Biotechnology*.
- Mendes, A., Reis, A., Vasconcelos, R., Guerra, P., & Silva, T. L. (2008). *Cryptocodinium cohnii* with emphasis on DHA production: a review. *21(2)*. doi:10.1007/s10811-008-9351-3
- Mercer, P., & Armenta, R. E. (2011). Developments in oil extraction from microalgae. *European Journal of Lipid Science and Technology*. doi:10.1002/ejlt.201000455
- Moniz, P., Andrade, G., Reis, A., & Lopes da Silva, T. (2022). *Cryptocodinium cohnii* Lipid Fractionation for the Simultaneous DHA and Biodiesel Production. *Chemical Engineering Transactions*. doi:10.3303/CET2293043
- Moniz, P., Silva, C., Oliveira, A. C., Reis, A., & Lopes da Silva, T. (2021). Raw Glicerol Based Medium for DHA and Lipids Production, Using the Marine Heterotrophic Microalga *Cryptocodinium cohnii*. *Processes*. doi:10.3390/pr9112005
- Mottaleb, M. A., & Sarker, S. D. (2012). Accelerated Solvent Extraction for Natural Products Isolation. *Methods in Molecular Biology*. doi:10.1007/978-1-61779-624-1_4
- Nikodinovic-Runic, J., Guzik, M., Kenny, S. T., Babu, R., Werker, A., & Connor, K. E. (2013). Carbon-rich Wastes as Feedstocks for Biodegradable Polymer (Polyhydroxyalkanoate) Production Using Bacteria. *Advances in Applied Microbiology*. doi:10.1016/B978-0-12-407673-0.00004-7
- Oh, C.-E., Kim, G.-J., Park, S.-J., Choi, S., Park, M.-J., Lee, O.-M., Son, H.-J. (2020). Purification of high purity docosahexaenoic acid from *Schizochytrium* sp. SH103 using preparative-scale HPLC. *Applied Biological Chemistry*. doi:10.1186/s13765-020-00542-w
- Pratas, M. J., Freitas, S. V., Oliveira, M. B., Monteiro, S. C., Lima, Á. S., & Coutinho, J. A. (2011). Biodiesel Density: Experimental Measurements and Prediction Models. *Energy & Fuels*. doi:10.1021/ef2002124
- Ratledge, C., Kanagachandran, K., Anderson, A., Grantham, D., & Stephenson, J. (2001). Production of Docosahexaenoic Acid by *Cryptocodinium cohnii* Growth in a pH-Auxostat Culture with Acetic Acid as Principal Carbon Source. *Lipids*. doi:10.1007/s11745-001-0838-x
- Remize, M., Brunel, Y., Silva, J., Berthon, J.-Y., & Filaire, E. (2021). Microalgae n-3 PUFAs Production and Use in Food and Feed Industries. *Marine Drugs*. doi:10.3390/md19020113
- Rivas, B., Moldes, A., Domínguez, J., & Parajó, J. (2004). Development of culture media containing spent yeast cells of *Debaryomyces hansenii* and corn steep liquor for lactic acid production with *Lactobacillus rhamnosus*. *International Journal of Food Microbiology*. doi:10.1016/j.ijfoodmicro.2004.05.006
- Sáez-Plaza, P., Michalowski, T., Navas, M. J., Asuero, A. G., & Wybraniec, S. (2013). An Overview of the Kjeldahl Method of Nitrogen Determination. Part I. Early History, Chemistry of the Procedure, and Titrimetric Finish. *Critical Reviews in Analytical Chemistry*. doi:10.1080/10408347.2012.751786

- Safdar, W., Shamooun, M., Zan, X., Haider, J., Sharif, H., Shoaib, M., & Song, Y. (2017). Growth kinetics, fatty acid composition and metabolic activity changes of *Cryptothecodinium cohnii* under different nitrogen source and concentration. *AMB Express*. doi:10.1186/s13568-017-0384-3
- Sanders, T. (2009). DHA status of vegetarians. *Prostaglandins, Leukotrienes and Essential Fatty Acids*. doi:10.1016/j.plefa.2009.05.013
- Setywardhani, D. A., Sulisty, H., Sediawan, W. B., & Fahrurrozi, M. (2015). Separating poly-unsaturated fatty acids from vegetable oil using urea complexation: the crystallisation temperature effects. *Journal of Engineering Science and Technology*.
- Sharma, J., Sarmah, P., & Bishnoi, N. R. (2020). Market Perspective of EPA and DHA Production from Microalgae. In *Nutraceutical Fatty Acids From Oleaginous Microalgae (A Human Health Perspective)*.
- Swanson, D., Block, R., & Mousa, S. (2012). Omega-3 Fatty Acids EPA and DHA: Health Benefits Throughout Life. *American Society of Nutrition*. doi:10.3945/an.111.000893
- Taborda, T., Moniz, P., Reis, A., & Lopes da Silva, T. (2021). Evaluating low-cost substrates for *Cryptothecodinium cohnii* lipids and DHA production, by flow cytometry. *Journal of Applied Phycology*. doi:10.1007/s10811-020-02304-z
- Tuttle, R., & Loeblich, A. (1975). An optimal growth medium for the dinoflagellate *Cryothecodinium cohnii*. *Phycologia*. doi:10.2216/i0031-8884-14-1-1.1
- Yang, F., Hanna, M. A., & Sun, R. (2012). Value-added uses for crude glycerol—a byproduct of biodiesel production. *Biotechnology for Biofuels*. doi:10.1186/1754-6834-5-13
- Zhou, K., Yu, J., Ma, Y., Cai, L., Zheng, L., Gong, W., & Liu, Q.-a. (2022). Corn Steep Liquor: Green Biological Resources for Bioindustry. *Applied Biochemistry and Biotechnology*. doi:10.1007/s12010-022-03904-w

Annex I – Materials and Reagents

Table 14 - Materials and reagents used in this work.

Name	Chemical Formula	Purity (%)	Brand	Application
Acetyl chloride	C ₂ H ₃ ClO	98.5	PanReac	Fatty acid analysis (transmethylation)
Amphotericin B	C ₄₇ H ₇₃ NO ₁₇	-	PanReac AppliChem	Culture medium
Anhydrous sodium sulphate	Na ₂ SO ₄	99.0	Merck	Fatty acid analysis; Lipid fractionation
Boric acid	H ₃ BO ₃	98.8	Merck	Total nitrogen determination
Bromothymol blue	C ₂₇ H ₂₈ Br ₂ O ₅ S	-	Merck	Total nitrogen determination (pH indicator)
Carbofluorescein diacetate (CFDA)	C ₂₉ H ₁₉ NO ₁₁	-	Life Technologies	Flow cytometry
Chloramphenicol	C ₁₁ H ₁₂ Cl ₂ N ₂ O ₅	>98.0	TCI	Culture medium
Cooper sulphate	CuSO ₄	≥99	Merck	Total nitrogen determination (catalyst mixture)
Corn steep liquor (CSL)	-	-	COPAM	Culture medium
Dimethyl sulfoxide (DMSO)	(CH ₃) ₂ SO	≥99.7	Riedel-de Haën	Culture medium (Antifungal dilution)
Ethanol	C ₂ H ₅ OH	≥99.8	Honeywell	Lipid fractionation
Heptadecanoic acid	C ₁₇ H ₃₄ O ₂	-	Nu-Check-Prep	Fatty acid analysis
Hydrochloric acid	HCL	-	Merck	Culture medium; total nitrogen determination; pH adjustments
Liquid glycerine	C ₃ H ₈ O ₃	99.95	José Manuel Gomes dos Santos, LDA	Culture medium
Methanol	CH ₃ OH	99.8	Honeywell	Fatty acid analysis (transmethylation)
Monohydrated D-Glucose	C ₆ H ₁₂ O ₆ ·H ₂ O	≥99	Chem-Lab	Culture medium
n-heptane	C ₇ H ₁₆	99.0	Fisher Chemical	Fatty acid analysis
n-hexane	C ₇ H ₁₄	95	Fisher Chemical	Soxhlet; ASE; Lipid fractionation
Penicillin G potassium salt	C ₁₆ H ₁₇ N ₂ NaO ₄ S	-	AlfaAesar	Culture medium
Petroleum ether (80-110°C)	-	-	Chem-Lab	Fatty acid analysis (Dissolution of C17:0)
Phosphate buffered saline (PBS)	-	-	Oxoid	Flow cytometry (samples dilution)
Potassium hydroxide	KOH	-	Merck	Lipid Fractionation
Potassium sulphate	K ₂ SO ₄	99	Chem-Lab	Total nitrogen determination (catalyst mixture)
Propidium iodide (PI)	C ₂₇ H ₃₄ I ₂ N ₄	-	Life technologies	Flow cytometry
Sea salt	-	-	OceanusIberica	Culture medium
Sodium hydroxide	NaOH	-	José M. Vaz Pereira, S.A.	Total nitrogen determination; pH adjustments
Streptomycin sulphate	(C ₂₁ H ₃₉ N ₇ O ₁₂) ₂₂ ·3H ₂ SO ₄	-	PanReac AppliChem	Culture medium
Sulfuric acid	H ₂ SO ₄	96	Merck	Total Nitrogen
Urea	CH ₄ N ₂ O	≥99	Sigma-Aldrich	Lipid Fractionation
Yeast extract powder	-	-	HiMedia	Culture medium

Annex II – EU Standard for Biodiesel

Table 15 - Requirements of biodiesel properties according to the European standard EN 14214.

Property	Unit	Minimum value	Maximum value
Ester content	%(w/w)	96.5	-
Density at 15°C	g cm ⁻³	0.86	0.90
Kinematic Viscosity at 40°C	mm ² s ⁻¹	3.5	5.0
Flash point	°C	>101	-
Sulphur content	mg kg ⁻¹	-	10
Cetane number	-	51	-
Sulphated ash content	%(w/w)	-	0.02
Water content	mg kg ⁻¹	-	500
Total contamination	mg kg ⁻¹	-	24
Copper band corrosion (3h at 50°C)	rating	Class 1	Class 1
Oxidation stability, 110°C	hour	6	-
Acid value	mg KOH g ⁻¹	-	0.5
Iodine value	-	-	120
Linolenic Acid methyl ester	%(w/w)	-	12
Polyunsaturated (≥4 double bonds) methyl ester	%(w/w)	-	1
MeOH content	%(w/w)	-	0.2
Monoglyceride content	%(w/w)	-	0.7
Diglyceride content	%(w/w)	-	0.2
Triglyceride content	%(w/w)	-	0.2
Free glycerol	%(w/w)	-	0.02
Total glycerol	%(w/w)	-	0.25
Alkaline Metals (Na + K)	mg kg ⁻¹	-	5
Phosphorus content	mg kg ⁻¹	-	4

Annex III – Calculation of the Specific Growth Rate

The specific growth rate (μ) was calculated using Equation 7, presented in section 2.5.8. of Methodology. This parameter was calculated, for each assay, in the period between the lag and stationary phases (exponential phase), in which the logarithm of the dry weight over time fits a straight line. Figure 45 contains the graph of the natural logarithm of the DCW of all assays, over fermentation time, with the points and trendlines used to calculate the specific growth rate.

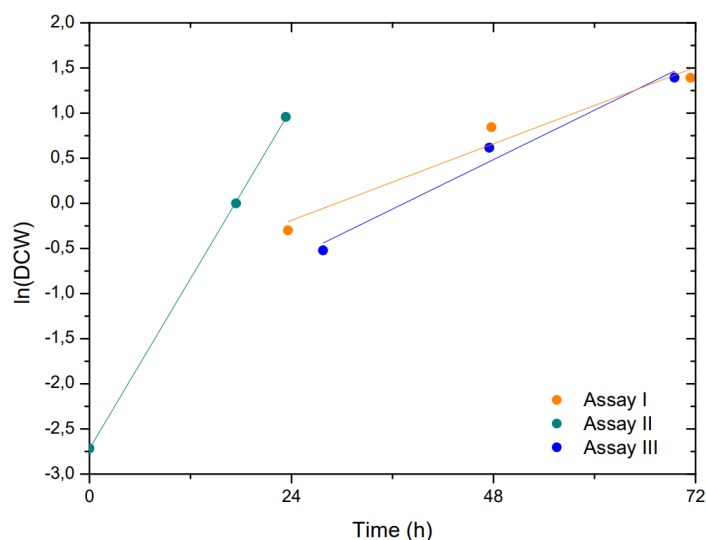


Figure 45 - Natural logarithm of dry cell weight (DCW) of the assays over fermentation time for the points used to calculate specific growth rate, along with the trendlines used.

Table 16 contains the specific growth rate, standard deviation and the coefficient of determination (R^2) for all assays. These data was calculated by MS Excel's LINEST function, according to data presented in Figure 45.

Table 16 - Specific growth rate, calculated standard deviation and coefficient of determination (R^2) for each assay.

Assay	μ (h^{-1})	Standard Deviation	R^2
I	0.0354	0.00698	0.9625
II	0.1572	0.00120	0.9998
III	0.0457	0.00642	0.9612

Annex IV – Calibration curves to determine carbon content in the culture medium by HPLC

To assess the carbon concentration in the culture medium during each fermentation of *C. cohnii* (glycerol or glucose, depending on the carbon source used in each assay) all samples collected were analyzed by HPLC. For a correct analysis of the carbon concentration in each sample, correlations were established to relate the peak areas obtained with each carbon source concentration. These correlations were calculated through HPLC analysis of glycerol, glucose and fructose standard solutions of known concentration, by linear regression between these concentrations and the correspondent peak areas obtained.

The calibration curves for glycerol, glucose and fructose are shown in Figures 46 and 47.

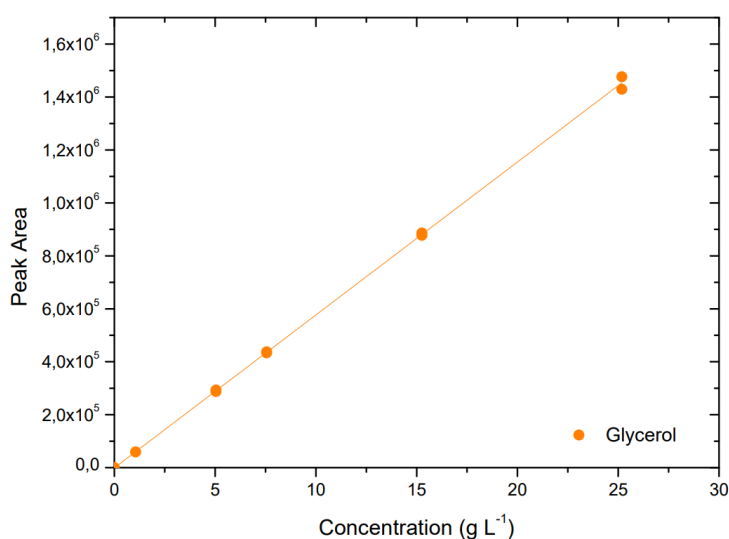


Figure 46 - Calibration curve for glycerol.

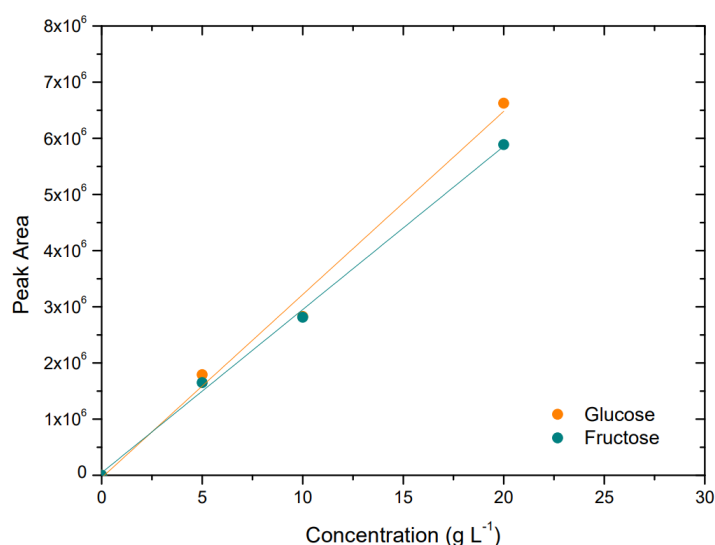


Figure 47 - Calibration curves for glucose and fructose.

Table 17 contains the correlations obtained for glycerol, glucose and fructose, as well as the the coefficient of determination (R^2) for each curve. This data was calculated by MS Excel's LINEST function, according to data presented in Figures 46 and 47.

Table 17 - Glycerol, glucose and fructose correlations.

	Intercept	Slope	R²
Glycerol	-888.9713	57772.9253	0.9994
Glucose	-43129.9084	326191.5758	0.9861
Fructose	44938.4230	290598.3607	0.9964